Anticancer activities of oxidant-redox drug combinations in lipid excipients

MC Haigh

orcid.org 0000-0002-5666-2252

B.Pharm

Dissertation submitted in partial fulfilment of the requirements for the degree *Master of Science* in Pharmaceutics at the North-West University

Supervisor:	Prof LH du Plessis
Co-supervisor:	Dr JM Viljoen
Assistant supervisor:	Prof RK Haynes

Graduation May 2018

Student number: 23500417

To those who inspired it

And will not read it

ACKNOWLEDGEMENTS

"I blame all of you. Writing this dissertation has been an exercise in continuous suffering. The normal reader may, perhaps, exempt themselves from excessive guilt, but for those of you who have played the larger role in prolonging my agonies with your encouragement and support, well… you owe me." ~ Chezanné Haigh

I would like to acknowledge my deepest gratitude to my parents, John and Ann Haigh, my sisters, Chezanné and Tammlyn Haigh, my brother, Struanné Haigh, and brother-in-law, Casper Uys. Your unfailing love and support, encouragement and patience, helped me make lemon juice when life gave me lemons.

To my supervisors, Prof Lissinda du Plessis, Dr Johanna Viljoen and Prof Richard Haynes. Thank you for all your advice, support and encouragement, but most of all, thank you for sharing your knowledge with me. A special thanks to the National Research Foundation (NRF) for their financial support and to Prof Lissinda and Prof Haynes for nominating me for the bursary.

Angelique Lewies and Dr Jaco Wentzel, the help and expertise you gave so freely, was invaluable to this dissertation. Thank you kindly.

And, Johan Reynecke, who went the through hard times with me, cheered me on and celebrated each accomplishment. Thank you for being the most supportive, understanding and encouraging person I've gotten to know.

ABSTRACT

Genetic alterations in the redox status of cancer cells promotes a continuous and elevated production of reactive oxygen species (ROS), associated in the initiation and progression of tumours. The body's potent antioxidant system effectively neutralises ROS produced in normal cells, however, owing to high metabolic rates of cancer cells, ROS is generated at levels beyond the capacity of this antioxidant system. Many cancers are characterised by poor prognosis and high mortality, despite extensive research and substantial efforts for developing targeted cancer chemotherapeutics.

Skin cancer represents the most frequent occurring cancers and melanoma, the leading cause of skin cancer related deaths. Breakthroughs in chemotherapeutics have been achieved in certain cancers, though marginal advances have been made in treatments for other malignancies such as metastatic melanoma. Strategies aimed at altering redox dysregulation in the presence of ROS inducers, present a promising new approach to cancer chemotherapeutics. This can be achieved by elevating oxidative stress beyond the toxicity threshold of cancer cells, sparing normal cells.

This study considered the increasing incidence of skin cancer and the challenges of current therapeutic strategies. An alternative treatment strategy was proposed and investigated. Combination therapy of artemisone, elesclomol and lipid excipients; oleic acid, stearic acid and cholesterol is investigated, for the first time, for potential anticancer activity against A375 human melanoma cells. This study forms part of initial screenings for a larger project, *"Rational development of combinations of known and novel drugs for chemotherapy of cancer"*, wherein rational oxidant and redox drug combinations are developed to target hypoxic and proliferating cancer cells. This approach relies on the susceptibility of cancer cells to oxidative stress.

The *in vitro* cytotoxicity of the proposed combinations against A375 melanoma cells was assessed relative to cell viability, using the 3-(4,5-dimethylthiazol-2-yl)-2,5-diphenyl tetrazolium bromide (MTT) assay and intracellular ROS accumulation, using the 2',7'- Dichlorofluorescein-diacetate (DCFH-DA) assay. The main findings in this study showed, for the first time, enhanced anticancer activity of artemisone and Cu(ll)-elesclomol when combined with lipid excipients, oleic acid, stearic acid and cholesterol. Combinations caused a dose dependant decrease in cell number and increase in ROS generation. Taken together, redox directed combinations with lipid excipients, should be thought of as potential alternative to traditional therapies and warrants further investigation.

Key terms: Skin cancer; Artemisone; Elesclomol; Oleic acid; Stearic acid; Cholesterol; Oxidative stress.

UITTREKSEL

Genetiese veranderinge in die redoks karakter van kanker selle bevorder die voordurende en verhoogde produksie van reaktiewe suurstofspesies (RSS), wat op hul beurt verwant is aan die oorsprong en progressie van kankaraardige gewasse. Die liggaam se natuurlike antioksidantstelsel kan die RSS wat in normale selle geproduseer word effektief neutraliseer. As gevolg van die die hoë metaboliese tempo van kanker selle word RSS egter teen verhoogde vlakke geproduseer, wat die kapasiteit van die antioksidantstelsel oorskrei. Menigde kankers word gekenmerk deur swak progose en hoë vlakke van afsterwing, ten spyte van breedvoerige navorsing en aansienlike pogings in die ontwikkelling van doelgerigte kanker chemoterapeutika. Velkanker verteenwoordig die mees prominentste van kankers, met melanoom die hoof oorsaak van velkanker verwante sterftes. Deurbrake in chemoterapeutika is behaal vir sekere kankers, alhoewel minimale vordering gemaak is in die behandeling van ander kwaadaardige velkankers, soos metastatiese melanomas. Stratigieë gerig op die verandering van redoks wanregulasie in die teenwoordigheid van RSS induseerders bied ‘n belowende nuwe benadering tot kanker chemoterapeutika. Die bogenoemde kan bereik word deur die oksidatiewe spanning te verhoog sodat die toksiese drumpel van die kankerselle oorskrei word, terwyl normale selle ongeraak bly.

Hierdie studie het die verhoogde voorvalle van velkanker en die uitdagings van die huidige terapeutiese stratigieë, oorweeg. ‘n Alternatiewe strategie van behandeling was voorgestel en ondersoek. Vir die eerste keer is die gekombineerde terapie van artemisoon, elesklomol en lipied hulpstowwe; oleïensuur, steariensuur, en cholesterol; ondersoek vir potensiële kankervegtende eienskappe teen A375 menslike melanoom selle. Hierdie studie vorm deel van aanvanklike proewwe vir ‘n groter projek onder die tietel *“Rasionele ontwikkeling van kombinasies van bekende en nuwe geneesmiddels vir chemoterapie van kanker”,* waarin rasionele oksidant en redoks geneesmiddel kombinasies ontwikkel word om hipoksiese en verspreidende kankerselle te teiken. Hierdie benadering maak staat op die vatbaarheid van kankerselle vir oksidatiewe spanning.

Die *in vitro* sitotoksisiteit van die voorgestelde kombinasies teen A375 melanoom kankerselle was geëvalueer relatief tot sel lewensvatbaarheid, met behulp van die 3-(4,5-dimielthiazool-2-yl)-2,5-difeniel tetrazolium bromied (MTT) toets en intrasellulêre RSS-akkumulasie, met behulp van die 2’,7’- dichlorofluoresien-diacetaat (DCFH-DA) toets. Die belangrikste bevindinge van hierdie studie het, vir die eerste keer, verhoogde kankervegtende effekte van artemisoon en Cu(II)-elesklomol in kombinasies met lipied hulpstowwe; oleïensuur, steariensuur en cholesterol; getoon. Kombinasies het 'n dosis-afhanklike afname in sel lewensvatbaarheid en ‘n toename in intrasellulêre RSS-generasie veroorsaak. Met die bogenoemde in ag geneem, kan redoksgerigte

kombinasies met lipied hulpstowwe beskou word as 'n potensiële alternatief tot tradisionele terapie en regverdig verdere ondersoek.

Sleutelterme: Vel kanker; Artemisoon; Elesklomol; Oleïensuur; Steariensuur; Cholesterol; Oksidatiewe stress.

TABLE OF CONTENTS

LIST OF ABBREVIATIONS

AK	Actinic keratosis
ANOVA	Analysis of Variance
et al	And others (Latin)
ATM	Artemisone
ART	Artemisinin
API	Active pharmaceutical ingredient
BCC	Basal cell carcinomas
BCG	Bacillus Calmette-Guérin
β-ESA	Beta-eleostearic acid
CO_2	Carbon dioxide
CSO-SA	Chitosan oligosaccharide
Cu	Copper
Cu(n)	Copper anion (n=I, II)
CMM	Cuteneous malignant melanoma
Da	Dalton
DFC	2',7' Dichlorofluorescein
DCFH-DA	2',7'- Dichlorofluorescein-diacetate
DMEM	Dulbecco's Modified Eagle's Medium
DMSO	Dimethyl Sulfoxide
DNA	Deoxyribonucleic acid
EDTA	Ethylenediaminetetraacetic acid

$FAD(H)_2$	Flavin adenine dinucleotide
Fre	Flavin reductase
FBS	Fetal Bovine serum
FDA	Food and drug administration
FU	Fluorouracil
G6PD	Glucose-6-phosphate dehydrogenase
GSH	Glutathione
GSSG	Glutathione disulphide
GR	Glutathione reductase
A375	Human melanoma cancer cell cultures
HO	Hydroxyl anion
H_2O_2	Hydrogen peroxide
IC_{10}	Inhibiting concentration at 10%
IC_{50}	Inhibiting concentration at 50%
IC_{90}	Inhibiting concentration at 90%
IFE	Inter-follicular epidermis
LBDDS	Lipid-based drug delivery systems
LDH	Lactate dehydrogenase
MM	Malignant melanoma
MED	Minimal erythematous dose
MTT	3-(4,5-dimethylthiazol-2-yl)-2,5-diphenyl tetrazolium bromide
MR	Mycothiol reductase
NADP(H)	Nicotinamide adenine dinucleotide phosphate

NEAA	Non-essential amino acids
NMSC	Nonmelanocytic skin cancers
NWU	North-West University
O_2	Oxygen
PBS	Phosphate buffered saline
P/S	1% Penicillin-Streptomycin
PFS	Progression-free survival
ROS	Reactive oxygen species
RNA	Ribonucleic acid
SCC	Squamous cell carcinomas
SFM	Serum free media
SLNP	Solid lipid nanoparticles
TrxR	Thioredoxin reductase;
EDTA	Trypsin-Versene
US	United States
UV	Ultraviolet
H_2O	Water
WHO	World Health Organisation

LIST OF SYMBOLS

cm^2	Centimetre squared
°C	Degrees Celsius
g	Gravitational acceleration
µl	Microliter
µM	Micromolar
mg	Milligram
mM	Millimolar
M	Molar
MW	Molecular weight
nm	Nanometre
nM	Nano molar
%	Percentage
x*g*	Times gravity

LIST OF TABLES

Chapter 2

Chapter 3

Annexure A

LIST OF FIGURES

Chapter 1

Chapter 2

Chapter 3

Chapter 4

Annexure A

CHAPTER 1

ANTICANCER ACTIVITIES OF OXIDANT-REDOX DRUG COMBINATIONS IN LIPID EXCIPIENTS

AN INTRODUCTION

1.1 Introduction

This study considers the increasing incidence of skin cancer and the challenges of current therapeutic strategies. An alternative treatment strategy is proposed and investigated. Combination therapy of artemisone, elesclomol and lipid excipients; oleic acid, stearic acid and cholesterol is investigated for potential anticancer activity on A375 human melanoma cells. This study forms part of initial screenings for a larger project titled *"Rational development of combinations of known and novel drugs for chemotherapy of cancer*", wherein rational oxidant and redox drug combinations are developed to target hypoxic and proliferating cancer cells. This approach relies on the susceptibility of cancer cells to oxidative stress.

The body organ in which neoplasms occur most frequently is the skin, with over one million skin cancer cases detected annually (Simões *et al.*, 2014). It serves as an essential environmental interface imparting a protecting sheath that is vital for homeostasis. At the same time, the skin is a key target for toxic insult by various chemical and physical agents capable of altering the skin's structure and function, for example reactive oxygen species (ROS). Accounting for approximately 40% of all new diagnosed cancers, skin cancer represents a leading and growing public health problem (Narendhirakannan & Hannah, 2012). Skin cancers are categorised into two main groups based on the cell of origin and clinical behaviour. First, there is non-melanoma skin cancers (NMSC), comprising of basal cell carcinomas (BCCs) and squamous cell carcinomas (SCCs); and secondly, cutaneous malignant melanoma skin cancers (D'Orazio *et al*., 2013; Simões *et al.*, 2014).

Non-melanoma skin cancers represent the most frequent form of cancer with an annual worldwide occurrence of 2 to 3 million cases; this rate is expected to double within the next 30 years (Simões *et al.*, 2014). Both BCCs and SCCs originate from epidermal keratinocytes. The incidence of these skin cancers vastly outnumbers that of malignant melanomas. Non-melanoma skin cancers however, have the tendency to remain confined to the site of origin, making treatment easier with improved long-term prognosis (D'Orazio *et al*., 2013).

Cutaneous malignant melanomas are profoundly malignant tumours arising from altered melanocytes or nevus cells (Oppermann *et al*., 2005). The American Cancer Society (2017) estimates 87 110 new cases of melanoma will be diagnosed in the United States (US) in 2017, of which 9 730 are estimated to result in death. In 2000 the crude incidence rate of cutaneous melanoma (per 100 000) in South Africa was 3.8 for men and 3.6 for woman and unfortunately, no newer statistics are available. Although invasive melanomas only account for 1% of all skin cancers, they are responsible for the vast majority of skin cancer deaths (American Cancer Society, 2017). They are the most severe and progressive form of skin cancer, with notorious resistance to all current modalities of cancer chemotherapy, despite a vast number of clinical trials in a wide range of anticancer approaches. These approaches range from surgery to radio-, immune- and chemotherapy; the average patient survival rate is only 6 to 10 months after diagnosis. Malignant melanoma prognosis would be auspicious if detected at very early stages of the disease, i.e. before the malignant melanoma becomes intrusive. Regrettably, melanoma lesions remain asymptomatic or unnoticeable for prolonged periods before diagnosis. Furthermore, metastatic melanoma cells tend to disseminate to multiple organs (including brain, bone, liver and lungs) as it is seldom limited to single foci, rendering treatment strategies challenging as opposed to NMSCs that often remain at the site of origin (Soengas & Lowe, 2003).

As previously mentioned, ROS may act as environmental toxicants capable of altering the skin's structure and function. These ROS are highly reactive with biological molecules; and may result in oxidative modification and altered function of biological molecules, including deoxyribonucleic acid (DNA), lipids and proteins, during free radical reactions (Trachootham *et al*., 2009). Cellular ROS may arise from interactions with exogenic sources such as xenobiotic compounds, or during the process of mitochondrial oxidative phosphorylation (Ray *et al*., 2012). A novel therapeutic strategy of modulating ROS has arisen to selectively target the destruction of cancer cells. Reactive oxygen species are produced at low concentrations in normal cells and are effectively neutralised by the potent antioxidant system of cells (Krishner *et al*., 2008; Narendhirakannan & Hannah, 2012). In contrast, the high metabolic activity of cancer cells results in elevated levels of ROS; above the capacity of the antioxidant system; resulting in a chronic state of oxidative stress promoting carcinogenesis and cancer progression. Opposed to the tumour-promoting abilities of ROS, increasing ROS levels beyond the threshold capacity of cancer cells can induce cancer cell arrest and apoptosis (Krishner *et al*., 2008). This enhanced oxidative stress of ROS, targets three major stages of cancer pathogenesis namely: proliferation, metastasis and resistance (Galadari *et al*., 2017).

The combination concept of oxidant drug and redox drug, based on the transition of metal ions, was one of the focus points for this study. Redox-oxidation of this proposed combination of oxidant drug and redox drug, rests on the irreversible reduction of an oxidant drug, as well as the

reversible reduction of a redox drug for the interception of electrons from crucial cofactors of redox enzymes otherwise responsible for redox homeostasis (Asahi *et* al., 2014; Haynes *et al*., 2010; Haynes *et al*., 2011; Haynes *et al*., 2012;; Trachootham *et al*., 2009). It was proposed that the reduced form of the redox drug would be oxidised, to generate ROS. The combined effects of the oxidant and the redox drugs generating ROS, would result in loss of redox homeostasis and subsequent apoptotic cell death. Metastasis would be counteracted by the increase in oxidative stress of this proposed redox-oxidation drug combination emerging from elevated ROS levels. Overall, it was suggested that an initial rapid build-up, succeeded by a sustained ROS production, would result in a catastrophic loss of redox homeostasis and ultimately, apoptosis (Figure 1.1). The proposed oxidant drug for this study was artemisone and the redox drug was elesclomol with copper as the transition metal.

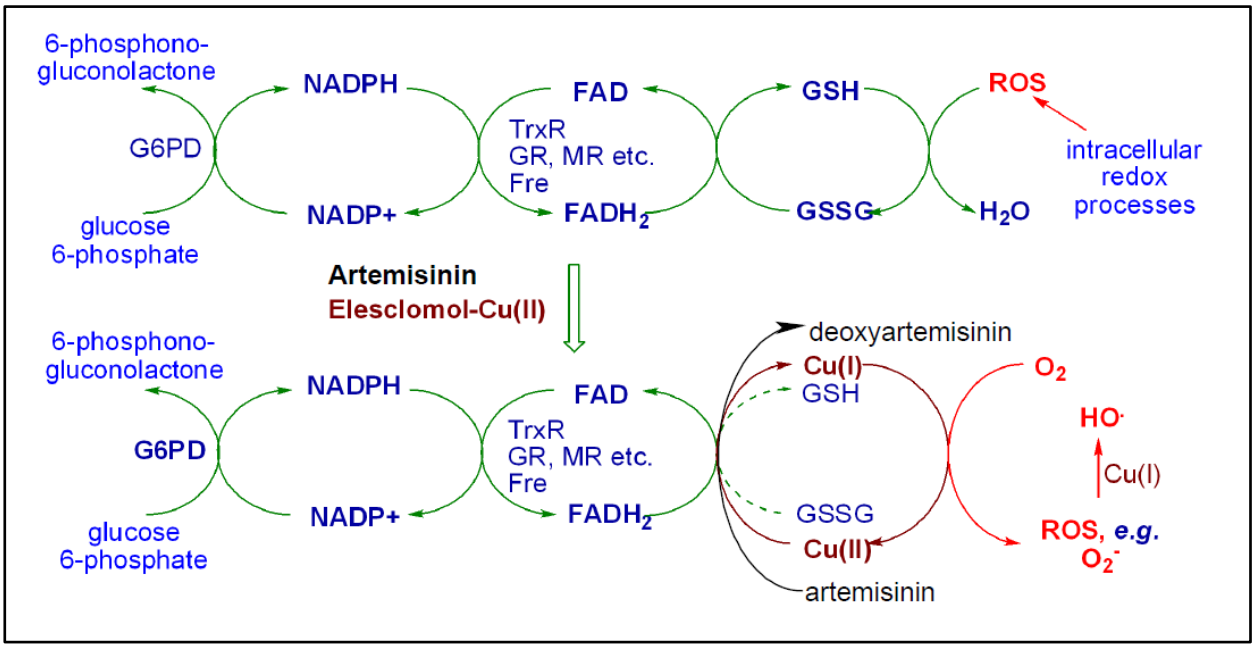

Figure 1.1: Combination concept of oxidant drug artemisinin and redox drug elesclomol based on transition metal ions. Immediate ROS generation followed by exhaustion of artemisinin. ROS generation is maintained continuous chelation of redox metal ion (Cu). (Used with permission from Haynes *et al*., 2012). G6PD = glucose-6-phosphate dehydrogenase; NADP(H) = nicotinamide adenine dinucleotide phosphate; FAD(H_2) = flavin adenine dinucleotide; TrxR = thioredoxin reductase; GR = glutathione reductase; MR = mycothiol reductase; Fre = flavin reductase; GSH = glutathione; GSSG = glutathione disulphide; ROS = reactive oxygen species; H_2O = water; Cu = copper; O_2 = oxygen; HO = hydroxyl anion.

Artemisinins are currently the most valuable antimalarial. They are isolated from the Chinese traditional herb, ginghao (*Artemisia annua)*, a plant traditionally used for its antifebrile properties (Haynes & Krishna, 2004). In the early 1970s, the principal artemisinin was first isolated and shown to be highly active as an antimalarial drug. Since then, it has become the backbone treatment for multi-drug resistant malaria strains (Gravett *et al*., 2011). Despite the efficacy of

artemisinin against the *Plasmodium* parasite, this compound exhibits pharmacokinetic limitations such as poor aqueous and oil solubility, as well as a short *in vivo* half-life due to its fast degradation and low bioavailability, thus limiting its effectiveness (Crespo-Ortiz & Wei, 2012). In addition, artemisinin displays neuro- and embryotoxicity, therefore limiting the widespread use of the compound (Fishwick *et al*., 1995). Due to these shortcomings, derivatives of artemisinin (collectively known as artemisinins), artemisone for instance, have been developed to overcome some of these pharmacokinetic drawbacks (Crespo-Ortiz & Wei, 2012; Woodrow *et al*., 2005).

Artemisone is a second generation semi-synthetic 10-allylaminoartemisinin that exhibits both superior activity and safety in comparison to artemisinin resulting in enhanced antimalarial efficacy, improved bioavailability, metabolic stability, prolonged half-life (*in vivo*) and the absence of neurotoxicity (Crespo-Ortiz & Wei, 2012; Haynes *et al*., 2006). Studies showed that additional to artemisone's potent antimalaria activity, this compound exhibits significant antitumor activity (Crespo-Ortiz & Wei, 2012; Gravett *et al*., 2011). Both the malaria parasite and cancer cells share fundamental characteristics, associated with the metabolic requirements related to the cell's high proliferation rates. The parasiticidal and anticancer mechanisms of artemisinins have been linked to an environment rich in free- or heme-bound intracellular iron and apoptosis induction (Van Huijsduijnen *et al*., 2013). The endoperoxide moiety of artemisinins has shown to be of importance for both antimalaria and anticancer activity via the generation of ROS to induce cellular damage, however the precise mechanism remains controversial (Ho *et* al., 2014; Nakase *et al*., 2008). Crespo-Ortiz and Wei (2012) suggested that artemisinins enhance the generation of ROS in an intracellular environment and do so by interfering with intracellular mechanisms associated with the control of oxidative stress. In this way, artemisinins may act as oxidant drugs in redox-oxidation reactions in this study (Figure 1.1).

Gravett *et al*. (2011) evaluated the *in vitro* anticancer effects of artemisone. Their findings established that application of artemisone resulted in reduced cell (tumour) numbers, induced cell cycle blockage and affected proteins that regulate cell cycling and enhanced the effect of cancer chemotherapeutic agents. All effects were attributed to disruptions in the cell cycle, thus resulting in growth arrest and hindering disease progression (Crespo-Ortiz & Wei, 2012; Gravett *et al*., 2011). Additionally, artemisone showed superior activity when compared to artemisinin in both breadth and magnitude (Gravett *et al*., 2011).

As stated, the proposed redox drug in this study is elesclomol. Elesclomol is a novel investigatory drug which through ROS generation results in subsequent apoptosis activation and consequently exerts anticancer activity (Krishner *et al*., 2008). Nagai *et al*. (2012) found that the strong binding of copper to elesclomol is fundamental for its anticancer activity, whereas in the absence of copper, the compound exhibits no discernible activity. Copper (Cu) chelates outside of cells and

enters as elesclomol-Cu(ll) complexes. Reactive oxygen species are generated by the redox cycling of Cu(II) to Cu(I). Continued copper accumulation within mitochondria is achieved by the repetitive shuttling of elesclomol-Cu complexes from the extracellular to the intracellular compartments upon initial dissociation from the elesclomol-Cu(ll) complex (Figure 1.1). This ROS generation results in oxidative stress levels incompatible with cell survival (Blackman *et* al., 2012; Nagai *et al*., 2012). As with artemisone, elesclomol displayes anticancer activity against various cancer cells and have shown improved efficacy when in combination with other chemotherapeutics, such as paclitaxel in human tumour xenograft models (Krishner *et al*., 2008).

Surgical excision is currently the standard treatment for skin cancers. However, not all patients, especially those with NMSCs, can be treated in this manner; and therefore, alternative treatment options must be considered (D'Orazio *et al*., 2013). Topical chemotherapy, including the use of imiquimol, has become an important alternative for patients who cannot be treated by surgical excision. Other reagents for topical chemotherapy include 5-fluorouracil, altretinoin, diclofenac sodium, and ingenol mebutate, however, the treatment period required for these preparations is extensive, some for up to 90 days; the high recurrence rate of 33 to 54% is also a concern. This failure in therapy, reinforces the need for the development of novel topical therapies (D'Orazio *et al*., 2013; Haque *et al*., 2015). Topical formulations against skin cancer has become an attractive alternative, opposed to traditional therapies, as not all NMSCs are easily treated with surgical excision (D'Orazio *et al*., 2013). Topical treatment of skin cancers is considered when the tumours are present on the top layers of the skin. Due to improved skin appearance as well as an increase in "quality-of-life" of patients, topical treatment plays an important role in the management of NMSCs (Haque *et al*., 2015).

Current topical melanoma therapies include 5-fluorouracil, imiquimol and photodynamic therapy using a photosensitive cream containing methyl aminolevulinate, all of which are suitable for superficial BCCs treatment. Diclofenac sodium gel is also available for pre-cancerous lesions (Simões *et al.*, 2014). These preparations frequently produce an intense inflammatory response causing discomfort to patients, in addition to frequent and often long-term dosing durations, reinforcing the need for alternative topical therapies for melanoma treatment (Haque *et al*., 2015).

Excipients are included in topical dosage forms to aid manufacturing and administration by improving the solubility of poorly soluble drugs. They increase dissolution- and/or drug release rates, ensure stability and decrease undesirable side effects of the pharmaceutical formulation (Dave *et al*., 2015; Kalinkova, 1999). Excipients for topical chemotherapy formulations include alcohol, polyethylene glycol, hydroxypropyl cellulose, polysorbate and paraffin. Some of these excipients may however intensify the condition being treated or lead to toxic side effects (Haque *et al*., 2015; Simões *et al.*, 2014). As a result, lipid excipients are considered as an alternative due

to their enhanced safety and efficacy profile. Furthermore, lipid formulations can be modified to meet a large variety of requirements specific for the condition or drug such as improved bioavailability, stability, solubility and toxicity (McGillis & Fein, 2004; Shrestha *et al*., 2014).

The lipid excipients chosen in this study were oleic acid (fatty acid), stearic acid (monoglyceride) and cholesterol (sterol). The potential of each of the chosen lipid excipients to induce cytotoxicity in cancer cells through increased intracellular ROS production has been explored. Excipients typically exert little to no therapeutic effects, however certain lipid excipients, such as oleic acid, display potential anticancer activity through ROS generation, leading to apoptosis induction (Garg *et al*., 2015; Hatanaka *et al*., 2013; Schröter *et al*., 2015). Carrillo *et al*. (2012) showed that in numerous cancer cell lines, oleic acid induced the inhibition of cell proliferation and apoptosis resulting in cancer cell death, potentially resulting from increased intracellular ROS generation. In two separate studies, stearic acid displayed cytotoxicity on human lung and bladder carcinoma cells through elevated ROS generation, leading to oxidative stress and apoptosis induction (Hu *et al*., 2012; Sun *et al*., 2012). The third lipid excipient in this study surprisingly displayed enhanced carcinogenesis in colorectal cancer via ROS elevation, in contrast to the other two lipid excipients anticancer action of ROS induced apoptosis (Wang *et al*., 2017). In contrast, the works of Kotla *et al*. (2017) showed cholesterol exhibited no cytotoxic effects nor influenced the proliferation of human leukaemia cells.

1.2 Research problem

Current skin cancer chemotherapy does not provide a noteworthy therapeutic benefit. Success is minimal and remission is often observed in melanoma tumours. Furthermore, the response rates are low; and mild to severe toxicity has been reported with the current cancer chemotherapeutic agents (Finn *et al*., 2012; Soengas & Lowe, 2003). This failure in current cancer therapy emphasises the need for alternative therapies (topical applications for example) and the possibility of utilising novel compounds, such as artemisone and elesclomol for cancer treatment.

This study focused on the *in vitro* cytotoxic activity and ROS-formation of the oxidant drug artemisone and the redox drug elesclomol, both alone and in combination with one another, on human melanoma cancer cell cultures (A375). This combination was proposed based on the anticipated synergism between the compounds enabling a decrease in the respective drug amounts required so in order ameliorate toxicity; and to decrease proliferation as well as hypoxic cancer cells. In an attempt to overcome the physiochemical shortcomings of artemisone, specific lipid excipients, namely oleic acid, stearic acid and cholesterol, were selected for intended topical application, as a route of drug delivery. These lipids were tested for their *in vitro* toxicity and ROS

generating properties as well as any synergistic or antagonistic interaction of the lipid excipients with the oxidant and redox agent combinations.

1.3 Aim and objectives

The aim of this study is to investigate the *in vitro* cytotoxic activity and intracellular ROS-generation of artemisone and elesclomol in combination with selected lipid excipients. In an attempt to meet this aim, the following objectives were set, to:

1. Determine the *in vitro* efficacy of:
    - Artemisone on A375 human melanoma cells.
    - Elesclomol and Cu(ll)-elesclomol on A375 human melanoma cells.
    - The selected lipid excipients; oleic acid, stearic acid and cholesterol; on A375 human melanoma cells.
2. Establish the inhibiting concentrations (IC) at 10%, 50% and 90% of artemisone and Cu(ll)-elesclomol on A375 human melanoma cells.
3. Evaluate the *in vitro* cytotoxicity of:
    - Artemisone in combination with each of the selected lipid excipients; oleic acid, stearic acid and cholesterol; on A375 human melanoma cells.
    - Cu(ll)-elesclomol in combination with each of the selected lipid excipients; oleic acid, stearic acid and cholesterol; on A375 human melanoma cells.
    - Artemisone–Cu(ll)-elesclomol in combination with each of the selected lipid excipients; oleic acid, stearic acid and cholesterol; on A375 human melanoma cells.
4. Detect the intracellular reactive oxygen species of:
    - Artemisone in combination with each of the selected lipid excipients; oleic acid, stearic acid and cholesterol; on A375 human melanoma cells.
    - Cu(ll)-elesclomol in combination with each of the selected lipid excipients; oleic acid, stearic acid and cholesterol; on A375 human melanoma cells.
    - Artemisone–Cu(ll)-elesclomol in combination with each of the selected lipid excipients; oleic acid, stearic acid and cholesterol; on A375 human melanoma cells.

1.4 References

American Cancer Society. 2017. Cancer facts & figures 2017. Atlanta: American Cancer Society. https://www.cancer.org/content/dam/cancer-org/research/cancer-facts-and-statistics/annual-cancer-facts-and-figures/2017/cancer-facts-and-figures-2017.pdf Date of access: 2 Nov. 2017.

Asahi, H., Tolba, M.E., Tanabe, M., Suqano, S., Abe, K. & Kawamoto. 2014. Perturbation of copper homeostasis is instrumental in early developmental arrest of intraerythrocytic *Plasmodium falciparum*. *BMC Microbiology*, 14(167). https://bmcmicrobiol.biomedcentral.com/articles/10.1186/1471-2180-14-167 Date of access: 6 Oct. 2017.

Blackman, R.K., Cheung-Ong, K., Gebbia, M., Proia, D.A., He, S., Kepros, J., Jonneaux, A., Marchetti, P., Kluza, J., Rao, P., Wada, Y., Giaever, G. & Nislow, C. 2012. Mitochondrial electron transport is the cellular target of the oncology drug elesclomol. *Plos One*, 7(1):e29798.

Carrillo, C., Cavia, M.A. & Alonso-Torre, S.R. 2012. Antitumor effect of oleic acid; mechanisms of action; a review. *Nutricion Hospitalaria*, 27(6):1860–1865.

Crespo-Ortiz, M. & Wei, M.Q. 2012. Antitumor activity of artemisinin and its derivatives: from a well-known antimalarial agent to a potential anticancer drug. *Journal of Biomedicine and Biotechnology,* 2012:247597.

Dave, V.S., Saoji, S.D., Raut, N.A. Haware, R.V. 2015. Excipient variability and its impact on dosage form functionality. *Journal of Pharmaceutical Sciences*, 104(3):906–915.

D'Orazio. J., Jarrett, S., Amaro-Ortiz. A. & Scott. T. 2013. UV radiation and the skin. *International Journal of Molecular Sciences,* 14(6):12222–12248.

Finn, L., Markovic, S.N. & Joseph, R.W. 2012. Therapy for metastatic melanoma: the past, present, and future. *BMC Medicine*, 10(23). https://bmcmedicine.biomedcentral.com/articles/10.1186/1741-7015-10-23 Date of access: 6 Sep. 2016.

Fishwick, J., McLean, W.G., Edwards, G. & Ward, S.A. 1995. The toxicity of artemisinin and related compounds on neuronal and glial cells in culture. *Chemico-Biological Interactions*, 96(3):263–271.

Galadari, S., Rahman, A., Pallochankandy, S. & Thayyullathil, F. 2017. Reactive oxygen species and cancer paradox: to promote or to suppress? *Free Radiacal Biology and Medicine*, 104(2017):144–164.

Garg, T., Rath, G. & Goyal, A.K. 2015. Comprehensive review on additives of topical dosage forms for drug delivery. *Drug Delivery*, 22(8):969–987.

Gravett, A.M., Liu, W.M., Krishna, S., Chan, W., Haynes, R.K., Wilson, N.L. & Dalgleish, A.G. 2011. *In vitro* study of the anti-cancer effects of artemisone alone or in combination with other chemotherapeutic agents. *Cancer Chemotherapy and Pharmacology*, 67(3):569–577.

Haque, T., Rahman, K.M., Thurston, D.E., Hadgraft, J. & Lane, M.E. 2015. Topical therapies for skin cancer and actinic keratosis. *European Journal of Pharmaceutical Sciences,* 77(1):279–289.

Hatanaka, E., Dermargos, A., Hirata, A.E., Vinolo, M.A.R., Carpinelli, A.R., Newsholme, P., Armelin, H.A. & Curi, R. 2013. Oleic, linoleic and linolenic acids increase ROS production by fibroblasts via NADPH oxidase activation. *Plos One*, 8(4):e58626.

Haynes, R.K., Chan, W.C., Wong, H.N., Li, K.Y., Wu, W.K., Fan, K.M., Sung, H.H., Williams, I.D., Prosperi, D., Melato, S., Coghi, P. & Monti, D. 2010. Facile oxidation of leucomethylene blue and dihydroflavins by artemisinins: relationship with flavoenzyme function and antimalarial mechanism of action. *ChemMedChem*, 5(8):1282–1299.

Haynes, R.K., Cheu, K.W., Chan, H.W., Wong, H.N., Li, K.Y., Tang, M.M., Chen, M.J., Guo, Z.F., Guo, Z.H., Sinniah, K., Witte, A.B., Coghi, P. & Monti, D. 2012. Interactions between artemisinins and other antimalarial drugs in relation to the cofactor model – a unifying proposal for drug action. *ChemMedChem*, 7(12):2204–2226.

Haynes, R.K., Cheu, K.W., Tang, M.M.K., Chen, M.J., Guo, Z.F., Guo, Z.H., Coghi, P. & Monti, D. 2011. Reactions of antimalarial peroxides with each of leucomethylene blue and dihydroflavins: flavin reductase and the cofactor model exemplified. *ChemMedChem*, 6(2):279–291.

Haynes, R.K., Fugmann, B., Stetter, J., Rieckmann, K., Heilmann, H.D., Chan, H.W., Cheung, M.K., Lam, W.L., Wong, H.N., Croft, S.L., Vivas, L., Rattray, L., Stewart, L., Peters, W., Robinson, B.L., Edstein, M.D., Kotecka, B., Kyle, D.E., Beckermann, B., Gerisch, M., Schmuck, G., Steinke, W., Wollborn, U., Schmeer, K. & Römer, A. 2006. Artemisone – a highly active antimalarial drug of the artemisinin class. *Angewandte Chemie*, 45(13):2082–2088.

Haynes, R.K. & Krishna, S. 2004. Artemisinins: activities and actions. *Microbes and Infection,* 6(14):1339–1346.

Ho, W.E., Peh, H.Y., Chan, T.K. & Wong, W.S.F. 2014. Artemisinins: pharmacological actions beyond anti-malarial. *Pharmacology & Therapeutics*, 142(1):126–139.

Hu, P., Wang, T., Xu, Q., Chang, Y., Tu, H., Zheng, Y., Zhang, J., Xu, Y., Yang, J., Yaun, H., Hu, F. & Zhu, X. 2012. Genotoxicity evaluation of stearic acid grafted chitosan oligosaccharide nanomicelles. *Mutation Research*, 751(2):116–126.

Kalinkova, G.N. 1999. Studies of beneficial interactions between active medicaments and excipients in pharmaceutical formulations. *International Journal of Pharmaceutics*, 187(1):1–15.

Kotla, S., Singh, N.K. & Rao, G.N. 2017. ROS via BTK-p300-STAT1-PPARγ signalling activation mediated cholesterol crystals-induced CD36 expression and foam cell formation. *Redox Biology*, 11(2017):350–364.

Krishner, J.R., He, S., Balasubramanyam, V., Kepros, J., Yang, C., Zhang, M., Du, D., Barsoum, J. & Bertin, J. 2008. Elesclomol induces cancer cell apoptosis through oxidative stress. *Molecular Cancer Therapeutics*, 7(8):2319–2327.

McGillis, S.T. & Fein, H. 2004. Topical treatment strategy for non-melanoma skin cancer and precursor lesions. *Seminars in Cutaneous Medicine and Surgery,* 23(3):174–183.

Nagai, M., Vo, N.H., Ogawa, L.S., Chimmanamada, D., Inoue, T., Chu, J., Beaudette-Zlatanova, B.C., Lu, R., Blackman, R.K., Barsoum, J., Koya, K. & Wada, Y. 2012. The oncology drug elesclomol selectively transports copper to the mitochondria to induce oxidative stress in cancer cells. *Free Radical Biology and Medicine,* 52(2012):2142–2150.

Nakase, I., Lai, H., Singh, N.P. & Sasaki, T. 2008. Anticancer properties of artemisinin derivatives and their target delivery by transferrin conjugation. *International Journal of Pharmaceutics*, 354(1-2):28–33.

Narendhirakannan, R.T. & Hannah, M.A.C. 2012. Oxidative stress and skin cancer: an overview. *Indian Journal of Clinical Biochemistry*, 28(2):110–115.

Oppermann, M., Geilen, C.C., Fecker, L.F., Gillissen, B., Daniel, P.T. & Eberle, J. 2005. Caspase-independent induction of apoptosis in human melanoma cells by the proapoptotic Bcl-2-related protein Nbk/Bik. *Oncogene*, 24(49):7369–7380.

Ray, P.D., Huang, B. & Tsuji, Y. 2012. Reactive oxygen species (ROS) homeostasis and redox regulation in cellular signalling. *Cellular signalling*, 24(5):981–990.

Shrestha, H., Bala, R. & Arora, S. 2014. Lipid-based drug delivery systems. *Journal of Pharmaceuticals*, 2014:801–820.

Simões, M.C.F., Sousa, J.J.S. & Pais, A.A.C.C. 2014. Skin cancer and new treatment perspectives: a review. *Cancer Letters*, 357(2015):8–42.

Schröter, J., Griesinger, H., Reuß, E., Schulz, M., Riemer, T., Süß, R., Schiller, J. & Fuchs, B. 2015. Unexpected products of the hypochlorous acid-induced oxidation of oleic acid: a study using high performance thin-layer chromatography-electrospray ionization mass spectrometry. *Journal of Chromatography A*, 1439(2016):89–96.

Soengas, M.S. & Lowe, S.W. 2003. Apoptosis and melanoma chemoresistance. *Oncogene*, 22(20):3138–3151.

Sun, Z., Wang, H., Ye, S., Xiao, S., Liu, J., Wang, W., Jiang, D., Liu, X. & Wang, J. 2012. Beta-eleostearic acid induced apoptosis in T24 human bladder cancer cells through reactive oxygen species (ROS)-mediated pathway. *Prostaglandins and Other Lipid Mediators*, 99(1-2):1–8.

Trachootham, D., Alexandre, J. & Huang, P. 2009. Targeting cancer cells by ROS-mediated mechanisms: a radical therapeutic approach? *Nature reviews: Drug discovery*, 8(7):579–591.

Van Huijsduijnen, R.H., Guy, R.K., Chibale, K., Haynes, R.K., Peitz, I., Kelter, G., Phillips, M.A., Vennerstrom, J.L., Yuthavong, V. & Wells, T.N.C. 2013. Anticancer properties of distinct antimalarial drug classes. *Plos One*, 8(12):e82962.

Wang, C., Li, P., Xuan, J., Zhu, C., Liu, J., Shan, L., Du, Q., Ren, Y. & Ye, J. 2017. Cholesterol enhances colorectal cancer progression via ROS elevation and MAPK signalling pathway activation. *Cellular Physiology and Biochemistry*, 42(2):729–742.

Woodrow, C.J., Haynes, R.K. Krishna, S. 2005. Artemisinins. *Postgraduate medical journal*, 81(952):71–78.

CHAPTER 2
SKIN CANCER AND ITS TREATMENT
A BACKGROUND

2.1 Introduction

Cancer may be defined as an assortment of diseases characterised by the sporadic growth and spread of abnormal cells, which if not controlled may result in death. While the cause of many cancers, especially childhood cancers, remains unknown, factors contributing to the disease may include external or lifestyle factors such as excessive body mass and tobacco use, and internal non-modifiable factors such as hormone imbalance, inherent genetic mutations and immune conditions. A considerable number of cancers may be prevented, including those caused by a combination of poor nutrition, extensive alcohol consumption, tobacco use, physical inactivity and excessive body mass. Furthermore, several cancers caused by infectious agents, including human immunodeficiency virus, human papillomavirus, hepatitis B and C viruses and *Helicobacter pylori* bacteria, may in principle be prevented through vaccination, behavioural changes or treatment of the infection. Using skin protection against extreme sun exposure and refraining from the use of indoor tanning devices, many of the 5 million annually diagnosed skin cancer cases could be prevented. Another preventative measure is screening for early detection of certain cancers, such as cervical and colorectal cancers, which enables the detection and removal of precancerous lesions (American Cancer Society, 2017).

The most common malignancy in the Caucasian population includes non-melanoma skin cancers and malignant melanomas. The incidence of these cancers is increasing, with a 0.6% annual rise of malignant melanomas for adults over 50 years. The projected number of new cases of melanoma skin cancers in 2016 is 76 380, representing 4.5% of all new cancer cases. The incidence of non-melanoma skin cancers in Caucasians is significantly higher, approximately 18-20 times higher than that of melanoma (Apalla *et al.*, 2016). Even though cutaneous malignancies are not as common in populations other than Caucasian, mortality rates are considerably higher when compared to their white counterparts; late detection and biologically more aggressive tumours may attribute to this discrepancy in outcomes. The most frequently occurring primary cutaneous malignancies in sub-Saharan African include squamous cell carcinoma, Kaposi sarcoma, malignant melanoma and basal cell carcinomas. A retrospective study of melanoma in non-white South Africans indicated that 43% of patients died within a year of diagnosis and only a minority survived beyond 3 years. A primary contributing factor to this predisposition toward poor prognosis is delayed diagnosis and treatment. Although the aetiology of melanoma in dark-

skinned individuals is intensely debated, the role of ultraviolet (UV) rays is evidently important, as it has been established that cultured melanocytes from both dark and light skin exposed to simulated UV-radiation resulted in cytotoxic damage. Therefore, no one is immune to skin cancer (Gohara, 2014).

Primary therapy or cancer treatment includes surgery and radiotherapy, however, in many cases these are inadequate. An ideal anticancer agent should be highly potent and specific to cancer cell death with no significant toxicity to normal cells (Das, 2015). Regardless of advances in chemotherapy that result in improved responses and patient survival, cancer therapy remains challenging due to the frequent occurrence of side effects and poor quality-of-life associated with current anticancer agents (Das, 2015; Orthaber *et al.*, 2017).

2.2 Skin structure and physiology

On average, the human skin embodies approximately 16% of the body mass, rendering it the largest organ (D'Orazio *et al*., 2013). The skin is a multi-lamellar organ composed of a variety of cell types and organellar bodies that act as an interface between internal organs and the external environment (Eckart, 1992; Haque *et al.,* 2015). Knowledge of the skin's structure and the function of its appendages are paramount to understanding the biology of healthy skin and the pathophysiology of skin diseases such as skin cancers (Lai-Cheong & McGrath, 2009). It was previously thought to be an impermeable membrane, however according to the works of Bos and Meinardi (2000), exogenous molecules smaller than 500 Da (Dalton) can diffuse through the skin barrier. This property of permeability holds great importance in topical drug delivery.

The main layers of the skin consist of the epidermis (surface layer), dermis (connective tissue layer) and hypodermis (subcutaneous layer) (Figure 2.1). The epidermis is an overlying layer of epithelial cells above the dermis. The internal layer of adipose tissue (hypodermis) supports both the dermis and epidermis (Eckart, 1992).

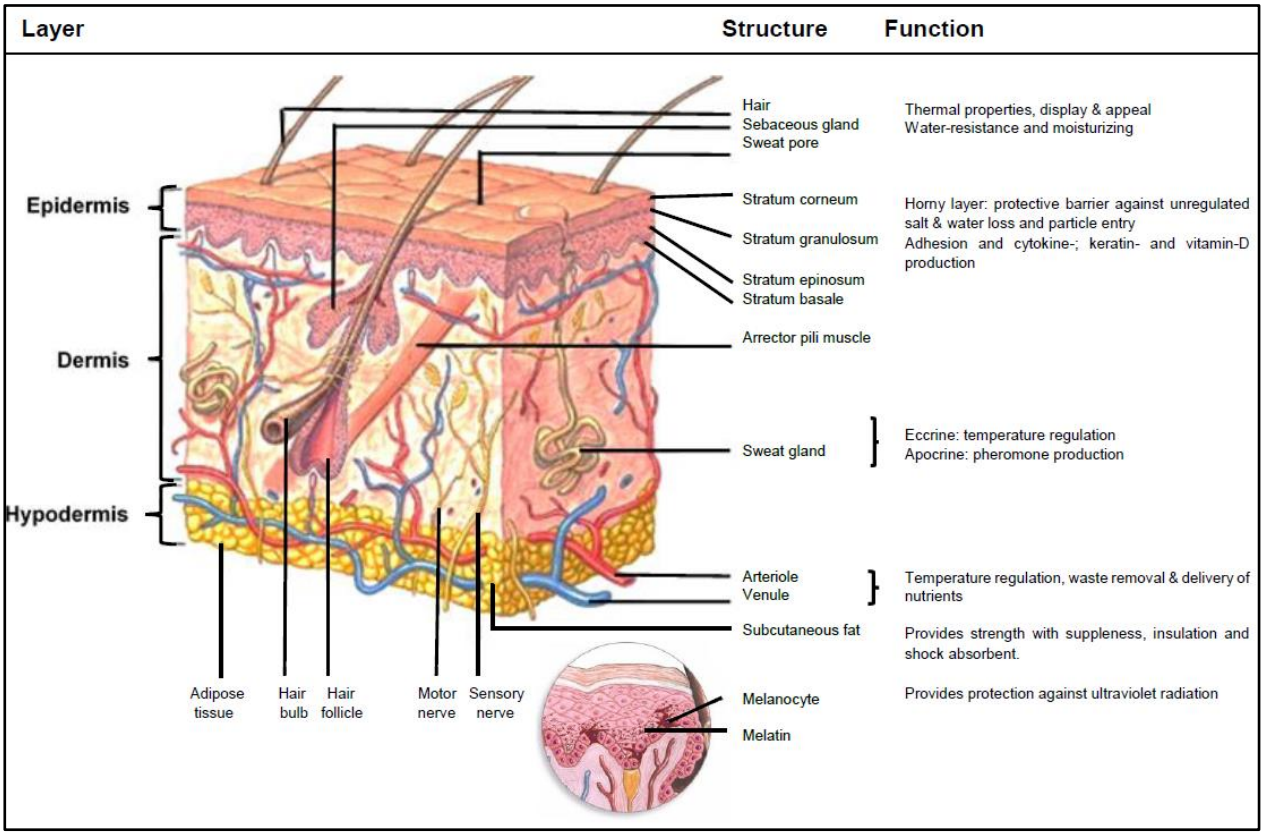

Figure 2.1: An illustration of the skin anatomy and function. Three main layers can be seen, namely the epidermis, dermis and hypodermis all with specialised cells and appendages each with unique functions (Adapted from Venus *et al*., 2011).

2.2.1 The epidermis

The epidermis is a multi-layered structure composed of four major skin layers: the stratum basale, stratum spinosum, stratum granulosum and stratum corneum (Figure 2.1). This layer varies in dimensions, ranging from 0.06 mm on the eyes to 0.8 mm on the palms of the hands and soles of the feet, forming the outermost layer of the skin (Eckart, 1992). It is a continuously renewing structure, regenerating from epidermal stem cells (Silverberg, 2012). Keratinocytes are the most abundant cells found in the epidermis; other cells of this layer include melanocytes and Langerhans and Merkel cells (Eckart, 1992). Melanocytes synthesise two melanin pigments, eumelanin and phaemelanin. These pigments are stored in specialised organelles present in melanocytes known as melanosomes. By directly absorbing UV photons and free radicals, melanin protects the skin from UV-induced radiation (Haque *et al.,* 2015).

2.2.1.1 Stratum basale

This is the layer at the epidermal/dermal barrier, and is generally a one cell thick continuous layer made up of dividing or non-dividing keratinocytes. These cells make up more than 90% of the epidermal layer and their major function is to form a protective sheath that repels foreign material, as well as being abrasion resistant and preventing fluid loss (Eckart, 1992; Venus *et al*., 2011). The cells in the stratum basale undergo mitosis and migrate through each sequential layer until they are shed from the skin surface (Bianchi & Cameron, 2008).

2.2.1.2 Stratum spinosum

Basal cells differentiate towards the surface to form the stratum spinosum layer of polyhedral cells. This layer is composed of keratinocytes that synthesise the fibrous protein keratin that is a major component of the horny stratum corneum. Langerhans cells are present in this layer and function as part of the body's immune system (McGraft *et al*., 2008). The name of this layer is derived from the 'spines' or intercellular bridges that extend among the keratinocytes composed of desmosomes; this 'spiny/prickly' appearance is visible with a light microscope (Marks & Miller, 2013; Venus *et al*., 2011). Desmosomes are extensions of keratin within the keratinocytes that functionally hold cells together (Eckart, 1992; Marks & Miller, 2013).

2.2.1.3 Stratum granulosum

Differentiation continues within the stratum granulosum in which the keratinocytes start to flatten and lose their organelles. These cells acquire additional keratin containing intracellular granules of keratohyalin. Smaller lamellated granules, called Odland bodies, are present within the cytoplasm of the stratum granulosum, the name of which is derived from the granules present in the layer (Marks & Miller, 2013; Venus *et al.,* 2011).

2.2.1.4 Stratum corneum

The stratum corneum represents the hydrophobic outermost layer of the epidermis (Figure 2.1), commonly referred to as the horny layer. It consists of non-nucleated cells that have lost their cytoplasmic organelles and migrated from the stratum granulosum; these cells are known as corneocytes. The corneocytes flatten, and filaments of keratin align into the disulfide cross-linked macrofibres (McGraft *et al*., 2008; Venus *et al*., 2011). This layering can be described as a brick-and-mortar style arrangement where the corneocytes, now dead, flattened and hardened by keratin, represent the "bricks" and the lipid bilayer composed of ceramides, cholesterol, cholesteryl esters and fatty acids from the "mortar". This mortar forms a structured environment that prevents water loss from the skin and invasion of microbial pathogens, toxic substances and

allergens into the body (Elias *et al.,* 2013; Foldvari, 2000). The stratum corneum varies in thickness between 10–20 µm at the different anatomical regions (Haque *et al.,* 2015; Venus *et al*., 2011). The stratum lucidum is an additional zone present in the palmoplantar skin between the stratum granulosum and the stratum corneum. The cells of this layer are still nucleated and are often referred to as “transitional” cells (Haque *et al.,* 2015; McGraft *et al*., 2008).

2.2.2 The dermis

The dermis represents the largest fraction of skin and is approximately 20–30 times thicker than the epidermis. It is responsible for providing the skin’s structural strength, nutrition supplementation, regulating the temperature and elimination of waste. The dermis is comprised mainly of elastic fibrils that are responsible for skin strength and holding skin tissue intact, and elastic connective tissue that provides flexibility. As seen in Figure 2.1, cells present in the dermis include fibroblasts, lymphocytes, mast cells, macrophages and melanocytes; it also contains blood vessels, nerves and skin appendages such as sebaceous and sweat glands required to sustain the epidermis (Eckart, 1992; Haque *et al.,* 2015; Potts *et al*., 1992).

2.2.3 The hypodermis

The hypodermis is a specialised layer of adipocytes or fat cells which forms the innermost layer of the skin. It acts as a cushion between the internal structures such as muscle and bone and the external skin. Additionally, it provides heat insulation, an energy reserve, allows for skin mobility and acts as a mechanical shock absorber (Eckart, 1992; Haque *et al.,* 2015).

2.3 Skin cancer

The global incidence of skin cancer and actinic keratosis (AK) has dramatically increased in recent years with over a million cases detected annually (Simões *et al.*, 2014). The primary cause of these neoplasms is failure of the body’s deoxyribonucleic acid (DNA) repair mechanism after damage of skin cell DNA due to UV-radiation (Haque *et al.,* 2015). A defective apoptosis mechanism is a characteristic of skin cancers, where too little apoptosis occurs thus resulting in uncontrollable cell development (Erb *et al.*, 2005; Lippens *et al.*, 2009). Another contributor is reactive oxygen species (ROS). In virtually all cancers, elevated ROS levels have been detected where they promote tumour growth and progression (Liou & Storz, 2010). This is of significance to this study and will be discussed in Section 2.5.1. Skin cancers can be differentiated into two main classes, namely non-melanoma skin cancers (NMSCs) and melanoma skin cancers (D’Orazio *et al.*, 2013). As illustrated in Figure 2.2, skin cancers may appear in different layers of the skin and with distinct clinical and anatomical presentations; this will be further discussed in Sections 2.3.1–2.3.2.

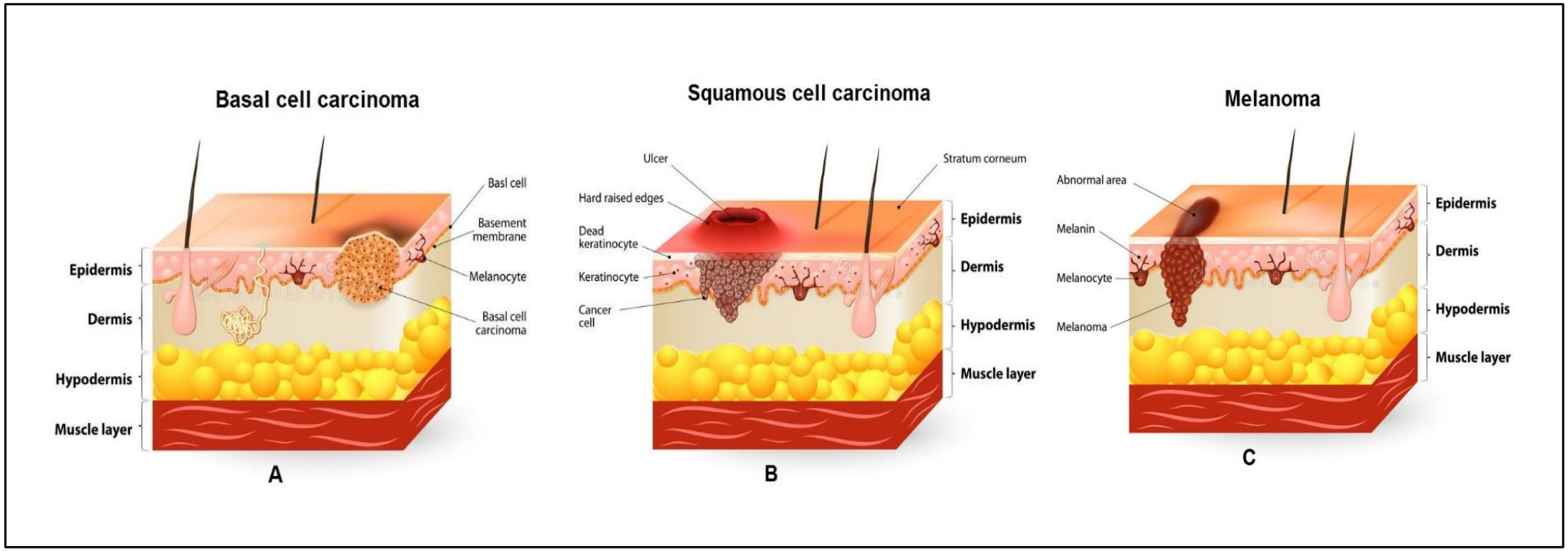

Figure 2.2: Anatomical presentation of the three major types of skin cancers. A and B representing non-melanoma skin cancers and C denoting melanoma skin cancers. (**A**) Basal cell carcinoma, presents typically with raised telangiectatic edges, it is small and translucent/pearly. (**B**) Squamous cell carcinoma, presents typically with hard raised edges, sometimes ulcerative. (**C**) Melanoma, presents typically as a discoloured and abnormal area. (Image obtained from Dreamstime. Royalty free image)

2.3.1 Non-melanoma skin cancer

Non-melanoma skin cancer (NMSC), also known as keratinocyte carcinoma, is the term primarily used to define basal cell carcinomas (BCCs) and squamous cell carcinomas (SCCs). A wide variety of additional primary cutaneous neoplasms arising from other cells present in the skin, such as Merkel-cell carcinomas, adnexal tumours and cutaneous lymphomas are also classified as NMSC, however, these entities are quite rare relative to BCCs and SCCs (Madan *et al*., 2010; Ridky, 2007).

Non –melanoma skin cancers represent the most frequent occurring form of human cancers, with an annual worldwide prevalence of 2–3 million cases. The incidence of NMSCs continues to rise despite increased public awareness efforts highlighting harmful effects of exposure to the sun (Diepgen & Mahler, 2002; D'Orazio *et al*., 2013; Madan *et al*., 2010). Key components in the pathogenesis of NMSCs are sunlight, viral infections, immune-suppression in recipients of organ transplants, genetic mutations and certain dietary factors (Ahmed *et al*, 2008).

Ultraviolet radiation (UV) from sun exposure remains the chief causative factor of NMSCs as it acts as a complete carcinogen or as a carcinogenesis promoter (Ahmed *et al*, 2008). Solar UV-radiation can be classified into three types: UV-A, UV-B and UV-C. Since UV-C is absorbed by the atmospheric ozone, ambient sunlight is predominantly only UV-A (90-95%) and UV-B (5–10%), with UV-B radiation being considered more mutagenic than UV-A radiation. UV-B radiation directly damages DNA and RNA (ribonucleic acid) by formation of covalent bonds between adjacent pyrimidines resulting in the generation of mutagenic photoproducts such as pyrimidine-pyrimidine dimers and cyclopyrimidine dimers. UV-A radiation results in indirect damage through the generation of ROS via the photo-oxidative-stress-mediated mechanism. These reactive oxidative species generate intermediates that combine with DNA to form adducts through the interaction with lipids, proteins and DNA. In order to prevent the harmful effects of these pre-mutagenic adducts, numerous complex DNA repair systems are needed (Madan *et al*, 2010). The significance of ROS is described in Section 2.5.1.

A major determinant of UV-sensitivity and skin cancer risk is skin pigmentation. The "Fitzpatrick Scale" is a semi-quantitative measure of UV-radiation and cancer risk based on six phototypes that describe skin colour by basal complexion, melanin level and inflammatory response (Table 2.1). The minimal erythematous dose (MED) is a quantitative method used to define the amount of UV-radiation (especially UV-B) required to induce sunburn in skin 24 to 48 hrs post exposure by determining oedema (swelling) and erythema (redness) as

endpoints. Individuals who are more sensitive to UV-radiation will thus have a lower MED for their skin.

Table 2.1 Fitzpatrick phenotyping scale. Numerical classification table for human skin colour as a means to estimate the response of diverse skin types to ultraviolet radiation (Adapted from D'Orazio *et al*., 2013).

Fitzpatrick phototype	Phenotype	Epidermal eumalanin	Cutaneous response to UV	MED* (mJ/cm^2)	Cancer risk
I	• Bright white unexposed skin • Typically, blue/green eyes • Easily freckling • British or Northern European	+/-	• Burns • Peels • Never tans	15-30	++++
II	• White unexposed skin • Eye colour: Blue, brown or hazel • Hair colour: red, blond or brown • Scandinavian/ European	+	• Burns easily • Peels • Minimal tanning	25-40	+++/+++
III	• Fair unexposed skin • Eye colour: Brown • Hair colour: dark • Southern or Central European	++	• Moderate burning • Moderate tanning	30-50	+++
IV	• Light brown unexposed skin • Eye colour: dark • Hair colour: dark • Asian, Latino or Mediterranean	+++	• Minimal burning • Easy tanning	40-60	++
V	• Brown unexposed skin • Eye colour: dark • Hair colour: dark • African, Latino, Native American or East Indian	++++	• Burns rarely • Easy and substantial tanning	60-90	+
VI	• Black unexposed skin • Eye colour: dark • Hair colour: dark • African or Aboriginal descent	+++++	• Virtually never burns • Ready and profuse tanning ability	90-150	+/-

*Minimal erythematous dose (MED) is described as the least amount of UV-radiation causing sunburn.

↓ MED of an individual's skin = ↑ UV sensitive.

2.3.1.1 Basal cell carcinoma

Basal cell carcinomas first described by Jacob (1827) are malignant neoplasms derived from the stratum basale, where they develop from the basal cells (Figure 2.1). BCCs account for 80% of all skin cancers and are the most frequent occurring NMSC characterised by their slow growth, non-visible pre-malignant phases and general development on the face and back of the hands (Ahmed *et al*., 2008; Haque *et al*., 2015; Lauth *et al*., 2004). BCCs may be differentiated into nodular, superficial and morpheaform subtypes. Nodular BCCs typically present as smooth and insensitive telangiectasia, commonly found on sun-exposed skin and associated with cell strands in the dermis and distinct nodules with a “pearly” appearance. Superficial BCCs present with one or more dry or scaly erythematous lesions. Another subtype of BCCs may have the appearance of thin threads of cells embedded in the supportive tissue. This type is known as morpheaform or sclerosing BCC. Additionally, a rare type of BCC can be found on the natal cleft or the lower trunk area and characterised by extended strands of basaloids linked to the superimposing epidermis. This type is known as fibroepithelloma of Pinkus (Ahmed *et al*., 2008; Haque *et al*., 2015). BCCs are rarely metastasising tumours, having a metastasis rate of <0.1%, but nevertheless are highly invasive and have the ability to cause extensive tissue damage with substantial morbidity (Ahmed *et al*., 2008; Lauth *et al*., 2004).

Lesions may appear on sun-protected skin as well as sun-exposed skin, the latter occurring more frequently. BCCs typically arise in the in the fourth decade of a patient’s life and beyond, however, exceptions can occur as with specific genodermatoss or in immune compromised patients. Patients with light skin phenotypes are particularly predisposed as sun exposure is a major factor in the development and transformation of BCCs. Although UV-radiation is by far the principal factor in the development and progression of lesions, exposure to arsenic, coal tar derivatives and irradiation are additional risk factors (Goldberg, 1996). Both BCCs and SCCs may occur as scars, ulcers, burn sites, draining sinuses and foci of chronic inflammation. Due to impaired immune surveillance of oncogenic viruses, immune compromised patients are at higher risk of BCCs because of decreased epidermal pigmentation enhancing the risk of UV-light induced oncogenic transformation or the promotion of genotype instabilities (Crowson *et al*., 1996). A variety of other lesions has been associated with BCCs in the same anatomic location, for example desmoplastic trichilemmoma (in up to 19% of reported BCC cases), warts nevi sebaceous and epidermal nevi, neurofibromata, cysts of the hair follicular derivations and pilomatricomas (Crowson, 2006).

The typical appearance of a BCC is a flesh or pearly pink coloured papule with telangiectasia. Lesions may present as translucent or somewhat erythematous, with sharp contours and a smooth margin, often with accompanied bleeding, crusting and scaling (Figure 2.2 A). Frequent ulcerations, with local destruction of the eye, ears and nasal area, are common with aggressive growth tumours (Boyd, 2004).

The architectural growth pattern is the only histologically proven prognosticator of biological BCC behaviour and thus the primary determinant of what constitutes a suitable therapeutic intervention. The differentiation patterns must be identified as part of BCCs histological spectrum and a determinant influencing differential diagnosis, as their misidentification for Merkel cell carcinomas, eccrine, follicular or sebaceous neoplasms may run the risk of over or under treatment (Crowson, 2006).

BCCs are derived from basaloid epithelia located in the follicular bulges and matrix cells, anagen hair bulbs and in specific basaloid cells of the interfollicular epidermis, (Crowson, 2006; Crowson, *et al*., 1996; Goldberg, 1996). BCCs arising in childhood originate from epithelial germ cells, whilst BCCs in adulthood arise from pluripotent progenitor epithelia (Shimizu *et al*., 1989). These neoplasms are distinct from that of adjacent epidermal basal layer epithelia, as BCCs manifest as a keratin profile resembling that of the lower part of the hair follicle and therefore are often referred to as hair-follicle-derived tumours (Crowson, 2006; Lauth *et al*., 2004).

2.3.1.2 Squamous cell carcinoma

Squamous cell carcinomas (SCCs) are the second most frequently occurring cancer in the Western world, accounting for 16% of all skin cancers. Thus, SCCs occur less frequent than BCCs in a ratio of 1:4. However, SCCs are generally more destructive neoplasms and have a substantial metastasis propensity (Ahmed *et al*., 2008; Haque *et al*., 2015; Lauth *et al*., 2004). SCCs are malignant epidermal keratinocyte tumours that regularly manifest as a wart-like growth, rough keratotic papule or a tender protrusion (fast growing, commonly with a central keratinous core) (Figure 2.2 B) (Ahmed *et al*., 2008). The head and neck are the most regularly affected areas, predominantly due to recurrent UV-radiation. As with BCCs, individuals with light skin phenotypes or immune compromised patients are at higher risk of developing a SCC (Lauth *et al*., 2004).

In contrast to BCCs, which are considered hair-follicle-derived tumours, inter-follicular epidermis (IFE) differentiation is associated with SCCs. Inter-follicular progenitor cells found in the IFE, have the capacity for accumulation of critical mutations (Lauth *et al*., 2004).

Subtypes of SCCs may be distinguished according to their diverse presentations. Atypical keratinocytes constitute the carcinoma itself, which may present in single layers or all the layers of the epidermis. Defective cornification, pale/vacuolated cytoplasm and nucleated cells in the stratum corneum (known as parakeratosis) are common presentations of SCC cells. Atypical keratinocytes are characterised by their tendency to remain within the epidermis and not penetrate into the dermis. In contrast, invasive SCCs penetrate into the dermis from the epidermis in which it originates and presents as sheets, strands and nests of atypical keratinocytes. Both parakeratosis and dyskeratosis (premature cell keratinisation of cells in the inner layers) may be present in the tumour in variable quantities. Additionally, SCCs may be further sub-divided subjected to the extent of keratinisation or differentiation (Haque *et al*., 2015). The risk of metastatic spread is considerably heightened due to increasing depth of penetration of the tumour. Generally, cutaneous SCCs have a 1% metastasising rate, however certain locations (such as the lip) have higher reported metastatic rates (Ahmed *et al*., 2008; Haque *et al*., 2015).

Additionally, squamous cell carcinomas include the pre-cancerous actinic keratosis (AK) lesions (Ahmed *et al*, 2008; Lauth *et al*, 2004). Ahmed *et al* (2008) described AK as a histologically strong tumour bordering on that of a well-distinguished SCC arising from a rapid growth phase for the first 4 to 8 weeks with the potential for self-induced regression after 3 to 6 months. AK develops because of UV-radiation inducing DNA damage and mutations. The progression of AK to SCC is due to the infiltration of AK lesions that grow or extend into the dermis from a ‘hot spot’ accumulation of small microscopically transformed cells to aggregates of keratinocytes showing qualities of atypia and pleomorphism. The typical presentation of an AK lesion is dry and/or crusty patches varying in size with a pink, red or brown appearance (Haque *et al*., 2015).

2.3.2 Cutaneous malignant melanomas

Cutaneous malignant melanomas (CMMs) are profoundly malignant tumours arising from altered melanocytes or nevus cells and account for less than 5% of all skin cancers, with a worldwide prevalence of 132 000 new cases and 65 000 deaths per year (D’Orazio *et al*., 2013; O Nestle & Kerl, 2003; Oppermann *et al*., 2005). Nonetheless, they are the most severe and progressive form of skin cancer with notorious resistance to all current modalities of cancer chemotherapy despite a vast number of clinical trials in a wide range of anticancer approaches. These approaches range from surgery to radio-, immune- and chemotherapy with an average patient survival rate of only 6 to 10 months after diagnosis (Jemal *et al*., 2002; O Nestle & Kerl, 2003; Soengas & Lowe, 2003).

The eyes and mucous membranes of the sinuses, oropharynx, anus and vagina are anatomical locations other than the skin where melanoma development may occur. UV-B radiation remains the major causative factor of malignant melanomas, especially after intense intermittent UV exposure. Individuals at the greatest risk of melanoma development are those with skin phenotypes I and II (Table 2.1) (Haque *et al.*, 2015). Suggestive clinical features of malignant melanomas (MMs) include major signs such as change in size, shape and colour of melanoma lesions; itching, bleeding or inflammation of lesions are considered as minor signs of MMs. High risk lesions include those that meet the ABCDE criteria of asymmetry, border abnormality, colour variation, diameter >6 mm and growing (Figure 2.2 C) (Mangas *et al*, 2010; Weiner & Yoon, 2010).

All primary MMs begin with melanocyte proliferation at the epidermal-dermal junction, become invasive as atypical melanocytes and migrate into the dermis individually or as aggregates. The stage classification of MM progress is as follows: Stage I and II are characterised by localised tumours that are confined to the skin; Stage III MM is tumours that undergo metastasis and/or lymph node involvement; MMs in which the metastasis spread to other organs or distant lymph nodes are classified as Stage IV MMs (Haque *et al*, 2015). Primary CMMs can be categorised into four sub-groups: superficial spreading melanoma (70%), nodular melanoma (15%), acral lentiginous melanoma (10%) and lentigo malignant melanoma (5%) (Weiner & Yoon, 2010). The presentation and preference sites of each of the CMM sub-groups are summarised in Table 2.2.

Table 2.2 The typical presentation of CMM sub-groups with their preference sites (Adapted from Weiner & Yoon, 2010)

CMM sub-group	Presentation	Preference sites
Superficial spreading melanoma	• Papule or • Nodule	• Men: backs • Women: backs and legs
Nodular melanoma	• Dark blue/black papule or • A rapid developing nodule	• Head • Neck • Trunk More commonly found in men
Acral lentiginous melanoma	• Brown to black macules with colour variations and asymmetrical edges • May also present as nodules or papules	• Palms • Beneath the nail bed • Soles A common type in individuals with dark complexions
Lentigo maligna melanoma	• Large, asymmetrically shaped papules or macules with tan, brown or black pigment variations • A nodular or popular component may ultimately develop	• Sun damaged skin (particularly the face and forearms) Occurs typically in the elderly

Malignant melanoma prognosis would be auspicious if detected at very early stages of the disease, i.e. before the malignant melanoma becomes intrusive. Regrettably, melanoma lesions remain asymptomatic or unnoticeable for prolonged periods before diagnosis. Furthermore, metastatic melanoma cells tend to disseminate to multiple organs (including brain, bone, liver and lungs) as it is seldom limited to single foci, rendering treatment strategies challenging as opposed to NMSCs which often remain at the site of origin (Soengas & Lowe, 2003). Additionally, treatment options are very limited. The only two United States Food and Drug Administration (FDA) approved drugs for metastatic melanoma treatment are decarbazine and interleukin-2, both of which have low response rates of 6.8% and 12.0% respectively (O'Day *et al*., 2009). Melanoma is potentially curable when diagnosed and surgically removed whilst located in the outermost skin layer. However, prognosis is poor with deeper lesions and metastasis with 6 to 9 months expected median survival for patients with stage IV metastatic melanoma (Kirshner *et al*., 2008).

2.4 Current therapeutic modalities

Lesion size, location and shape as well as patient age are the determining factors for local therapeutic intervention of NMSCs. Currently the main treatment approaches include radiotherapy and surgery (Haque *et al*, 2015). As SCCs tend to be more aggressive and have a higher propensity for metastasis development, lymph node dissection is often considered (McGuire *et al*., 2009). Other treatment strategies include oral chemotherapy with cisplatin and retinoids, topical chemotherapy with imiquimod, retinoids, sodium diclofenac and fluorouracil (FU), photodynamic therapy and laser surgery (Haque *et al*., 2015; Telfer *et al*., 2008).

Malignant melanoma treatment is dependent on the stage of the cancer. Treatment approaches range from surgery to chemo-, immune-, targeted- and radiotherapy. However, the primary treatment option is surgery. Immuno-modulators such as ipilimumab, the Bacillus Calmette-Guérin (BCG) vaccine and cytokines (interleukin-II and interferon-alpha) are often used to boost patient immune response (Haque *et al*, 2015; Simões *et al*., 2014).

Surgical excision is currently the standard treatment for skin cancers. However, not all patients, especially those with NMSCs, can be treated in this manner and therefore alternative treatment options must be considered (D'Orazio *et al.*, 2013). In addition, poor cosmetic outcome is a frequent result of such techniques. Topical chemotherapy, including use of imiquimod, has become an important alternative for patients who cannot be treated by surgical excision. Other reagents for topical chemotherapy include 5-fluorouracil, sodium diclofenac and ingenol mebutate. Still, the treatment period required for these preparations are extensive,

some for up to 90 days; the high recurrence rate of 33–54% as well as high treatment costs are also a concern. This failure in therapy, reinforces the need for the development of novel non-invasive topical therapies (D'Orazio *et al.*, 2013; Haque *et al*., 2015; Madan *et al*., 2010; Simões *et al*., 2014).

2.5 Novel approach to melanoma treatment

Unfortunately, the occurrence of severe adverse side effects and emergence of drug resistance often hamper established chemotherapy treatment currently available for tumours, warranting the development of less toxic agents, which retain activity against otherwise chemo-resistant cancer cells (Efferth *et al*., 2001). Breakthroughs in chemotherapeutic intervention have been achieved in certain areas including urogenital oncology targeting testicular cancer and paediatric oncology targeting childhood leukaemia where remarkable survival rates are currently attained. Nonetheless, only marginal advances have been made in treatment of other important malignancies, such as metastatic melanoma, glioblastoma and pancreatic carcinoma, where no effective chemotherapeutic options are presently available. Patient survival following diagnosis is regularly measured in months (Wondrak, 2009).

Reactive oxygen species have emerged as potential targets for anticancer drug discovery. ROS mediate cellular oxidative stress and redox dysregulation involved in initiation and progression of cancer. The causative involvement of redox alterations in tumour progression has been extensively researched and well documented, particularly in metastatic melanoma and pancreatic carcinoma (Wondrak, 2009). Selective targeting by redox chemotherapeutics, such as redox modulators and direct- and indirect-acting pro- and antioxidants, represents a promising approach to cancer therapy by exploiting cancer cells' particular vulnerability to inherently elevated cellular oxidative stress levels and dependence on antiapoptotic and mitogenic ROS signalling (Das, 2015; Wondrak, 2009).

Utilisation of agents typically used for diseases other than cancer has attracted much attention for chemotherapy treatment of skin cancer. Artemisone is an example of such an agent. Artemisone, an artemisinin derivative, is a well-established antimalarial agent, yet, an influx of studies and data have emerged displaying its therapeutic value beyond malaria, including anticancer properties. (Ho *et al*., 2014). Gravett *et al*. (2011) indicated that artemisone may exhibit anti-cancer effects through cancer cell cycle disruptions by apoptosis induction, consequently hindering disease progression. In addition, artemisone enhanced anti-proliferation effects when in combination with established anti-cancer agents. (Gravett *et al*., 2011). Another possible antitumour mechanism of action involves the generation of ROS

formation to induce oxidative stress resulting in apoptosis and cell death (Crespo-Ortiz & Wei, 2012).

Efferth (2017) suggested that artemisinin-type drugs should be used as part of combination therapy rather than monotherapy when applied in clinical oncology. The antineoplastic activity of artemisone could add independent anticancer action with no/reduced side effects when used in combination therapy (Das, 2015). Combinations of established or investigatory agents (like artemisinin-type drugs) with novel synthetic compounds have gained much interest in cancer therapeutics (Efferth, 2017). One example of such a novel synthetic compound is elesclomol, a small investigatory drug that selectively induces apoptosis in cancer cells through elevating ROS levels resulting in oxidative stress (Nagai *et al*., 2012; Qu *et al*., 2009).

2.5.1 Redox balance in skin cancer

Reactive oxygen species (ROS) are continually generated in response to environmental stimuli and intracellular metabolism. For most cells, the major source of ROS is via the mitochondrial respiratory chain and excessive ROS production is involved in apoptosis of cells. In general, ROS is released by neutrophils as defence molecules to destroy exogenous pathogens such as bacteria. In signal transduction, they can also act as secondary messengers. However, physio-pathological changes, including cell cycle disruptions, apoptosis and necrosis, can result from excessively high oxidative stress and weakened antioxidative defence damaging macromolecules essential for cellular functions (Qu *et al*., 2009).

A novel approach to target cancer cell destruction selectively by modulating ROS levels has been proposed. The collective term ROS refers to the chemical species that are generated as by-products of normal oxygen metabolism and includes hydrogen peroxide, the hydroxyl radical and superoxide anion. ROS production in normal cells are low due to the effective neutralisation by the potent antioxidant system of the cells opposed to cancer cells that generate elevated ROS levels. Excessive ROS levels generated and maintained in cancer cells compared to normal cells are partially due to increased metabolic activity, initiation of proliferative signalling pathways, and mitochondrial DNA mutations, resulting in defects in the electron transport chain, which ultimately leads to a state of chronic oxidative stress (Kirshner *et al*., 2008; Qu *et al*., 2009). Carcinogenesis and cancer progression are promoted by elevated ROS levels through DNA damage that amplifies genomic instability, and through redox modulation of key regulatory proteins, which directly stimulate tumour promoting signalling pathways. Through signalling pathways, activation that stimulates proliferation and transformed phenotype maintenance, oxidative stress promotes growth advantages in cancer

cells. In contrast to ROS's tumour promoting abilities, induction of cell cycle arrest and apoptosis may result from excessive ROS levels beyond the cells' antioxidant capacity (Kirshner *et al*., 2008). Thus, due to already elevated ROS levels, cancer cells are particularly vulnerable to agents that can further raise ROS levels to a critical point resulting in the initiation of apoptosis, whereas with low production of ROS and high antioxidant capacity, normal cells have reduced sensitivity to oxidative stress inducing agents. Therefore, targeting oxidative stress in cancer cells represents an innovative class of anticancer therapeutics for solid tumours (Kirshner *et al*., 2008; Qu *et al*., 2009).

2.5.2 Artemisone

Artemisia annua L (qinghao, sweet wormwood or annual wormwood) is an indigenous plant historically used in Chinese traditional remedies for its antipathogenic properties (Gravett *et al.*, 2011; Klayman, 1985). Earliest mentions of qinghao's medicinal value includes treatment of haemorrhoids (found on a piece of unearthed silk from the Mawangdui Han dynasty tomb, 168 B.C) and fever (written in 340 A.D, the author of Handbook of Prescriptions for Emergency Treatments, Ge Hong, advised one handful of qinghao should be soaked in 1 L of water, strained then swallowed) (Klayman, 1985; Liu, 2017). It was only in 1972 when the antimalarial principal qinghaosu (now generally known as artemisinin) was first isolated by Chinese scientist Professor You-You Tu, who was awarded the 2015 Nobel Prize in Physiology and Medicine for her discovery (Gravett *et al.*, 2011; Liu, 2017; Zhang, 2016). Despite artemisinin's efficacy, pharmacokinetic limitations occurred, such as low oil/water solubility, limited bioavailability and a short half-life *in vivo*. To overcome some of these problems, the prototype artemisinin has been structurally modified leading to the establishment of various derivatives, collectively known as artemisinins (Crespo-Ortiz & Wei, 2012; Gravett *et al.*, 2011; Meshnick *et al.* 1996). Today artemisinins are the most potent and rapidly acting antimalarial agents used as a component in first-line treatment for malaria recommended by the World Health Organization (WHO) (Gravett *et al.*, 2011; Haynes *et al.,* 2006*;* Krishna *et al.*, 2008).

Artemisone is a newer artemisinin derivative, which has become more popular as a therapeutic candidate with good efficacy and tolerability. Furthermore, artemisone exhibits an improved pharmacokinetic profile, including increased activity against *Plasmodium falciparum* with sustained activity in plasma (in contrast to other derivatives), improved bioavailability and metabolic stability, longer half-life (*in vivo*) and neglectable neurotoxicity (Das, 2015; Gravett *et al.*, 2011; Haynes *et al.*, 2006).

2.5.2.1 Artemisone – therapeutic value beyond antimalarial activity

Artemisinins are currently well-established agents for treating malaria, including highly resistant strains (Krishna *et al.*, 2008). With its established safety profile in millions of malarial patients, artemisinins have been submitted to studies investigating other therapeutic uses (Ho *et al.*, 2014; Krishna *et al.*, 2008). Accumulating evidence collaborates that artemisinins display activity in various *in vitro* and/or *in vivo* disease models of infection, inflammation, allergic disorders, autoimmune disease and cancer (Figure 2.3) (Ho *et al.*, 2014; Krishna *et al.*, 2008; Zhang, 2016).

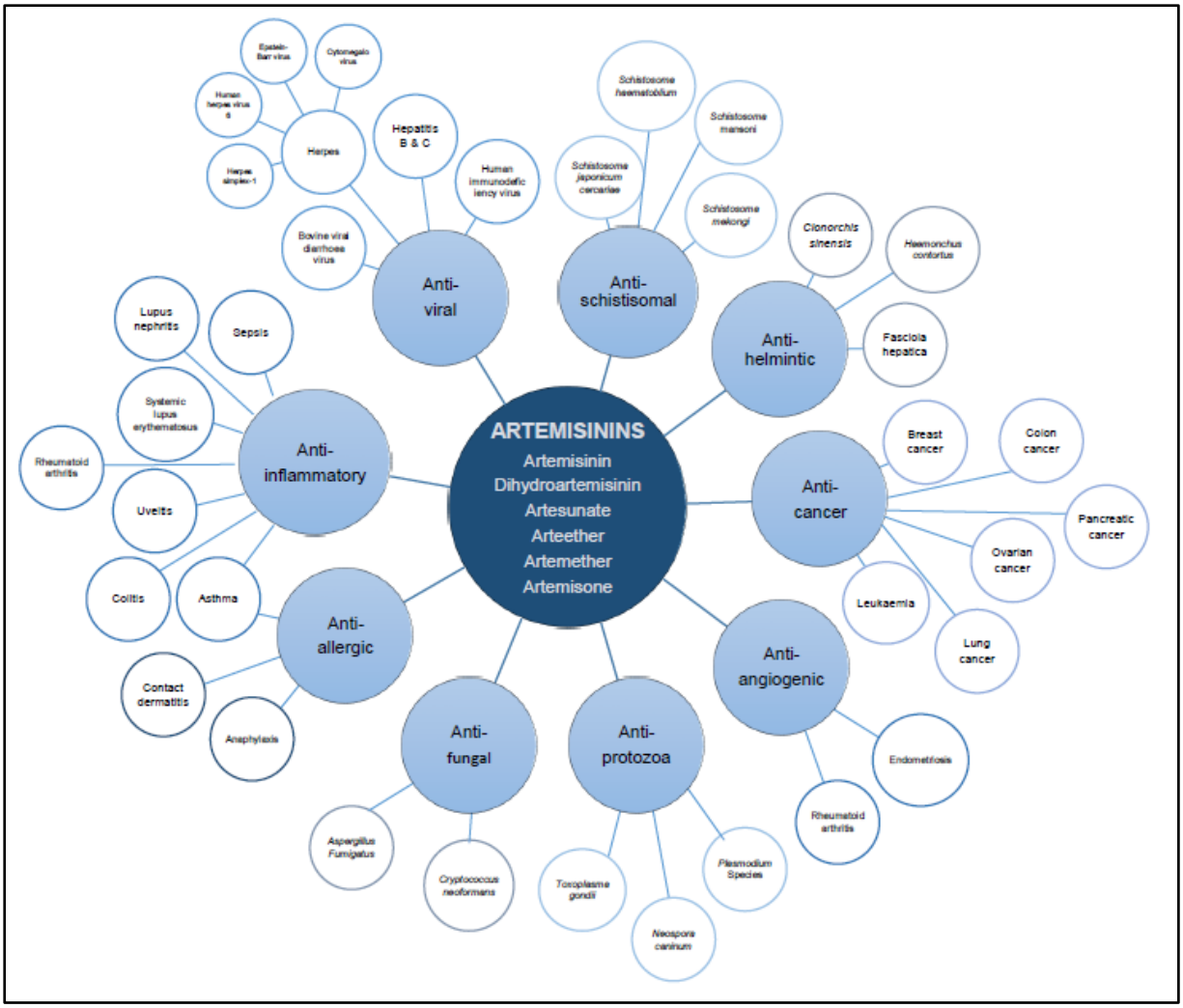

Figure 2.3: Bubble map outline of artemisinins diverse biological activities and potential clinical application in various diseases. Solid circles signify different biological activities, and transparent circles denote potential application of corresponding biological activities to various human diseases. (Adapted from Ho *et al*., 2014)

The antiviral activity of artemisinins is attributed to the inhibitory effects against double-strained deoxyribonucleic acid (DNA) herpes viruses, including herpes simplex virus, cytomegalovirus and Epstein-Barr virus (Efferth *et al.*, 2008; Ho *et al.*, 2014). Romero *et al.* (2005) showed artemisinins to have synergistic effects when in conjunction with lamivudine (established antiviral) against the hepatitis B virus.

In an *in vivo* murine model of toxoplasmosis, artemisone suppressed the *Toxoplasma gondi* parasite replication and reduced mortality (Dunay *et al.*, 2009). Furthermore, D'Angelo *et al.* (2009) showed that artemisinins have the ability to inhibit multiple steps of *Toxoplasma gondi's* lytic cycle, demonstrating therapeutic potential for human *Toxoplasmosis* prevention and treatment.

Due to their favourable safety profile and potent pharmacological actions, artemisinins have been investigated in an array of inflammatory diseases such as autoimmune diseases (rheumatoid arthritis, systemic lupus erythematosus and inflammatory bowel disease), allergic inflammation (dermatitis, allergic- anaphylaxis and asthma) and septic inflammation. In the early 1980s, artesunate was first discovered to hold immunosuppressive effects displayed by *in vitro* inhibition of mitogen-stimulated mouse spleen cells and human peripheral lymphocytes (Ho *et al.*, 2014; Shen *et al.*, 1984).

In recent years, the artemisinins demonstrated anticancer properties due to their ability to reduce cell numbers in multiple solid tumours *in vitro* and *in vivo*. Multiple potential mechanisms of its anticancer actions have been identified, including induction of cell cycle arrest, pro-apoptotic, antiangiogenetic, antiproliferation and antimigratory and metastasis inhibition (Gravett *et al.*, 2011; Zhang, 2016).

Thus, artemisinins are a group of potent bioactive molecules with a variety of biological activities surpassing anti-malarial actions, which include antiviral, anti-parasitic, antiprotozoal, antifungal, anti-inflammatory and anticancer, as summarised in Figure 2.3.

2.5.2.2 Artemisone – From antimalarial to anticancer agent

In the malaria parasite, the antimalarial mechanism of artemisinin's action is attributed to transport protein interference, parasitic mitochondrial function disruptions and immune function modulation, angiogenesis inhibition and early stage inhibition of parasite development that have invaded red blood cells (Haynes & Krishna, 2004; Liu, 2017). The endoperoxide moiety of artemisinins has been reported as pharmacologically significant and an absolute requirement for antimalarial activity (Crespo-Ortiz & Wei, 2012; Das, 2015; Haynes & Krishna, 2004). It is postulated that this endoperoxide bond is activated by reduced haem or ferrous

iron resulting in cytotoxic carbon-centred radicals (highly alkylating agents). Essential parasite macromolecules are targeted by these radicals triggering parasitic death, possibly via alkylation (Crespo-Ortiz & Wei, 2012; Das, 2015). However, the precise mode of action and principal target of artemisinin remains controversial and under study (Gravett *et al.*, 2011; Meshnick, 2002).

Artemisinins have also been investigated as anticancer agents. The rationale is that both cancer cells and malaria parasites contain high concentrations of free iron. As with malaria, carbon-centred free radicals are generated through haem/iron-mediated decomposition of the endoperoxide bridge. The formation of free radicals has been hypothesised to trigger cell death (Lai *et al.*, 2012; Meshnick, 2002). These radicals (superoxide anions and hydroxyl radicals) are formed in response to the formation of ROS to induce cellular damage through the induction of direct oxidative stress to cancer cells (Ho *et al.*, 2014). Other potential mechanisms have been identified by which artemisinins can act against cancer cells. They have shown to be pro-apoptotic and antiproliferative. Other modes of action include the inhibition of metastasis/invasion (of malignant cells to other organs), angiogenesis- and growth inhibition (Crespo-Ortiz & Wei, 2012; Efferth *et al*., 2001; Gravett *et al.*, 2011; Liu, 2017).

Artemisinin's anticancer effects were reported as early as the 1980s and 1990s. An *in vitro* study showed artesunate resulted in a >63% reduction in proliferation of human leukaemia cells (Shen *et al.*, 1984). Woerdenbag *et al*. (1993) described the cytotoxicity of artemisinins in 1993 on Ehrlich ascites tumour cells (*in vitro)* and since then, a wealth of studies on artemisinins as anticancer agents have emerged (Crespo-Ortiz & Wei, 2012; Gravett *et al.*, 2011). The semi-synthetic artemisinin, artesunate, was analysed by Efferth *et al.* (2001) for its anticancer activity against 55 cancer cell lines (*in vitro*) in collaboration with the Developmental Therapeutics Program of the National Cancer Institute, USA. Artesunate displayed inhibitory activity against leukaemia, colon, breast, central nervous system and melanoma cancer cells (among others), being most active against leukaemia and colon cancer cell lines, typically resistant cell lines. Furthermore, activity was displayed in molar ranges comparable to those of established antitumour agents and no cross-resistance in drug-resistant cell lines was observed (Efferth *et al*., 2001).

One newer artemisinin derivative, artemisone has emerged as a notable therapeutic candidate for cancer therapy owing to its improved pharmacokinetic profile, including longer half-life and reduced toxicity in comparison to other artemisinins (Crespo-Ortiz & Wei, 2012; Das, 2015). Gravett *et al.* (2011) showed artemisone effective against several cancer cell lines including melanoma, colon, breast and pancreatic cancers. Artemisone exhibited a dose dependant decline in cell number and arrest in cell cycling, as well as a consistent superiority to

artemisinin, with half the maximal inhibitory concentrations (IC_{50}), which is notably lower in comparison to artemisinin (Gravett *et al.*, 2011).

2.5.2.3 Cancer combination therapy with artemisone

Drug combination therapy is a general practice used to treat many infectious diseases such as tuberculosis, the human immunodeficiency virus and malaria and the general principle applies to cancer treatment as well (Cui & Su, 2009). Artemisinins are well established in drug combination therapies for drug-resistant malaria treatment, thus, artemisinin-type drugs to be used in oncology ought to be (with a high probability) part of combination therapy protocols rather than monotherapy (Efferth, 2017; Krishna *et al.*, 2008). Principles pertaining to combination therapy protocols with established anticancer agents, would also apply for artemisinin-type drug combinations, that is (1) combining drugs with diverse modes of action and targets to prevent development of resistance; (2) minimise the occurrence of severe and fatal toxicities through dispersion of adverse effects to various tissues in the body; (3) each component of the combination therapy is required to exhibit anticancer activity.

An array of results has been published in literature in recent years on the addition or synergistic combinations of artemisinins with other compounds to enhance tumour growth inhibition in various cell lines and animal experiments (Efferth, 2017). Such effects were shown in a study with artemisone in combination with common anticancer drugs gemcitabine, oxaliplatin and thalidomide on several cell lines including melanoma. Enhanced activity was observed in each of the combinations with artemisone, all resulting in cell cycle arrest. Furthermore, the antiproliferative effect of artemisone was heightened in combination with the other drugs, whereas combinations with artemisinin displayed antagonistic properties (Gravett *et al.*, 2011). These synergistic effects of artemisone-drug combinations promote the potential clinical utility of artemisinin-type therapeutic combinations in melanoma therapy.

Combination therapy with novel synthetic compounds has become an appealing alternative to standard chemotherapy combinations, with drugs such as doxorubicin, gemcitabine, oxiplatin and thalidomide. An important part of anticancer drug development lies in the synthesis of novel cytotoxic compounds to be used in combination therapy (Efferth, 2017). Elesclomol is an example of a novel synthesis molecule that can be utilised for combination therapy with artemisone for melanoma treatment. The rationalisation for this potential drug combination rests on both artemisone and elesclomol's ability to generate ROS levels (beyond a critical threshold), thus inducing cellular damage/death (Ho *et al.*, 2014; Kirshner *et al*., 2008).

2.5.3 Elesclomol

Elesclomol is a novel anticancer candidate drug, derived from a phenotypic screen for small molecules, which exhibits potent apoptotic activity. Elesclomol has been evaluated in a selection of clinical trials and displayed anticancer activity against a broad range of cancer cell lines. Elesclomol was found to be well tolerated with a prolonged progression-free survival (PFS) time, and enhanced the efficacy of chemotherapeutic agents when in combination (Kirshner *et al*., 2008; Nagai *et al*., 2012). This was seen in a Phase III clinical trial for patients with advanced melanoma, where the anticancer activity of an elesclomol-paclitaxel combination was enhanced compared to paclitaxel alone. The combination also yielded a doubling median PFS and a 41.7% risk reduction for disease progression/death (O'Day *et al*., 2009).

Elesclomol displays anticancer activity through the generation of ROS inducing cell cycle arrest and activation of apoptosis (Kirshner *et al*., 2008; Nagai *et al*., 2012). Apart for the prevailing role of mitochondria during cellular energy production, mitochondria are also critical regulators of apoptosis. Cancer cells' mitochondria are structurally and functionally altered from those of normal cells, and thus are able to control the activation of apoptotic effector mechanisms. Altered redox status and elevated ROS levels are typically seen in the mitochondria of cancer cells. A promising approach for cancer therapy (as previously stated) involves the disruption of redox homeostasis and increasing ROS levels beyond the threshold compatible with cellular survival (Nagai *et al*., 2012).

The first-in-class investigatory drug, elesclomol, exerts anticancer action through the selective mitochondrial ROS induction. Consequently, activation of apoptosis through oxidative stress is achieved (Nagai *et al*., 2012; Yadav *et al*., 2013). Elesclomol-induced ROS production is contingent on chelation and redox cycling of copper (Cu) within the mitochondria. This drug chelates copper outside of cells, which in turn facilitates its uptake into cells as Cu(ll)-elesclomol complexes. The complexes rapidly and selectively transport copper into the mitochondria of cells where Cu(II) is reduced to Cu(I) resulting in ROS generation. Reduction of Cu(II) to Cu(I) within the mitochondria is a fundamental requirement for elesclomol's anticancer activity, as elesclomol alone exhibits no discernible activity in the absence of copper. Continued copper accumulation within the mitochondria is resultant of continued shuttling of elesclomol-copper complexes causing a state of oxidative stress (Blackman *et* al., 2012; Nagai *et al*., 2012).

This distinct characteristic of elesclomol displayed by mitochondrial selectivity is unique to the compound and not shared by other chelators, including disulfiram (Nagai *et al*., 2012). The

selective mitochondrial ROS induction and anticancer enhancing effects of elesclomol when in combination with other agents, represents a potential approach to anticancer therapy and an appealing candidate for combination therapy with other ROS inducing agents, such as artemisone.

2.5.4 Lipid excipients

Literature documents the lack of efficient and effective skin cancer treatment, and how current therapies are insufficient in meeting the needs of patients, and focus is on the development of new therapeutic agents. Besides the urgent need for new agent development in skin cancer, innovative approaches for drug delivery must also be considered (Efferth *et al*., 2001; Zhao *et al*., 2009).

Current treatment options for skin cancer may include modalities such as cryosurgery, electrodessication, systemic chemotherapy and chemical peeling (McGillis & Fein, 2004; Sonavane *et al*., 2012). The emergence of severe side effects and extensively long treatment times are associated with some of the previously mentioned modalities (Haque *et al*., 2015). Cryosurgery and electrodessication represent the primary treatment options for skin cancer. Granted, surgery is effective in treating selected skin cancers but it's worth has been hampered by the fact that not all patients are good surgical candidates (elderly for example), extended postoperative recovery times, high costs to patients and its potential side effect profile, including scarring and pigment alterations (McGillis & Fein, 2004). Consequently, topical/transdermal drug delivery using lipid excipients has become an attractive alternative for therapy of certain skin cancers (Haque *et al*., 2015).

2.5.4.1 Topical and transdermal drug delivery

The skin provides a remarkable surface area for molecular transport providing several advantages over some conventional preparations, such as oral dosage forms when formulated in topical and transdermal drug delivery systems (Naik *et al*., 2000). These advantages include:

- The skin provides a large and readily accessible surface area for drug absorption (Naik *et al*., 2000);
- The application of these systems is non-invasive, can be self-administered and generally inexpensive, thus improving patient compliance (Prausnitz & Langer, 2008).
- Sustained drug release may be obtained, beneficial for API's with short biological half-lives ((Naik *et al*., 2000; Prausnitz & Langer, 2008).
- Premature drug metabolism during the first-pass effect of the liver is prohibited (Prausnitz & Langer, 2008).

- Controlled input kinetics of transdermal systems for drugs with narrow therapeutic indexes (Naik *et al*., 2000).
- Reduction of systemic side effects (Guy, 1996).

Topical and transdermal drug delivery has a reputable role in the management of specific skin cancers, principally due to improved skin appearance and quality of life for patients. Current skin cancer chemotherapy used in topical/transdermal drug delivery includes retinoids, 5-fluorouracil, diclofenac and imiquimod. Conversely, some of these preparations are likely to exacerbate the condition being treated and treatment times are often overly long (Haque *et al*., 2015). In recent years, transdermal delivery systems have made a noticeable contribution to medical practices, however its full potential as an alternative to oral and other delivery systems has yet to be fully achieved (Prausnitz & Langer, 2008). Furthermore, Haque *et al.* (2015) mentions the lack of new emerging chemical entities for topical management of skin cancers.

Topical drug delivery is preferred to transdermal (and regional) delivery since it provides a protective and emollient function as well as delivering the therapeutic agent(s) to employ a local effect when applied to the skin (Garg *et al*., 2015). Topical chemotherapy is a method of drug delivery through the direct application of an anticancer drug formulation to the skin, usually in the form of a cream or an ointment (American Cancer Society, 2016). Topical drug delivery is primarily used to confine a pharmacological effect of a drug to the skin's surface or within the skin (Garg *et al*., 2015).

2.5.4.2 Lipid-based drug delivery

Pharmaceutical excipients (additives) are non-drug components used as inactive constituents for structuring dosage forms, mainly used to control the extent of absorption, improve stability and organoleptic properties, and maintain viscosity of the formulation. Ideal features or properties of excipients include: (1) non-toxic qualities; (2) they are commercially available at a quality grade; (3) affordable; (4) chemically and physically stable (Garg *et al*., 2015).

A promising concept for drug delivery using lipid excipients has gained significant importance due to their safety and efficiency profile. Lipid-based drug delivery systems (LBDDS) have the potential to provide time controlled delivery and improve the solubility and bioavailability of poorly soluble drugs. This type of formulation may be used in a wide range of pharmaceutical applications including topical, oral, parenteral and pulmonary delivery (Shrestha *et al*., 2014). Lipid excipients currently used may include fatty acids (e.g. oleic acid), monoglycerides (e.g. stearic acid), diglycerides (e.g. glycerol behenate), triglycerides (e.g. tristearin), steroids (e.g. cholesterol) and waxes (e.g. cetyl palmitate). These lipid excipients are also typically used in

solid lipid nanoparticle delivery systems that similarly possess the potential to enhance bioavailability and controlled site-specific drug delivery of an active pharmaceutical ingredient (Kalepu *et al*., 2013).

The lipid excipients chosen for this study are oleic acid, stearic acid and cholesterol. These lipids were chosen for their potential to improve solubility and bioavailability of agents used in LBDDS. Additionally, these lipids can be used in a broad range of formulations for diverse routes of administration, including the topical route (Shrestha *et al*., 2014).

2.5.4.3 Anticancer potential of lipid excipients

Typically, excipients exert little to no therapeutic value (Garg *et al*., 2015). However, certain lipid excipients have shown anticancer activity through ROS generation and apoptosis induction, for example oleic acid (Hatanaka *et al*., 2013; Schröter *et al*., 2015). Numerous investigations have reported the beneficial effects of oleic acid in cancer progression; herein, oleic acid induced cell proliferation inhibition in various cancer cell lines. Oleic acid was shown to suppress over-expression of human epidermal growth factor receptor 2, a well-known oncogene involved in the aetiology, invasive progression and metastasis in numerous human cancers, and displayed a potential role in intracellular calcium signalling pathways related to proliferation occurrence. It has been shown to induce apoptosis in cancer cells resulting in cell death, potentially resulting in increased intracellular ROS production or caspase 3 activity (Carrillo *et al*., 2012). In addition to its anticancer properties, oleic acid derived from olive oil in dietary-drug combinations has the potential to yield additives of synergistic protections against cancer progression (Schwartz *et al*., 2004). In other studies, oleic acid was described to act synergistically with cytotoxic drugs, resulting in an enhanced antitumor effect (Carrillo *et al*., 2012).

Lipids other than oleic acid used as pharmaceutical excipients, have displayed similar anticancer potential through ROS generation. Stearic acid, as stearic acid grafted chitosan oligosaccharide (CSO-SA) and beta-eleostearic acid (β-ESA, stearic acid isomer), exhibited cytotoxicity against human lung and bladder carcinoma cells, respectively, via excessive ROS production resulting in oxidative stress and the induction of apoptosis (Hu *et al*., 2012; Sun *et al*., 2012).

Another lipid excipient of interest is cholesterol. As with oleic acid and stearic acid, cholesterol likewise possesses the ability to generate ROS. In contrast to oleic and stearic acid's anticancer promoting effects through ROS generation resulting in apoptosis induction, elevated serum cholesterol levels are related to an increased risk of certain cancers, for

example colorectal adenoma and colorectal cancer (Wang *et al*., 2017). A study conducted by Wang *et al*. (2017) showed colorectal cancer progression was enhanced by cholesterol via ROS elevation. Interestingly, in another study, cholesterol crystals neither exhibited cytotoxic effects nor influenced the proliferation of human leukemic monocyte cells (Kotla *et al*., 2017). This unique quality of cholesterol to induce ROS production, resulting in diverse effects on various cancer cells, could hold a potential in chemotherapy and further evaluation of cholesterol's potential toxicity should be explored.

2.6 Summary

Taking past findings into consideration, this current study focuses on the combination therapy of the antimalarial drug artemisone, the novel investigatory molecule elesclomol and lipid excipients (oleic acid, stearic acid and cholesterol) as a potential new approach to anticancer treatment for skin cancer. Each component possesses the potential to generate ROS and in doing so, induce apoptosis resulting in cancer cell death. However, one component alone may not elevate ROS levels sufficiently over the critical threshold. By combining these three agents, ROS may potentially be generated over the critical threshold, leading to excessive oxidative stress and apoptosis induction and ultimately, cancer cell death.

2.7 References

Ahmed, A.H., Soyer, H.P., Saunders, N., Boukamp, P. & Roberts, M.S. 2008. Non-melanoma skin cancers. *Drug Discovery Today: Disease Mechanisms*, 5(1):e55–e62.

American Cancer Society. 2016. Local treatment other than surgery for basal and squamous cell skin cancers. https://www.cancer.org/cancer/basal-and-squamous-cell-skin-cancer/treating/other-than-surgery.html Date of access: 14 March 2017.

American Cancer Society. 2017. Cancer facts & figures 2017. Atlanta: American Cancer Society. https://www.cancer.org/content/dam/cancer-org/research/cancer-facts-and-statistics/annual-cancer-facts-and-figures/2017/cancer-facts-and-figures-2017.pdf Date of access: 2 Nov. 2017.

Apalla, Z., Nashan, D., Weller, R.B. & Castellsagué, X. 2016. Skin cancer: epidemiology, disease burden, pathophysiology, diagnosis, and therapeutic approaches. *Dermatology and Therapy,* 7(1):5–19.

Bianchi, J. & Cameron, J. 2008. Assessment of skin integrity in the elderly. *British Journal of Community Nursing*, 13(3):S26.

Blackman, R.K., Cheung-Ong, K., Gebbia, M., Proia, D.A., He, S., Kepros, J., Jonneaux, A., Marchetti, P., Kluza, J., Rao, P., Wada, Y., Giaever, G. & Nislow, C. 2012. Mitochondrial electron transport is the cellular target of the oncology drug elesclomol. *Plos One*, 7(1):e29798.

Bos, J.D. & Meinardi, M.M.H.M. 2000. The 500 dalton rule for skin penetration of chemical compounds and drugs. *Experimental dermatology*, 9(3):165–169.

Boyd, A.S. Tumours of the epidermis. (*In* Barnhill, R. & Crowson A.N., *ed*. Textbook of Dermatopathology. McGraw-Hill: New York. P.575–634.)

Carrillo, C., Cavia, M.A. & Alonso-Torre, S.R. 2012. Antitumor effect of oleic acid; mechanisms of action; a review. *Nutricion Hospitalaria*, 27(6):1860–1865.

Crespo-Ortiz, M. & Wei, M.Q. 2012. Antitumor activity of artemisinin and Its derivatives: from a well-known antimalarial agent to a potential anticancer drug. *Journal of Biomedicine and Biotechnology,* 2012(2012):247597.

Crowson, A.N. 2006. Basal cell carcinoma: biology, morphology and clinical implications. *Modern Pathology*, 19(2006):s127–s147.

Crowson, A.N., Magro, C.M., Kadin, M.E. & Stranc, M. 1996. Differential expression of the bcl-2 oncogene in human basal cell carcinoma. *Human Pathology*, 27(4);355–359.

Cui, L. & Su, X. 2009. Discovery, mechanisms of action and combination therapy of artemisinin. *Expert Review of Anti-infective Therapy*, 7(8):999–1013.

D'Angelo, J.G., Bordón, C., Posner, G.H., Yolken, R. & Jones-Brando, L. 2009. Atremisinin derivatives inhibit *Toxoplasma gondi in vitro* at multiple steps in the lytic cycle. *Journal of Antimicrobial Chemotherapy,* 63(1):146–150.

Das, A.K. 2015. Anticancer effect of antimalarial artemisinin compounds. *Annals of Medical and Health Sciences Research,* 5(2):93–102.

Diepgen, T. & Mahler, V. 2002. Epidemiology of skin cancer. *British Journal of Dermatology*, 146(61):1–6.

D'Orazio. J., Jarrett, S., Amaro-Ortiz. A. & Scott. T. 2013. UV radiation and the skin. *International Journal of Molecular Sciences,* 14(6):12222–12248.

Dunay, I.R., Chan, W., Haynes, R.K. & Sibley, L.D. 2009. Artemisone and artemiside control acute and reactivated toxoplasmosis in a murine model. *Antimicrobial Agents and Chemotherapy*, 53(10):4450–4456.

Eckert, R.L. 1992. The structure and function of skin. (*In* Mukhtar, H., *ed*. Pharmacology of the skin. Boca Raton: CRC Press. P.4–9).

Efferth, T. 2017. Cancer combination therapies with artemisinin-type drugs. *Biochemical Pharmacology* (In press).

Efferth, T., Dunstan, H., Sauerbrey, A., Miyachi, H. & Chitambar, C.R. 2001. The anti-malarial artesunate is also active against cancer. *International Journal of Oncology,* 18(4):767–773.

Efferth, T., Romero, M.R., Wolf, D.G., Stamminger, T., Marin, J.J.G. & Marschall, M. 2008. The antiviral activities of artemisinin and artesunate. *Clinical Infectious Diseases,* 47(6):804–811.

Elias, P.M., Eichenfield, L.F., Fowler, J.F., Horowitz, P. & McLoad, R.P. 2013. Update on the structure and function of the skin barrier: atopic dermatitis as an exemplar of clinical implications. *Seminars in Cutaneous Medicine and Surgery,* 32(2):21–24.

Erb, P., Ji, J., Wernli, M., Kump, E., Glaser, A. & Büchner, S.A. 2005. Role of apoptosis in basal cell and squamous cell carcinoma formation. *Immunology Letters*, 100(2015):68–72.

Foldvari, M. 2000. Non-invasive administration of drugs through the skin: challenges in delivery system design. *Pharmaceutical science & technology today,* 3(12):417–425.

Garg, T., Rath, G. & Goyal, A.K. 2015. Comprehensive review on additives of topical dosage forms for drug delivery. *Drug Delivery*, 22(8):969–987.

Gohara, M. 2014. Skin cancer: an African perspective. *British Journal of Dermatology*, 173(2):17–21.

Goldberg, L.H. 1996. Basal cell carcinoma. *Lancet*, 347(1996):663–667.

Gravett, A.M., Liu, W.M., Krishna, S., Chan, W., Haynes, R.K., Wilson, N. & Dalgleish, A.G. 2011. In vitro study of the anti-cancer effects of artemisone alone or in combination with other chemotherapeutic agents. *Journal of Chemical information and Modeling,* 53(9):1689–1699.

Gravett, A.M., Liu, W.M., Krishna, S., Chan, W., Haynes, R.K., Wilson, N. & Dalgleish, A.G. 2011. In vitro study of the anti-cancer effects of artemisone alone or in combination with other chemotherapeutic agents. *Journal of Chemical information and Modeling,* 53(9):1689–1699.

Guy, R.H. 1996. Current status and future prospects of transdermal drug delivery. *Pharmaceutical Research*, 13(12):1765–1769.

Haque, T., Rahman, K.M., Thurston, D.E., Hadgraft, J. & Lane, M.E. 2015. Topical therapies for skin cancer and actinic keratosis. *European Journal of Pharmaceutical Sciences,* 77(1):279–289.

Hatanaka, E., Dermargos, A., Hirata, A.E., Vinolo, M.A.R., Carpinelli, A.R., Newsholme, P., Armelin, H.A. & Curi, R. 2013. Oleic, linoleic and linolenic acids increase ROS production by fibroblasts via NADPH oxidase activation. *Plos One*, 8(4):e58626.

Haynes, R.K. & Krishna, S. 2004. Artemisinins: activities and actions. *Microbes and Infection,* 6(14):1339–1346.

Ho, W.E., Peh, H.Y., Chan, T.K. & Wong, W.S.F. 2014. Artemisinins: Pharmacological actions beyond anti-malarial. *Pharmacology and Therapeutics*, 142(1):126–139.

Hu, P., Wang, T., Xu, Q., Chang, Y., Tu, H., Zheng, Y., Zhang, J., Xu, Y., Yang, J., Yaun, H., Hu, F. & Zhu, X. 2012. Genotoxicity evaluation of stearic acid grafted chitosan oligosaccharide nanomicelles. *Mutation Research*, 751(2):116–126.

Jacob, A. 1827. Observations respecting an ulcer of peculiar character, which attacks the eyelids and other parts of the face. https://archive.org/details/b22333411 Date of access: 2 Feb. 2017.

Kalepu, S., Manthina, M. & Padavala, V. 2013. Oral lipid-based drug delivery systems – an overview. *Acta Pharmaceutica Sinica B*, 3(6):361–372.

Klayman, D.L. 1985. Qinghaosu (Artemisinin): An antimalarial drug from China. *American Association for the Advancement of Science*, 228(4703):1049–1055.

Kotla, S., Singh, N.K. & Rao, G.N. 2017. ROS via BTK-p300-STAT1-PPARγ signalling activation mediated cholesterol crystals-induced CD36 expression and foam cell formation. *Redox Biology*, 11(2017):350–364.

Krishna, S., Bustamante, L., Haynes, R.H & Staines, H.M. 2008. Artemisinins: their growing importance in medicine. *Trends in Pharmacological Sciences,* 29(10):520–527.

Krishner, J.R., He, S., Balasubramanyam, V., Kepros, J., Yang, C., Zhang, M., Du, D., Barsoum, J. & Bertin, J. 2008. Elesclomol induces cancer cell apoptosis through oxidative stress. *Molecular Cancer Therapeutics*, 7(8):2319–2327.

Lai, H.C., Singh, N.P. & Sasaki, T. 2013. Development of artemisinin compounds for cancer treatment. *Investigational New Drugs,* 31(1):230–246.

Lai-Cheong, J.E. & McGrath, J.A. 2009. Structure of and function of skin, hair and nails. *Medicine*, 37(5):223–226.

Liou, G. & Storz, P. 2010. Reactive oxygen species in cancer. *Free Radical Research*, 44(5):479–496.

Liu, C. 2017. Discovery and development of artemisinin and related compounds. *Chinese Herbal Medicines*, 9(2):101–114.

Lippens, S., Hoste, E., Vandenabeele, P., Agostinis, P. & Declercq, W. 2009. Cell death in the skin. *Apoptosis*, 14(4):549–569.

Madan, V., Lear, J.T. & Szeimies, R. 2010. Non-melanoma skin cancer. *Lancet*, 375(2010):673–685.

Mangas, C., Paradelo, C., Puig, S., Gallardo, F., Marcoval, J., Azon, A., Bartralot, R., Bel, S., Bigatà, Curtcó, N., Dalmau, J., Del Pozo, L.J., Ferrándiz, C., Formigón, M., González, A., Just, M., Llambrich, A., Llistosella, E., Malvehy, J., Martí, R.M., Nogués, M.E., Pedragosa, R., Rocamora, V., Sàbat, M. & Salleras, M. 2010. Initial evaluation, diagnosis, staging, treatment, and follow-up of patients with primary cutaneous malignant melanoma. *ACTAS Dermo-Sifiliográficas,* 101(2):129–142.

Marks, J.G. & Miller, J.J. 2013. Structure and function of the skin. (In Marks, J.G. & Miller, J.J., *ed.* Lookingbill and Marks' Principles of Dermatology. London: Elsevier Health Sciences. P.2–10).

McGillis,S.T. & Fein, H. 2004. Topical treatment strategy for non-melanoma skin cancer and precursor lesions. *Seminars in Cutaneous Medicine and Surgery,* 23(3):174–183.

McGraft, J.A., Eady, R.A.J. & Pope, F.M. 2008. Anatomy and organization of human skin. (*In* Burns, T., Breanthnach, S. Cox, N. & Griffiths, C., *ed.* Rook's Textbook of Dermatology. Massachusetts:Blackwell Publishing. P.45–128).

McGuire, J.F., Ge, N.N. & Dyson, S. 2008. Nonmelanoma skin cancer of the head and neck I: histopathology and clinical behaviour. *American Journal of Otolaryngology*, 30 (2):121–133.

Meshnick, S.R. 2002. Artemisinin: mechanism of action, resistance and toxicity. *Interbational Journal of Parasitology,* 32(16):1655–1660.

Meshnick, S.R., Taylor, T.E. & Kamchonwongpaisan, S. 1996. Artemisinin and the antimalarial endoperoxides: from herbal remedy to targeted chemotherapy. *Microbiology Reviews*, 60(2): 301–315.

Naik, A., Kalia, Y.N. & Guy, R.H. Transdermal drug delivery: overcoming the skin's barrier function. *Pharmaceutical Science & Technology Today,* 3(9):318–326.

Nagai, M., Vo, N.H., Ogawa, L.S., Chimmanamada, D., Inoue, T., Chu, J., Beaudette-Zlatanova, B.C., Lu, R., Blackman, R.K., Barsoum, J., Koya, K. & Wada, Y. 2012. The oncology drug elesclomol selectively transports copper to the mitochondria to induce oxidative stress in cancer cells. *Free Radical Biology and Medicine,* 52(2012):2142–2150.

O'Day, S., Gonzalez, R., Lawson, D., Weber, R., Hutchins, L., Anderson, C., Haddad, J., Kong, S., Williams, A. & Jacobson, E. 2009. Phase II, randomized, controlled, double-blinded trail of weekly elesclomol plus paclitaxel versus paclitaxel alone for stage IV metastatic melanoma. *Journal of Clinical Oncology,* 27(32):5452–5458.

Orthaber, K., Pristovnik, M., Skok, K., Perić, B. & Maver, U. 2017. Skin cancer and its treatment: novel treatment approaches with emphasis on nanotechnology. *Journal of Nanomaterials*, 2017(2017). https://doi.org/10.1155/2017/2606271 Date of access: 14 March 2017.

Potts, R.O., Bommannan, D.B. & Guy, R.H. 1992. Precutaneous absorption. (*In* Mukhtar, H., *ed.* Pharmacology of the skin. Boca Raton: CRC Press. P.4–9).

Prausnitz, M.R. & Langer, R. 2008. Transdermal drug delivery. *Nature Biotechnology,* 26(11):1261–1268.

Qu, Y., Wang, J., Sim, M., Liu, B., Giuliano, A., Barsoum, J. & Cui, X. 2009. Elesclomol, counteracted by Akt survival signalling, enhances the apoptotic effect of chemotherapy drugs in breast cancer. *Breast Cancer Research and Treatment*, 121(2):311–321.

Ridky, T.W. 2007. Nonmelanoma skin cancer. *Journal of the American Academy of Dermatology*, 57(3):484–501.

Romero, M.R., Efferth, T., Serrano, M.A., Castaño, B., Macias, R.I.R., Briz, O. & Marin, J.J.G. 2005. Effect of artemisinin/artesunate as inhibitors of hepatitis B virus production in an "*in vitro*" replicative system. *Antiviral Research*, 68(2005):75–83.

Schröter, J., Griesinger, H., Reuß, E., Schulz, M., Riemer, T., Süß, R., Schiller, J. & Fuchs, B. 2015. Unexpected products of the hypochlorous acids-induced oxidation of oleic acid: a study using high performance thin-layer chromatography-electrospray ionization mass spectrometry. *Journal of Chromatography A*, 1439(2016):89–96.

Schwartz, B., Birk, Y., Raz, A. & Madar, Z. 2004. Nutritional – pharmacological combinations: a novel approach to reducing colon cancer incidence. *European Journal of Nutrition,* 43(4):221–229.

Shen, M., Ge, H.L., He, Y.X., Song, Q.L. & Zhang, H.Z. 1984. Immunosuppressive action of Qinghaosu. *Scientia Sinica,* 27(4):398–406.

Shimizu, N., Ito, M., Tazawa, T. & Sato, Y. 1989. Immunohistochemical study on keratin expression in certain cutaneous epithelial neoplasms. *American Journal of Dermatopathology*, 11(6):534–540.

Shrestha, H., Bala, R. & Arora, S. 2014. Lipid-based drug delivery systems. *Journal of Pharmaceuticals*, 2014:801820.

Silverberg, N.B. 2012. The skin: an introduction. (*In* Preedy, V.R., *ed.* Handbook of diet, nutrition and the skin. Netherlands:Wageningen Academic Publishers. P.14–21).

Simões, M.C.F., Sousa, J.J.S. & Pais, A.A.C.C. 2014. Skin cancer and new treatment perspectives: a review. *Cancer Letters*, 357(2015):8–42.

Sonavane, K., Phillips, J., Ekshyyan, O., Moore-Medlin, T., Roberts Gill, J., Rong, X., Lakshmaiah, R.R., Abreo, F., Boudreaux, D., Clifford, J.L. & O'Nathan, C.A. 2012. Topical curcumin-based cream is equivalent to dietary curcumin in a skin cancer model. *Journal of Skin Cancer*, 30(2):121–133.

Sun, Z., Wang, H., Ye, S., Xiao, S., Liu, J., Wang, W., Jiang, D., Liu, X. & Wang, J. 2012. Beta-eleostearic acid induced apoptosis in T24 human bladder cancer cells through reactive oxygen species (ROS)-mediated pathway. *Prostaglandins and other lipid mediators*, 99(1–2):1–8.

Telfer, N.R., Colver, G.B. & Morton, C.A. 2008 Guidelines for the management of basal cell carcinoma. *The British Journal of Dermatology*, 159(1):35–48.

Venus, M., Waterman, J. & McNab, I. 2011. Basic physiology of the skin. *Surgery (Oxford)*, 29(10):471–474.

Wang, C., Li, P., Xuan, J., Zhu, C., Liu, J., Shan, L., Du, Q., Ren, Y. & Ye, J. 2017. Cholesterol enhances colorectal cancer progression via ROS elevation and MAPK signalling pathway activation. *Cellular Physiology and Biochemistry*, 42(2):729–742.

Weiner, R.S. & Yoon, J. 2010. Melanoma. (*In* Hall, B.J & Hall, J.C., *ed.* Sauer's manual of skin diseases. Lippincott Williams & Wilkins: Philadelphia. P.313–315).

Woerdenbag, H.J., Moskal, T.A., Pras, N. & Malingré, T.M. 1993. Cytotoxicity of artemisinin-relasted endoperoxides to Ehrlich ascites tumor cells. *Journal of Natural Products*, 56(6):849–856.

Wondrak, G.T. 2009. Redox-directed cancer therapeutics: molecular mechanisms and opportunities. *Antioxidants & Redox Signalling,* 11(12):3013–3069.

Yadav, A.A., Patel, D., Wu, X. & Hasinoff, B.B. 2013. Molecular mechanism of the biological activity of the anticancer drug elesclomol and its complexes with Cu(ll), Ni(ll) and Pt(ll). *Journal of Inorganic Biochemistry,* 126(2013):1–6.

Zhang, R. 2016. Artemisinin (Qinghaosu), Nobel Prize, anti-malaria, and beyond. *Chinese Journal of Natural Medicines,* 14(1):0001–0002.

Zhao, Q.H., Zhang, Y., Liu, Y., Wang, H.L., Shen, Y.Y., Yang, W.J. & Wen, L.P. 2009. Anticancer effects of realgar nanoparticles on mouse melanoma skin cancer *in vivo* via transdermal drug delivery. *Medical Oncology,* 27(2):203–212.

CHAPTER 3

IN VITRO CYTOTOXICITY ANALYSIS AGAINST HUMAN MELANOMA CELLS

MATERIALS & METHODS

3.1 Introduction

Skin cancers remain the most common occurring cancer worldwide, with an estimated global incidence of between 2 and 3 million cases each year (Lin *et al*., 2017). Chemotherapy currently available is often hindered by the occurrence of severe adverse effects and the development of drug resistance (Efferth *et al*., 2001). Surgical excision is presently used to treat a large majority of skin cancers. Apart from poor cosmetic outcomes frequently associated with surgical excisions, not all patients are candidates (D'Orazio *et al*., 2013). Hence, warranting the development of alternative chemotherapeutics for melanoma treatment.

A novel approach of modulating ROS to selectively target cancer cell destruction has been proposed. As described in Section 2.5.2, cancer cells are vulnerable to agents that may generate ROS beyond the critical point of cancer cells' antioxidant capacity, resulting in oxidative stress and apoptosis induction leading to cancer cell death (Kirshner *et al*., 2008; Qu *et al*., 2009). The constituents chosen in this study, artemisone, elesclomol and lipid excipients (oleic acid, stearic acid and cholesterol) each possesses the ability to generate ROS. The wealth of literature currently available on the prominent anticancer effects of the selected drug constituents, artemisone and elesclomol, further substantiates their significance in this study (Blackman *et al*., 2012; Crespo-Ortiz & Wei, 2012; Efferth *et al*., 2001; Gravett *et al*., 2011; Krishner *et al*., 2008; Lai *et al*., 2012; Nagai *et al*., 2009; Van Huijsduijnen *et al*., 2013; Woodrow *et al*., 2005).

Drug constituent 1, artemisone, is a second-generation derivative of artemisinin that exhibits a multi-modal character against cancer cells by displaying antiproliferative, antiangiogenic and antimigratory, as well as pro-apoptotic activity (Gravett *et al*., 2011; Lai *et al*., 2012). Research has demonstrated that the active endoperoxide bridge of artemisinins may be activated and fragmented by intracellular iron to generate carbon-centred radical species and ROS inducing oxidative stress, apoptosis and cell death (Wondrak, 2009).

Drug constituent 2, elesclomol, is a novel investigational drug presently undergoing clinical evaluation in a pivotal phase III melanoma trial (Blackman *et al*., 2012; Krishner *et al*., 2008). Nagai *et al*. (2009), showed elesclomol's binding to copper is a fundamental requirement for anticancer activity. The generation of ROS is attributed to the redox cycling of Cu (ll) to Cu (l) opposed to elesclomol in the absence of copper that resulted in no discernible activity (Blackman *et al*., 2012; Nagai *et al*., 2009). Furthermore, Cu(ll)-elesclomol renders a substantially greater loss in cell viability compared to elesclomol (Hasinoff *et al*., 2014).

The lipid excipients chosen in this study include oleic acid, stearic acid and cholesterol. Pharmaceutical excipients are included in dosage forms to aid in the manufacturing and administration of drugs. Moreover, it may be used to improve stability, solubility, absorption and organoleptic properties of active pharmaceutical ingredients (Garg *et al*., 2015). Lu *et al*. (1998) raised the possibility that lipid excipients, non-esterified fatty acids including oleic acid, may have the potential to generate reactive oxygen species. Bellenghi *et al*. (2015) studied the effect oleic acid has on the malignant melanoma cell line A375. Their results showed oleic acid reduced melanoma dissemination, inhibited changes in the secretion profile of cancer cells and protected against malignancy (Bellengi *et al*., 2015). A similar study showed that fatty acid esters of phlorizin; including oleic- and stearic acid; resulted in significant growth inhibition of carcinoma and leukaemia cells, leading to cell cycle arrest and apoptosis at concentrations non-toxic to normal human hepatocytes (Nair *et al*., 2014).

Artemisinins are notorious for their low aqueous solubility, poor and inconsistent absorption, low bioavailability and short half-lives (White, 2008). Since elesclomol is a novel investigatory drug, limited information is available on the compound's physiochemical properties. Lipid-based drug delivery systems offer the potential to enhance drug absorption and bioavailability of poor water-soluble drugs, such as artemisinins (Nanjwade *et al*., 2011). Wang and colleagues showed the anticancer efficacy of artemisinins are improved when using lipid-based drug delivery systems (Wang *et al*., 2012). Additionally, lipid-based nanoparticles have displayed the ability to effective: 1) enhance the selectivity of cancer chemotherapeutics; 2) reduce toxic side effects of anticancer agents by lowering its cytotoxicity in normal cells; 3) enhance the solubility of hydrophobic agents; and 4) provide prolonged and controlled drug release (Dwivedi *et* al., 2015; Yingchoncharoen *et al*., 2016).

Combination therapies has become the standard in numerous conditions and represent a promising approach for addressing unmet medical needs by exploiting chances for enhanced efficacy, reduced toxicity and decreased drug resistance of active pharmaceutical ingredients (Foucquier & Guedj, 2015). Gravett *et al*. (2011) showed combination therapy with artemisone beneficial in cancer with enhanced effects of known anticancer drugs gemcitabine and

oxaliplatin. Elesclomol displays similar effects when in combination resulting in significant enhanced efficacy of well-established chemotherapeutic agents, such as paclitaxel in human xenograft models (Krishner *et al*., 2008). Owing to this potential of enhanced activity of artemisone and elesclomol when used in combination therapy, drug and lipid excipient combinations were investigated in this study. Combining artemisone and elesclomol with selected lipid excipients represents a novel combination approach for melanoma treatment.

Using cultured cells for preliminary screenings of potential therapeutic agents has become a familiar practice as cell cultures can be selected to represent the relevant disease or biochemical anomalies associated with the selected condition (Van Tonder *et al*., 2015). Human melanoma cultured cells were exposed to the proposed anticancer agents for a fix duration of time and, afterwards, cell viability and ROS generation were determined using the 3-(4,5-dimethylthiazol-2-yl)-2,5-diphenyl tetrazolium bromide (MTT) assay and the 2',7'-dichlorofluorescein-diacetate (DCFH-DA) assay. Briefly, the MTT assay is an established quantitative colorimetric method to estimate the number of viable cells in proliferation and cytotoxicity studies (Sylvester, 2011). The DCFH-DA assay is a commonly used method to detect the production of reactive oxygen intermediates and for evaluating the overall oxidative stress in toxicological phenomenon (Afri *et al*., 2004). The assay principles are further described in Sections 3.5.1 and 3.6.2.

The primary purpose of this study was to investigate the *in vitro* cytotoxic activity and intracellular ROS-generation of artemisone and elesclomol in combination with selected lipid excipients; oleic acid, stearic acid and cholesterol. This study forms part of initial screenings for a larger project under the title *"Rational development of combinations of known and novel drugs for chemotherapy of cancer*"; in which rational combinations of oxidant and redox drugs are developed to target both hypoxic and proliferating cancer cells. Proposed synergism between components are expected to decrease required drug amounts and ameliorate toxicity. The strategy for this project relies on cancer cells' susceptibility to oxidative stress. In this chapter the experimental design, materials, cell culturing, experimental method and assays are explained and discussed.

3.2 Experimental optimisation and design

"Experimental observations are only experience carefully planned in advance, and designed to form a secure basis of new knowledge" (Fisher, 1937:9). Thus, an experiment is methodical, and related to knowledge previously obtained; the results are deliberately observed and accurately recorded; and this may be achieved by careful planning and design of an experiment (Fisher, 1937). Experimental design is a method used to design and execute

experiments, where independent and dependent variables are identified, and the way in which experiments are to be carried out, is indicated. The goal of an experimental design is to establish a pivotal connection between the dependant and independent variables and to minimise expenditure of resources while obtaining the maximum amount of information possible (Kirk, 2009).

The experimental approach for this study was to initially determine the effect of each of the selected constituents; artemisone, elesclomol, oleic acid, stearic acid and cholesterol; against A375 human melanoma cells, followed by establishing the inhibition concentrations at 10%, 50% and 90% for artemisone and elesclomol. The proposed drug and lipid excipient combinations against A375 cells were subsequently analysed assessing the 1) cell viability and 2) intracellular ROS (Figure 3.1). All experiments were performed on human melanoma cell line, A375 cells.

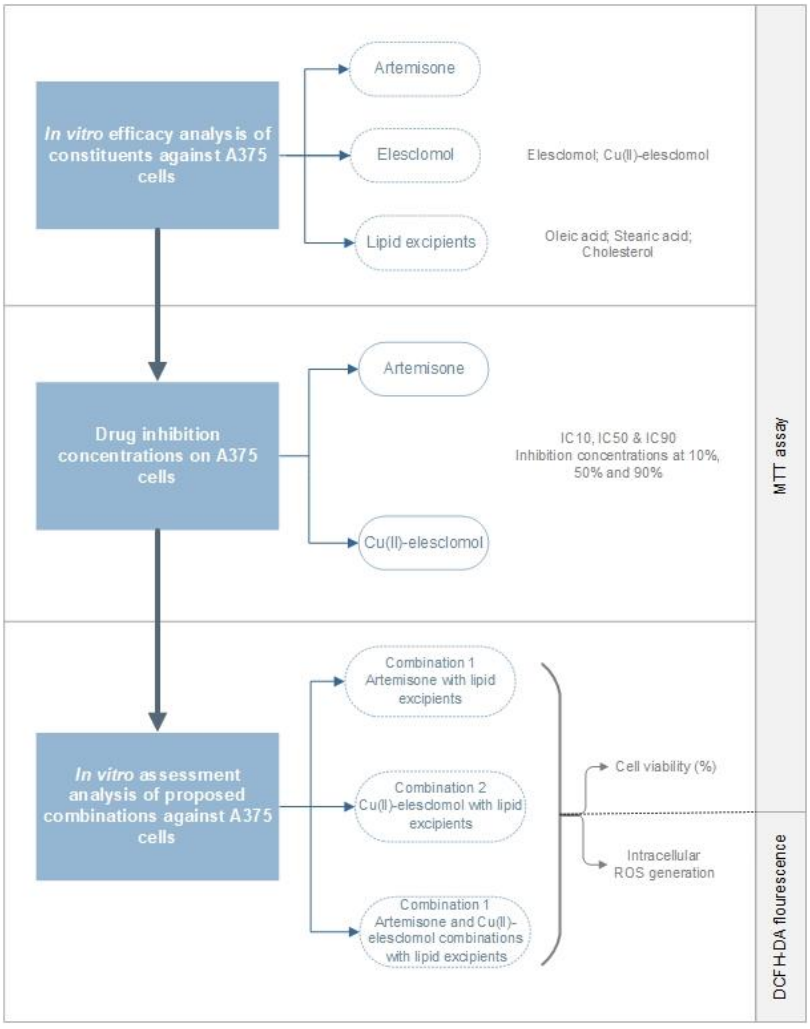

Figure 3.1: Experimental design flow diagram of the *in vitro* cytotoxicity studies on A375 human melanoma cells. Transparent column denotes the experimental procedure and solid column (far right) indicates the method used.

3.3 Selection of an appropriate cell line

When selecting a suitable cell line for a particular study, a few parameters (apart from specific functional requirements) must be taken into consideration. Freshney (2010) described these parameters as finite vs. continuous; human vs. non-human; normal vs. transformed cell line; availability of the cell line and its growth characteristics, among others. The antitumor effects of artemisone and elesclomol alone, and in combination with each other, as well as lipid excipients were under investigation on skin cancer in humans. Thus, the cell line had to be tumorigenic and originate from human skin tissue in order to meet the scope of this study. The human malignant melanoma cell line, A375 originating from skin tissue was selected as an appropriate cell line for the study. The human malignant melanoma cell line, A375 [A375] (ATCC® CRL1619™) was purchased from the American Type Culture Collection (ATCC™). Cells with a passage number between 15 and 25 were used in the experiments.

3.4 Non-analytical experimental procedures

Cell culturing, sub-culturing, freezing and preparation of cells were experimental proceedings performed prior to analytical assays. All procedures were conducted under sterile conditions, using sterile equipment and reagents. These procedures were carried out in the cell culturing laboratory in building G20 room G16 of the North-West University (NWU) Potchefstroom.

3.4.1 Materials

The active pharmaceutical ingredients (APIs), artemisone and elesclomol were kindly donated by Prof. R.K Haynes (Centre of Excellence for Pharmaceutical Sciences, Faculty of Health Sciences, NWU Potchefstroom). Oleic acid (fatty acid), cholesterol (sterol) and stearic acid (monoglyceride) were the lipid excipients used in combination with the APIs to determine their cytotoxic effects on A735 cells. All were purchased from Sigma-Aldrich, St Louis, USA.

Plastic consumables were purchased from Sigma-Aldrich® (Corning®) in aseptic packaging. To maintain the sterility, the handling of these items was conducted in the laminar flow hood (Filta-matrix Laminar Flow Cabinets Class 5). The reagents used are listed in Table 3.1.

Table 3.1: Reagents used during non-analytical experimental procedures

Reagent	Supplier	Catalogue number
Dulbecco's Modified Eagle's Medium (DMEM) with high glucose	Separations (Thermo Scientific)	SH30243.FS
Dimethyl Sulfoxide (DMSO)	Sigma- Aldrich®	D2650
10% Fetal Bovine serum (FBS)	WhiteSci (Lonza)	DE14-801FI
Human malignant melanoma cell line, A375	American Type Culture Collection (ATCC®)	CRL-1619™
Non-essential amino acids (NEAA)	WhiteSci (Lonza)	BE13-114E
1% Penicillin-Streptomycin (P/S)	WhiteSci (Lonza)	BE17-602E
Phosphate buffered saline (PBS)	Sigma- Aldrich®	P4417
Trypan Blue solution	Sigma- Aldrich®	T8154
Trypsin-Versene (EDTA)	WhiteSci (Lonza)	BE17-161F

3.4.2 Cell line maintenance and conditions

The human malignant melanoma cells, A375 were cultivated in 75 cm^2 culture flasks and grown in complete growth media comprising of DMEM supplemented with 1% P/S, 1% NEAA and 10% FBS (initial 20% FBS with cell start-up). The cell cultures were incubated at 37˚C in a 5% CO_2 in a humidified atmosphere. The growth media was renewed three times weekly.

Cell cultures were sub-cultured when once approximately 80% confluency was reached using trypsination (using 1.5 ml Trypsin-Versene) for cell detachment from the flask wall. After cell detachment, cell cultures were split into new culture flasks, labelled (date, cell type, passage and growth medium specifications) and incubated.

In order to maintain cell lines with earlier passages for extended periods, cells were cryopreserved, 1 ml freeze media consisting of 500 µl DMSO and 4.5 ml FBS per cryovial.

3.4.3 Cell count determination

The cell count was determined using the 0.4 % trypan blue dye exclusion method. This method rests on the concept that trypan blue dye is not taken up by viable cells, however, is permeable to non-viable cells. Therefore, on exposure to the dye, non-viable cells are stained and viable cells remain unstained (Griffiths, 2000).

The Countess™ automated cell counter (Invitrogen™) was used to determine the cell viability and cell count of cell culture samples required for seeding in 96-well plates. Cells were trypsinated (using 1.5 ml Trypsin-Versene) for cell detachment. Once detached, the cell suspension (re-suspended in 7 mL complete growth media and 3 ml trypsin) was centrifuged for 5 minutes at 250*g* to form the cell pellet. The media was decanted and the pellet was re-suspended with 3 ml serum free media (SFM). The cell suspension (50 µl) was added to 50 µl of 0.4% trypan blue dye in an Eppendorf® microtube, 10 µl of this sample mixture was pipetted into each of the chamber parts of the Countess™ cell counting chamber slides. The slide was then inserted into the Countess™ cell counter for examination and the percentage viability, total number of cells; viable cells and dead cells were obtained.

3.4.4 Preparation of 96-well plates

After determining the percentage viable cells and the live-cell concentration number of A375 cells with the Countess™ automated cell counter, a standard 96-well plate (Corning®, Sigma-Aldrich®, South Africa) was prepared for experimental proceedings. Briefly, a cell stock solution was prepared comprising of cell suspension and SFM. The total volume cell stock solution required was determined by multiplying the number of wells to be treated by the volume stock solution to be added to each well (0.1 ml). The volume cell suspension required was determined by dividing the desired cell density for A375 cells (25 000 cells/µl) by the mean live cell concentration number as obtained with the Countess™. The volume SFM required was determined by subtracting the volume cell suspension required from the total stock solution volume. Each well was treated with 100 µl of this cell stock solution and incubated overnight at 37°C in a 5% CO_2 in a humidified atmosphere. The percentage cell viability, as determined with the Countess™, had to be > 95% for cells to be considered viable. All the experiments in this study was conducted on viable cells (results not shown).

3.5 Experimental procedures

Experimental procedures were conducted on A375 cells using either the MTT assay or the DCFH-DA assay. The A375 cells were seeded into 96-well plates as described in Sections 3.4.3 & 3.4.4; and treated at different sample concentrations. With the exception of the intracellular detection of ROS; determined using the DCFH-DA assay method; the MTT assay was utilised for all other experiments in this study, assessing cell viability of treated samples.

3.5.1 Colorimetric Tetrazolium Dye assay

Cell viability was determined using the colorimetric tetrazolium dye assay. The 3-(4,5-dimethylthiazol-2-yl)-2,5-diphenyl tetrazolium bromide (MTT) assay is a quantitative colorimetric method for spectrophotometric determination of cell numbers as a function of mitochondrial activity in living cells as developed by Tim Mosmann (Mosmann, 1983). Purple water insoluble formazan crystals are obtained during the reduction of the yellowish tetrazolium MTT by means of mitochondrial dehydrogenases of viable cells that cleave to the tetrazolium ring. Afterwards, the crystals are dissolved in acidified isopropanol or dimethyl sulfoxide (DMSO). The resulting purple solution is measured spectrophotometrically and the degree of cytotoxicity is indicated by the amount of formazan formed. This formazan product serves as an indicator for viable cells as it is impermeable to cell membranes and thus accumulates within healthy cells (Figure 3.2) (Boncler *et al*, 2014; Fotakis & Timbrell, 2006).

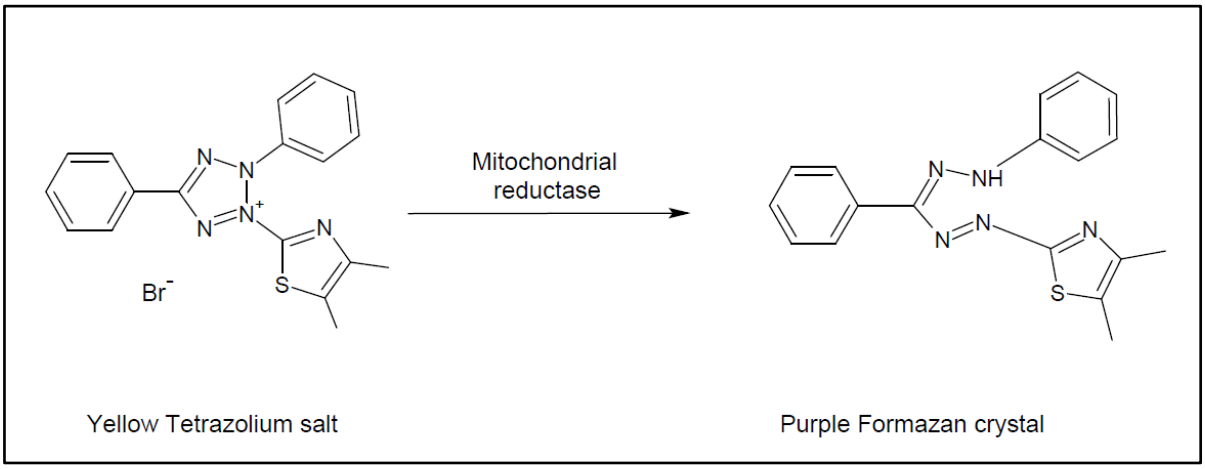

Figure 3.2: Principle of cytotoxic (MTT) assay. Mitochondrial reductases of viable cells cleave to the yellow tetrazolium ring, yielding aqueous insoluble purple formazan crystals.

The MTT-based *In Vitro* Toxicology Assay Kit (Sigma-Aldrich, St. Louis, USA) was used to determine cell viability with minor modifications. Briefly, A375 cells were seeded in 96-well plates as described in Section 3.4.4. and incubated overnight. Once approximately 90% confluency was reached, cells were exposed to treatments as described in Sections 3.5.2–3.5.5 and 3.6.1, for 24 h. Following treatments, culture medium was removed and cells was washed with 2 volumes of PBS to remove all tracts of the tested substances, 100 µl of SFM containing 0.5 mg/ml MTT solution was added to each well and incubated for 4 h. The MTT was removed and replaced with 100 µl DMSO to dissolve the resulting formazan crystals. DMSO was also added to wells containing no cells, serving as the blank. Cell viability was determined after 1 h of incubation using a microplate reader (SpectraMax® Paradigm™ Molecular Devices, Sunnyvale, CA, USA) at an absorbance wavelength of 560 nM and

background absorbance at 630 nM with DMSO measured as a blank. Triton X-100 was included as a positive control, which was added 1 h prior to MTT treatment. Blank and background measurements were subtracted and cell viability was expressed as a percentage relative to the untreated control, set as 100% viable using the following equation:

$$\%\,\text{Cell viability} = \left| \frac{(\Delta\,\text{Absorbance} - \Delta\,\text{Blank})}{(\Delta\,\text{Control} - \Delta\,\text{Blank})} \right| \times 100 \qquad \textbf{[1]}$$

Where: Δ Absorbance = absorbance at 360 nm; Δ Blank = mean blank at 360 nm – mean blank at 560 nm; and Δ Control = control absorbance at 360 nm – control absorbance at 560 nm.

3.5.2 *In vitro* efficacy analysis of artemisone against A375 cells

Literature documents the anticancer activities of artemisone on a variety of cancer cell lines, including melanoma cells; and the effects of other artemisinins on A375 human melanoma cells (Table 3.2). Some studies have investigated the effects of artemisone formulations on A375 cells, for instance, a study conducted by Dwivedi and collaborators (2015) investigated the anticancer effects of artemisone nano-vesicular formulations on A375 melanoma cells. However, studies of artemisone as a single agent on the A375 human melanoma cell line are ostensibly lacking.

Table 3.2: Studies of artemisone on cultured melanoma cells and artemisinins on A375 human melanoma cell lines.

Artemisinin derivative	Melanoma cell line	Reference
Artemisone	MJT3; KM	Gravette *et al*. (2011)
	1341L; 1729L; 276L; 462NL	Van Huijsduijnen *et al*. (2013)
Artemisone encapsulated nanovesicles and solid lipid niosomes	A375	Dwivedi *et al*. (2015)
Dihydroartemisinin	A375; G361; LOX	Cabello *et al*. (2012)
Artemisinin	A375P; A375M	Crespo-Oritz & Wei (2011)

The *in vitro* cytotoxicity of artemisone was analysed against A375 cells using the MTT assay. Briefly, artemisone was reconstituted at 10 mM in dimethyl sulfoxide (DMSO). A 96-well plate was prepared as described in Section 3.4.4. Following the 24 h cell attachment period, cells were treated with artemisone, in a serial dilution ranging from 112.50 µM to 1800 µM (to a final

volume of 100 µl/well) and incubated for 24 h at 37°C in a 5% CO_2 in a humidified atmosphere. The MTT assay as described in Section 3.5.1 was performed after 24 h and analysed using Prism version 5 software (GraphPad Software Inc., California USA). Triton X-100 was included as a positive control. Experiments were performed in triplicate.

3.5.3 *In vitro* efficacy analysis of elesclomol against A375 cells

As described in Sections 2.5.3 and 3.1, the binding of copper to elesclomol is a fundamental requirement for elesclomol's ROS generating activity (Figure 3.3). The cytotoxic effect of elesclomol and copper bound elesclomol, presented as Cu(II)-elesclomol was investigated on A375 cells.

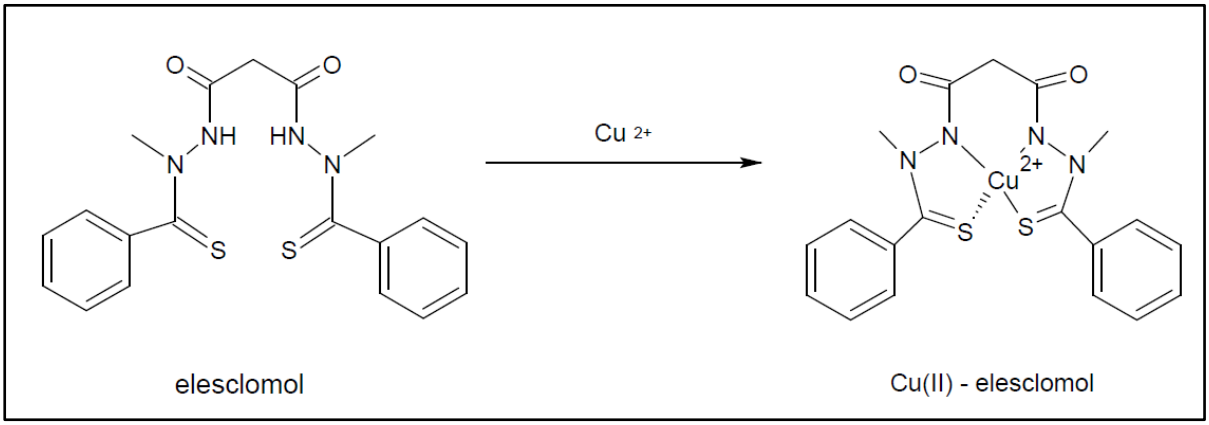

Figure 3.3: Structure of elesclomol and Cu(II)-elesclomol complex. Elesclomol reacts with the Cu^{2+} to form the Cu(II)-elesclomol complex.

Elesclomol and Cu(II)-sulphate was reconstituted at 100 µM in DMSO and 10 mM in SFM, respectively. The 96-well plates were prepared as described in Section 3.4.4. Following the 24 h cell attachment period, a set of cells were treated in a serial dilution of elesclomol ranging from 0.625 nM to 20 nM; another set was treated in a serial dilution with Cu(II)-elesclomol ranging from 0.625 nM to 20 nM elesclomol and 0.313 µM to 10 µM Cu(II)-sulphate. Each plate was treated to a final volume of 100 µl/well. The plates were incubated for 24 h at 37°C in a 5% CO_2 humidified atmosphere. Triton X-100 was included as the positive control. All experiments were performed in triplicate. The MTT assay as described in Section 3.5.1 was performed after the 24 h treatment period and analysed using Prism version 5 software (GraphPad Software Inc., California USA).

3.5.4 *In vitro* efficacy analysis of lipid excipients against A375 cells

Pharmaceutical excipients are commonly defined as inert constituents of a drug product used as a carrier, dilute and or vehicle for the active ingredient(s). The primary functions of excipients are to facilitate product manufacturing, drug release and provide bulk to the dosage

form. Excipients were historically viewed as pharmacologically inactive substances however, studies have demonstrated the impact excipients can have on the absorption, distribution, metabolism and elimination (ADME) processes of the co-administrated drug(s) (Elder *et al*., 2016; Wasan, 2009).

Lipid excipients has the ability to solubilise hydrophobic drugs within the matrix of the dosage form, often resulting in enhanced drug absorption mediated by a reduction in the barriers of poor water-soluble solubility and slow drug dissolution rate in the gastrointestinal fluids, in the case of oral drug delivery (Wasan, 2009). Lipid formulations have gained increasing interest in topical and transdermal drug delivery, displaying numerous processes in which drug delivery onto and in the skin, is facilitated and possibly enhanced by lipids. An example of a lipid penetration enhancer, is oleic acid (Cannon, 2014). Furthermore, lipids formulated in solid lipid nanoparticles (SLNPs) have been showed to enhance activities of various agents. In a study of artemisone encapsulated in SLNPs, the anticancer effects of artemisone was enhanced when formulated in SLNPs displaying highly selective cytotoxicity against A375 human melanoma cells in comparison to the free drug (Dwivedi *et al*., 2015).

In this study, the *in* vitro cytotoxic effects of lipid excipients, oleic acid; stearic acid and cholesterol; were investigated against A375 melanoma cells. Briefly, lipid excipients were reconstituted at 10 mM in DMSO for oleic acid and stearic acid; and 10 mM in methanol for cholesterol. A 96-well plate was prepared as described in S3.4.4. Following the 24 h cell attachment period, cells were treated with each lipid excipient, in a serial dilution ranging from 56.25 µM to 3600 µM (to a final volume of 100 µl/well) and incubated for 24 h at 37°C in a 5% CO_2 humidified atmosphere. The MTT assay as described in Section 3.5.1 was performed after 24 h and analysed using Prism version 5 (GraphPad Software Inc., California USA). Triton X-100 was included as a positive control and DMSO served as the blank. Experiments were performed in triplicate.

3.5.5 Drug inhibitory concentrations against A375 cells

In an attempt to understand the pharmacology and biological characteristics of chemotherapeutic agents, the half-maximal (50%) inhibition concentration (IC_{50}) is often determined as a parameter of an agent's efficacy in inhibiting a specific biological or biochemical function and is indicative of its antiproliferation potency (Griffiths & Sundaram, 2011; He *et al*., 2016). The IC_{50} is a quantitative measurement that represents a specific drug concentration required to inhibit a biological process (i.e. cancer cell growth) by 50%.

The inhibiting concentrations at 10%; 50% and 90% (IC_{10}; IC_{50} and IC_{90}) for artemisone and elesclomol (respectively) were chosen as the concentration range for experimental

procedures on A375 cells evaluating the *in vitro* cytotoxicity and intracellular ROS detection of the proposed combinations (see Section 3.6). These parameters were experimentally established using the MTT assay. The MTT assay, in contrast to traditional methods used for determining percentages of killed cells, is an easy technique to determine IC_{50} values and can be performed in 96-well plates. This assay determines cytotoxicity of an agent founded by reductions in intracellular nicotinamide adenine dinucleotide (NADPH) dependant oxidoreductase activity. The optical density of the control wells denotes the initial status of living cells, in which the mean is set as 100% survival rate (i.e., 0% inhibition rate). The IC_{50} value calculated at the concentration corresponding to a survival rate of 50% (He *et al*., 2016).

3.5.5.1 Artemisone preparation and treatment

Artemisone was reconstituted at 10 mM in DMSO. The 96-well plates were prepared as described in Section 3.4.4. Following the 24 h cell attachment period, cells were treated with artemisone in a serial dilution ranging from 112.50 µM to 3600 µM (to a final volume of 100 µl/well) and incubated for 24 h at 37°C in a 5% CO_2 humidified atmosphere.

3.5.5.2 Elesclomol preparation and treatment

Elesclomol and Cu(ll)-sulphate was reconstituted at 100 µM in DMSO and 10 mM in SFM, respectively. The 96-well plates were prepared as described in Section 3.4.4. Following the 24 h cell attachment period, cells were treated with 100 µl Cu(ll)-elesclomol in a serial dilution ranging from 0.625 nM to 20 nM elesclomol and 0.313 µM to 10 µM Cu(ll)-sulphate, respectively (to a final volume of 100 µl/well). The 96-well plates were subsequently incubated for 24 h at 37°C a 5% CO_2 humidified atmosphere.

Experiments were performed in triplicate. Both the artemisone- and elesclomol treated 96-well plates included the positive control, Triton X-100. After the 24 h treatment period, the MTT assay was performed as described in Section 3.5.1. Prism version 5 software (GraphPad Software Inc., California USA) was used to obtain the IC_{10}; IC_{50} and IC_{90} values.

3.5.6 *In vitro* efficacy analysis of proposed combinations against A375 cells

Combination therapy of two or more constituents that produce overtly similar effects exploits the chances for enhanced efficacy, ameliorated toxicity and decreased occurrence of drug resistance. Combinations are said to be synergistic when the combined effect is greater than individual potencies of each constituent (Foucquier & Guedj, 2015; Tallarida, 2011).

This study attempted to develop potentially synergistic combinations that targets hypoxic and proliferated cancer cells, relying on cancer cell's susceptibility to oxidative stress. Three

principal combinations were investigated, namely: (1) Artemisone combinations with lipid excipients: artemisone-oleic acid; artemisone-stearic acid; and artemisone-cholesterol; (2) Cu(ll)-elesclomol combinations with lipid excipients: Cu(ll)-elesclomol-oleic acid; Cu(ll)-elesclomol-stearic acid; and Cu(ll)-elesclomol-cholesterol; and (3) Artemisone–Cu(ll)-elesclomol combinations with lipid excipients: Artemisone–Cu(ll)-elesclomol–oleic acid; artemisone–Cu(ll)-elesclomol–stearic acid; and artemisone–Cu(ll)-elesclomol–cholesterol.

Concentration ranges was set at the IC_{10}, IC_{50} and IC_{90} values of both artemisone and elesclomol (see Section 4.5). The lipid excipients were chosen as the independent variables at a fix concentration of 45 µM see Annexure A.1. Artemisone was reconstituted at 10 mM in DMSO. Elesclomol and Cu(ll)-sulphate was reconstituted at 100 µM in DMSO and 10 mM in SFM, respectively. Lipid excipients were reconstituted at 10 mM in DMSO for oleic acid and stearic acid; and 10 µM methanol for cholesterol. The 96-well plates were prepared as described in Section 3.4.4. Following the 24 h cell attachment period, cells were treated with combinations 1–3 to a final volume of 100 µl/well:

- Combination 1: Cells were treated with artemisone at 30 µM, 140 µM and 600 µM (IC_{10}, IC_{50} and IC_{90}) alone and in combination with each lipid excipient at 45 µM (oleic acid, stearic acid and cholesterol).
- Combination 2: Cells were treated with Cu(ll)-elesclomol at 0.5 nM, 5 nM and 10 nM (IC_{10}, IC_{50} and IC_{90}) alone and in combination with each lipid excipient at 45 µM (oleic acid, stearic acid and cholesterol).
- Combination 3: Cells were treated in a 1:1 ration of artemisone:Cu(ll)-elesclomol at IC_{10} (30 µM artemisone + 0.5 nM Cu(ll)-elesclomol), IC_{50} (140 µM artemisone + 5 nM Cu(ll)-elesclomol) and IC_{90} (600 µM artemisone + 10 nM Cu(ll)-elesclomol) alone and in combination with each lipid excipient at 45 µM (oleic acid, stearic acid and cholesterol).

3.5.6.1 *In vitro* assessment of cell viability

Combination treatments were investigated using the MTT assay evaluating cell viability and proliferation as a function of *in vitro* cytotoxicity. The premise of the MTT assay is that cellular damage will inevitably result in failure of the cell's ability to maintain and provide energy required for metabolic cell function and growth (Rode, 2008).

The 96-well plates were prepared as described in Section 3.4.4. Following the 24 h cell attachment period, cells were treated with combinations 1 to 3 as described in Section 3.6. The plates were incubated for 24 h at 37°C in a 5% CO_2 humidified atmosphere. Triton X-100

was included as the positive control. All experiments were performed in triplicate. The MTT assay as described in Section 3.5.1 was performed after the 24 h treatment period and analysed using Prism version 5 software (GraphPad Software Inc., California USA).

3.5.6.2 Oxidative stress targeting in skin cancer

The ROS production was detected using the 2',7'- Dichlorofluorescein-diacetate (DCFH-DA) probe. DCFH-DA is a non-polar and cell permeable compound. After cell penetration, it is hydrolysed to the non-fluorescent derivative 2',7' Dichlorofluorescein (DFC) by intracellular esterase and trapped within the cells. As seen in Figure 3.4, this compound is oxidised by intracellular ROS to the highly fluorescent DCF in the presence of intracellular hydrogen peroxide (H_2O_2) (Bass *et al.*, 1983; Krishner *et al.*, 2008; Rosenkranz *et al*., 1992). Bass *et al*. (1983) showed that the cellular fluorescence intensity is directly proportionate to the level of formed DCF. Thus, DCF emits green fluorescence proportional to the intracellular ROS level. The accumulation of intracellular ROS is reflected by a change in DCF fluorescence (Yang *et al*., 2014).

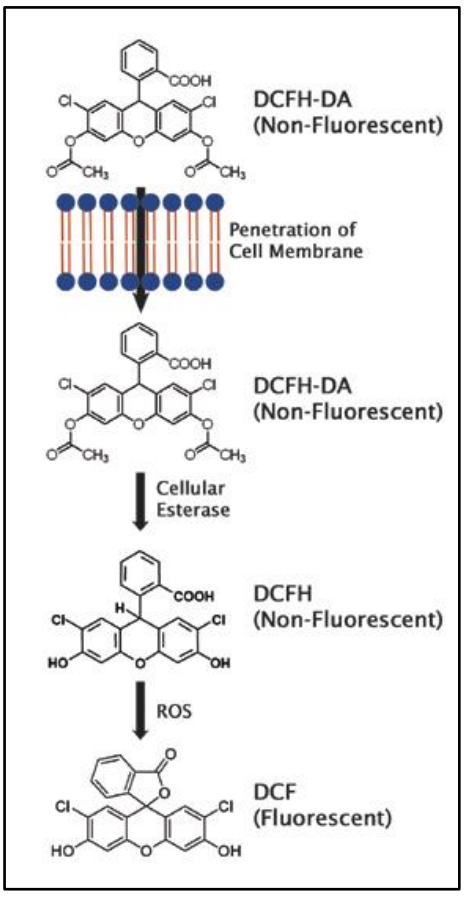

Figure 3.4: Principle of oxidative stress assay using DCFH-DA probe. The non-fluorescent DCFH-DA penetrates the cell membrane and is oxidised by intracellular ROS to produce the highly fluorescent DCF.

The combined methods using the fluorescent probe DCFH-DA, as described by Corasaniti *et al*. (2007) and Janda *et al*. (2015) were utilised in this study with minor modifications to measure intracellular ROS accumulation. In short, A375 cells were seeded at 25 000 cells/well in 96-well plates (Black plate, Tissue Culture treated, Clear bottom, Porvair, WhiteSci, Cape Town, South Africa) and incubated at 37°C in a 5% CO_2 humidified atmosphere until approximately 90% cell confluency was obtained. Serum-free DMEM without L-glutamine and phenol red (Lonza, WhiteSci, Cape Town, SA) was used for all experiments. Cells were stained for 30 minutes using preheated serum-free DMEM containing 5 µM DCFH-DA. Thereafter, the stain was removed and cells were gently washed twice with preheated serum-free DMEM and exposed to combination treatments as described in Section 3.6. Cells treated with 30% hydrogen peroxide was included as a positive control. All experiments were performed in triplicate. A kinetic analysis measuring the fluorescence at an excitation of 485 nm and an emission of 535 nm was conducted at 37°C using a microplate reader (SpectraMax® Paradigm™ Molecular Devices, Sunnyvale, CA, USA) at time 0 h and 1 h. The background fluorescence produced by the blank media controls and treated unstained cell controls were deducted from the DCFH-DA stained cells. For kinetic analysis, the DCF fluorescence measured at time 0 h (*i.e*. beginning of the analysis) was deducted from the DCF fluorescence at time 1 h. For the final measurement, the intracellular ROS accumulation was expressed as a fold change relative to the control set as 1.

3.6 Statistical analysis

Microsoft Office Excel 2016® and SpectraMax® Paradigm® (Molecular Devices, Sunnyvale, CA, USA) spectrophotometer equip with SoftMax® Pro Microplate Data Acquisition and Analysis software, was used to initially process data. GraphPad Prism™ version 5 software (GraphPad Software Inc., San Diego, CA, USA) was used to analysed data. Statistical significance was determined with one-way analysis of variance (ANOVA) with Dunnett multiple comparison post-test for non-parametric data. Significance was set at $P \leq 0.05$ and data was represented as the mean ± standard deviation (SD) or 95% confidence intervals in the case of IC_{50} values. Using the MTT data, IC_{50} values were calculated with GraphPad Prism 5 software. Data points were normalised to the positive control (Triton X-100) assumed as 0% viable and the negative control (untreated cell control) assumed at 100% viable; followed by log-transformation of values. Using the log (inhibition) vs. response function, the curve was fitted and the IC_{50} values determined. Column graphs of the DCFH-DA assay were fit with grouped analysis using one-way analysis of variance (ANOVA).

3.7 References

Afri, M., Frimer, A.A. & Cohen, Y. 2004. Active oxygen chemistry within the liposomal bilayer. Part IV: Locating 2',7'-dichlorofluorescein (DCF), 2',7'-dichlorodihydrofluorescein (DCFH) and 2',7'-dichlorodihydrofluorescein diacetate (DCFH-DA) in the lipid bilayer. *Chemistry and physics of lipids*, 131(1):123–133.

Bass, D.A., Parce, J.W., Dechatelet, L.R., Szejda, P., Seeds, M.C. & Thomas, M. 1983. Flow cytometric studies of oxidative product formation by neutrophils: a graded response to membrane stimulation. *Journal of Immunology*, 130(4):1910–1917.

Bellenghi, M., Puglisi, R., Pedini, F., De Feo, A., Felicetti, F., Bottero, L., Sangaletti, S., Errico, M.C., Petrini, M., Gesumundo, C., Denaro, M., Felli, N., Pasquini, L., Tripodo, C., Colombo, M.P., Carè, A. & Mattia, G. 2015. SCD5-induced oleic acid production reduces melanoma malignancy by intracellular retention of SPARC and cethepsin B. *Journal of Pathology,* 236(2015):315–325.

Blackman, R.K., Cheung-Ong, K., Gebbia, M., Proia, D.A., He, S., Kepros, J., Jonneaux, A., Marchetti, P., Kluza, J., Rao, P., Wada, Y., Giaever, G. & Nislow, C. 2012. Mitochondrial electron transport is the cellular target of the oncology drug elesclomol. *Plos One*, 7(1):e29798.

Boncler, M., Ròzalski, M., Krajewska, U., Podsedek, A. & Watala, C. 2041. Comparison of PrestoBlue and MTT assays of cellular viability in the assessment of anti-proliferative effects of plant extracts on human endothelial cells. *Journal of Pharmacological and Toxicological Methods*, 69(1):9–16.

Cabello, CM., Lamore, S.D., Bair, W.B., Qiao, S., Azimian, S., Lesson, J.L. & Wondrak, G.T. 2012. The redox antimalarial dihydroartemisinin targets human metastatic melanoma cells but not primary melanocytes with induction of NOXA-dependent apoptosis. *Investigational new drugs*, 30(4):1289–1301.

Cannon, J.B. 2014. Lipids in transdermal and topical drug delivery. *American Pharmaceutical Review*, 17(7). http://www.americanpharmaceuticalreview.com/Featured-Articles/170872-Lipids-in-Transdermal-and-Topical-Drug-Delivery/ Date of access: 2 Aug. 2017.

Corasaniti, M.T., Maiuolo, J., Maida, S., Fratto, V., Navarra, M., Russo, R., Amantea, D., Morrone, L.A. & Bagetta, G. 2007. Cell signalling pathways in the mechanisms of neuroprotection afforded by bergamot essential oil against NMDA-induced cell death in vitro. *British Journal of Pharmacology*, 151(4):518–529.

Crespo-Ortiz, M.P. & Wei, M.Q. 2012. Antitumor activity of artemisinin and its derivatives: from a well-known antimalarial agents to a potential anticancer drug. *Journal of Biomedicine and Biotechnology*, 2012(4):12222–12248.

D'Orazio. J., Jarrett, S., Amaro-Ortiz. A. & Scott. T. 2013. UV radiation and the skin. *International Journal of Molecular Sciences,* 14(6):12222–12248.

Dwivedi, A., Mazumder, A., du Plessis, L.H., du Preez, J.L., Haynes, R.K. & du Plessis, J. 2015. In vitro anti-cancer effects of artemisone nano-vesicular formulations on melanoma cells. Nanomedicine: Nanotechnology, Biology, and Medicine, 11(8):2041–2050.

Efferth, T., Dunstan, H., Sauerbrey, A., Miyachi, H. & Chitambar, C.R. 2001. The anti-malarial artesunate is also active against cancer. *International Journal of Oncology,* 18(4):767–773.

Elder, D.P., Kuentz, M. & Holm, R. 2016. Pharmaceutical excipients – quality, regulatory and biopharmaceutical considerations. *European Journal of Pharmaceutical Sciences*, 87(2016):88–99.

Fisher, R.A. 1937. The design of experiments. 2nd ed. Edinburgh: Oliver and Boyd.

Fotakis, G. & Timbrell, J.A. 2006. In vitro cytotoxicity assays: Comparison of LDH, neutral red, MTT and protein assay in hepatoma cell lines following exposure to cadmium chloride. *Toxicology Letters*, 160(2):171–177.

Foucquier, J. & Guedj, M. 2015. Analysis of drug combinations: current methodological landscape. *Pharmacy Research & Perspectives*, 3(3):e00149.

Freshney, R.I. 2010. Culture of animal cells: A manual of basic technique and specialized applications. 6th ed. New Jersey: John Wiley & Sons, Inc.

Garg, T., Rath, G. & Goyal, A.K. 2015. Comprehensive review on additives of topical dosage forms for drug delivery. *Drug Delivery*, 22(8):969–987.

Gravett, A.M., Liu, W.M., Krishna, S., Chan, W., Haynes, R.K., Wilson, N. & Dalgleish, A.G. 2011. In vitro study of the anti-cancer effects of artemisone alone or in combination with other chemotherapeutic agents. *Journal of Chemical information and Modelling,* 53(9):1689–1699.

Griffiths, B. 2000. Scaling-up of animal cell cultures. (*In* Masters, J.R.W *ed.* Animal Cell Culture. New-York: Oxford University Press. p. 19–67).

Griffiths, M. & Sundaram, H. 2011. Drug design and testing: profiling of antiproliferative agents for cancer therapy using a cell-based methyl-[$_3$H]-thymidine incorporation assay. *Methods in molecular biology*, 731(2011):451–465.

Hasinoff, B.B., Wu, X., Yadav, A.A., Patel, D., Zhang, H., Wang, D., Chen, Z. & Yalowich, J.C. 2014. Cellular mechanisms of the cytotoxicity of the anticancer drug elesclomol and its complex with Cu (II). *Biochemical Pharmacology,* 93(2015):266–276.

He, Y., Zhu, Q., Chen, M., Huang, Q., Wang, W., Li, Q., Huang, Y. & Di, W. 2016. The changing 50% inhibitory concentration (IC_{50}) of cisplatin" a pilot study on the artifacts of the MTT assay and the precise measurement of density-dependant chemoresistance in ovarian cancer. *Oncotarget*, 7(43):70803–70821.

Janda, E., Lascala, A., Carresi, C., Parafati, M., Apriqliano, S., Russo, V., Savoia, C., Ziviani, E., Musolino, V., Morani, F., Isidoro, C. & Mollace, V. Parkinsonian toxin-induced oxidative stress inhibits basal autophagy in astrocytes via NQO2/quinone oxidoreductase 2: Implications for neuroprotection. *Autophagy*, 11(7):1063–1080.

Kirk, R.E. 2009. Experimental design. (*In* Millsap, R.E. & Maydeu-Olivares, A., *ed.* The SAGE handbook of quantitative methods in psychology. London: Sage. p. 23–45).

Krishner, J.R., He, S., Balasubramanyam, V., Kepros, J., Yang, C., Zhang, M., Du, D., Barsoum, J. & Bertin, J. 2008. Elesclomol induces cancer cell apoptosis through oxidative stress. *Molecular Cancer Therapeutics*, 7(8):2319–2327.

Lai, H.C., Singh, N.P. & Sasaki, T. 2012. Development of artemisinin compounds for cancer treatment. *Invest New Drugs*, 31(2013):230–245.

Lin, B.S., Michael, K., Kalra, S. & Tizhoosh, H.R. 2017. Skin lesion segmentation: U-nest versus clustering. https://arxiv.org/pdf/1710.01248.pdf Date of access: 30 Oct. 2017.

Lu, G., Greene, E.L., Nagai T. & Egan, B.M. 1998. Reactive oxygen species are critical in the oleic acid–mediated mitogenic signalling pathway in vascular smooth muscle cells. *Hypertension,* 32(6):1003–1010.

Mosmann, T. 1983. Rapid colorimetric assay for cellular growth and survival: application to proliferation and cytotoxicity assay. *Journal of Immunological Methods*, 65(1983):55–63.

Nagai, M., Vho, N., Kostik, E., He, S., Kepros, J., Ogawa, L.S., Inoue, T., Blackman, R.K., Wada, Y. & Barsoum, J. 2009. The oxidative stress inducer elesclomol requires copper chelation for its anticancer activity. *Molecular Cancer Therapeutics*, 8(12):C11.

Nair, S.V.G., Ziaullah, H.P. & Rupasinghe, V. 2014. Fatty acid esters of phloridzin induce apoptosis of human liver cancer cells through altered gene expression. *Plos One,* 9(9):e107149.

Nanjwade, B.K., Patel, D.J., Udhani, R.A. & Manvi, F.V. 2011. Functions of lipids for enhancement of oral bioavailability of poor water-soluble drugs. *Scientia Pharmaceutica*, 79(4):705–727.

Qu, Y., Wang, J., Sim, M., Liu, B., Giuliano, A., Barsoum, J. & Cui, X. 2009. Elesclomol, counteracted by Akt survival signalling, enhances the apoptotic effect of chemotherapy drugs in breast cancer. *Breast Cancer Research and Treatment*, 121(2):311–321.

Rode, H., *ed.* 2008. How cell die: apoptosis and other cell death pathways. (*In* Rode, H., *ed.* Apoptosis, Cytotoxicity and Cell Proliferation. Mannheim: Roche Diagnostics. p. 116).

Rosenkranz, A.R., Schmaldienst, S., Stuhlmeier, K.M., Chen, W., Knapp, W. & Zlabinger, G.J. 1992. A microplate assay for the detection of oxidative products using 2',7'-dichlorofluorescin-diacetate. *Journal of Immunological Methods*, 156(1):39–45.

Sylvester, P.W. 2011. Optimisation of the tetrazolium dye (MTT) colorimetric assay for cellular growth and viability. (*In* Satyanarayanajois, S.D., *ed*. Drug design and discovery. Methods in Molecular Biology. New York: Human Press. p. 157–168).

Tallarida, R.J. 2011. Quantitative methods for assessing drug synergism. *Genes & Cancer*, 2(11):1003–1008.

Van Huijsduijnen, R.H., Guy, R.K., Chibale, K., Haynes, R.K., Peitz, I., Kelter, G., Phillips, M.A., Vennerstrom, J.L., Yuthavong, V. & Wells, T.N.C. 2013. Anticancer properties of distinct antimalarial drug classes. *Plos One*, 8(12):e82962.

Van Tonder, A., Joubert, A.M. & Cromarty, A.D. 2015. Limitations of the 3-(4,5-dimethylthiazol-2-yl)-2,5-diphenyl-2H-tetrazolium bromide (MTT) assay when compared to three commonly used cell enumeration assays. *BMC research notes*, 8(2015). https://www.ncbi.nlm.nih.gov/pmc/articles/PMC4349615/pdf/13104_2015_Article_1000.pdf Date of access: 31 Oct. 2017.

Wang, Z., Yu, Y., Ma, J., Zhang, H., Zhang, H., Wang, X., Wang, J., Zhang, X. & Zhang, Q. 2012. LyP-1 modification to enhance delivery of artemisinin or fluorescent probe loaded polymeric micelles to highly metastatic tumor and its lymphatics. *Molecular pharmaceutics*, 9(9):2646–2657.

Wasan, K.M. 2009. The biological functions of lipid excipients and the implications for pharmaceutical products development. *Journal of Pharmaceutical Sciences*, 98(2):379–382.

White, N.J. 2008. Qinghaosu (artemisinin): the price of success. *Science*, 320(5874):330–334.

Woodrow, C.J., Haynes, R.K. Krishna, S. 2005. Artemisinins. *Postgraduate medical journal*, 81(952):71–78.

Wondrak, G.T. 2009. Redox-directed cancer therapeutics: molecular mechanisms and opportunities. *Antioxidants & Redox Signalling,* 11(12):3013–3069.

Yang, H.L., Huang, P.J., Liu, Y.R., Kumar, K.J., Hsu, L.S., Lu, T.L., Chai, Y.C., Takajo, T., Kazunori, A. & Hseu, Y.C. 2014. Toona sinensis inhibits LPS-induced inflammation and migration in vascular smooth muscle cells via suppression of reactive oxygen species and NF-κB signaling pathway. *Oxidative Medicine and Cellular Longevity*, 2014(2014):901315.

Yingchoncharoen, P., Kalinowski, D.S. & Richardson, D.R. 2016. Lipid-based delivery systems in cancer: what is available and what is yet to come. *Pharmacological Reviews*, 68(3):701–787.

CHAPTER 4

IN VITRO CYTOTOXICITY ANALYSIS AGAINST HUMAN MELANOMA CELLS

RESULTS & DISCUSSION

4.1 Introduction

Skin cancers represent the most frequent occurring malignancy in humans. Surgical modalities are currently the mainstay of treatment, however, not always a suitable option (Simões *et al*., 2015). Combination therapy of two or more chemotherapeutic agents, has become a cornerstone for cancer therapy. Amalgamation of anticancer agents may result in synergistic or an additive effect that may in turn enhance the efficacy of the agents compared to its efficacy in monotherapy (Bayat *et al*., 2017).

Reactive oxygen species are the main mediators of cellular redox dysregulation and oxidative stress implicated in the initiation and progression of cancers. The dependence of malignant cells on mitogenic and survival signalling through ROS represents a specific vulnerability that can be selectively targeted by redox chemotherapeutics (Wondrak, 2009). In normal cells, ROS is produced at low concentrations and effectively neutralised by the potent antioxidant system of the cells. Cancer cells on the other hand, generate ROS levels above the capacity of the antioxidant system, resulting in a state of chronic oxidative stress. When ROS levels are further increased beyond the threshold capacity of cancer cells, apoptosis and cancer cell death can be induced (Krishner *et al*., 2008).

Redox directed combinations were investigated in which artemisone, proposed oxidant drug, and Cu(ll)-elesclomol, suggested redox drug, were combined to target hypoxic and proliferating cancer cells based on the susceptibility of cancer cells to oxidative stress. Anticipated synergism between artemisone and Cu(ll)-elesclomol will probably result in reduced required drug concentrations and ameliorated toxicity. Further reduced toxicity and enhanced selectivity of chemotherapeutic agents were investigated by combining lipid excipients, oleic acid, stearic acid and cholesterol with artemisone and Cu(ll)-elesclomol.

In this study, the anticancer effects of artemisone and Cu(ll)-elesclomol in combination with selected lipid excipients (oleic acid, stearic acid and cholesterol) were investigated against A375 human melanoma cells. Initially, the *in vitro* cytotoxicity of each constituent was investigated against A375 cells. This was done to evaluate the anticancer activity of each of

the constituents as monotherapy. Secondly, the inhibiting concentrations of artemisone and Cu(ll)-elesclomol at 10%, 50% and 90% were determined for the concentration range used in the experiments that followed. Experiments were concluded by the evaluation of drug combination treatments against A375 cells with regard to cell viability and ROS generation.

The efficacy of anticancer constituents can be classified as cytotoxic, meaning toxic to cells or killing cells; or cytostatic, denoting to stop cells from growing. The MTT assay measures cell viability in terms of the reductive activity of nicotinamide adenine dinucleotide phosphate (NADPH)-dependant cellular oxidoreductase enzymatic conversion of MTT to formazan (Berridge *et al*., 2015). This assay provides an estimation of the activity of metabolically active cells; and conclusions on cell proliferations, viability and cytotoxicity can be drawn. (Shoemaker, 2006).

Results were analysed using Microsoft Office Excel 2016® and GraphPad Prism™ version 5 software. All experiments were performed in triplicate. The error bars in figures represent the standard deviation between the mean of triplicate replications (n=3). One-way ANOVA, with Dunnett multiple comparison post-tests, were used to evaluate the difference in means between groups with a conventional threshold P-value for statistical significance defined as $P \leq 0.05$.

4.2 *In vitro* efficacy analysis of artemisone against A375 cells

The quantitative colorimetric MTT assay was used to evaluate artemisone's toxicity against A375 melanoma cells. Only one other study, to our knowledge, has examined the *in vitro* cytotoxic effects of artemisone against A375 melanoma cells. In that study artemisone was encapsulated in nano-vesicular formulations and the anticancer effects were determined against A375 melanoma cells (Dwivedi *et al*., 2015).

Results obtained from the MTT assay indicate that exposure to artemisone significantly suppressed melanoma cells ($P<0.0001$) in a dose dependant manner (Figure 4.1). At 143.5 µM ($R^2=0.9798$) with 95% confidence intervals of 110.8 to 185.8, artemisone suppressed 50% of the melanoma cell growth. These results are broadly consistent with those shown by Dwivedi and collaborators, in which 50% melanoma cell growth suppression was observed at an artemisone concentration of 0.06 mg/ml (149.43 µM) against A375 melanoma cells (Dwivedi *et al*., 2015). Results further indicated cytostatic effects at 112.5 µM and 225 µM, and cytotoxic effects at 450 µM to 3600 µM.

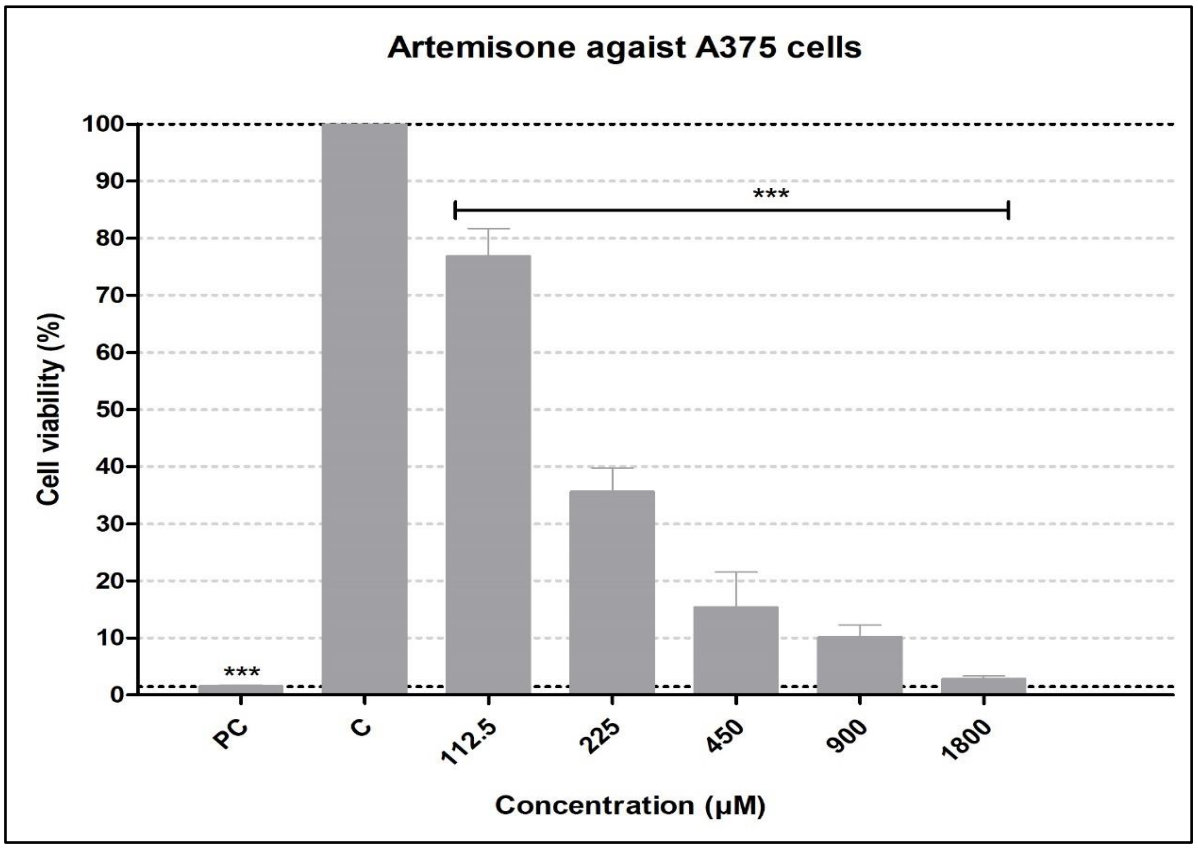

Figure 4.1: Cytotoxic effects against A375 cells following artemisone exposure (112.5-1800 µM). The percentage cell viability determined by the MTT assay over a period of 24 h, expressed relative to the untreated control (C), which was set at 100% viable. Triton X-100 (0.01%) was used as a positive control (PC). Bars signify the mean; and error bars signify the standard deviation (n=3). Asterisks indicate significant statistical differences in cell viability of exposed cells versus control cells (***P<0.0001).

These findings concur with the wealth of published results in literature on artemisinins and their growing importance in cancer chemotherapy (see Section 2.5.2.2). It is evident from these findings and previous studies, that artemisone is an attractive cancer chemotherapeutic drug candidate, particularly for melanoma.

4.3 *In vitro* efficacy analysis of elesclomol against A375 cells

The significance of bound copper to elesclomol required for the anticancer activity has been well highlighted in literature as described in Section 2.5.3. Nagai *et al*. (2012) demonstrated that in the absence of bound copper to elesclomol, no discernible anticancer activity was observed. However, when bound to copper, elesclomol displayed potent anticancer activities due to increased ROS and oxidative stress levels unfavourable for cellular survival (Blackman *et al*., 2012; Nagai *et al*., 2012).

The MTT assay was utilised to analyse the *in vitro* cytotoxicity of the elesclomol and Cu(II)-elesclomol at concentrations ranging from 0.63–20 nM. Figure 4.2 demonstrates the percentage cell viability after exposure to elesclomol and Cu(II)-elesclomol. The percentage cell viability serves as an indication of *in vitro* cytotoxicity relative to the cell control and the positive control.

Melanoma cells exposed to elesclomol treatment demonstrated no significant cell growth suppression ($P>0.05$) relative to the untreated control ($R^2=0.9909$). Elesclomol concentrations at 0.63–2.5 nM, depicted a negative impact on melanoma cell growth suppression ($P<0.0001$) and displayed no cytotoxic activity against melanoma cells. Higher concentrations of elesclomol (5–20 nM) resulted in similar effects with no significant cytotoxic activity at 10 nM and 20 nM. Melanoma cells exposed to Cu(II)-elesclomol significantly suppressed cell growth ($P<0.0001$), relative to the untreated control ($R^2=0.9915$). The results indicate a general concentration dependant decline in the percentage cell viability and substantial cytotoxic activity.

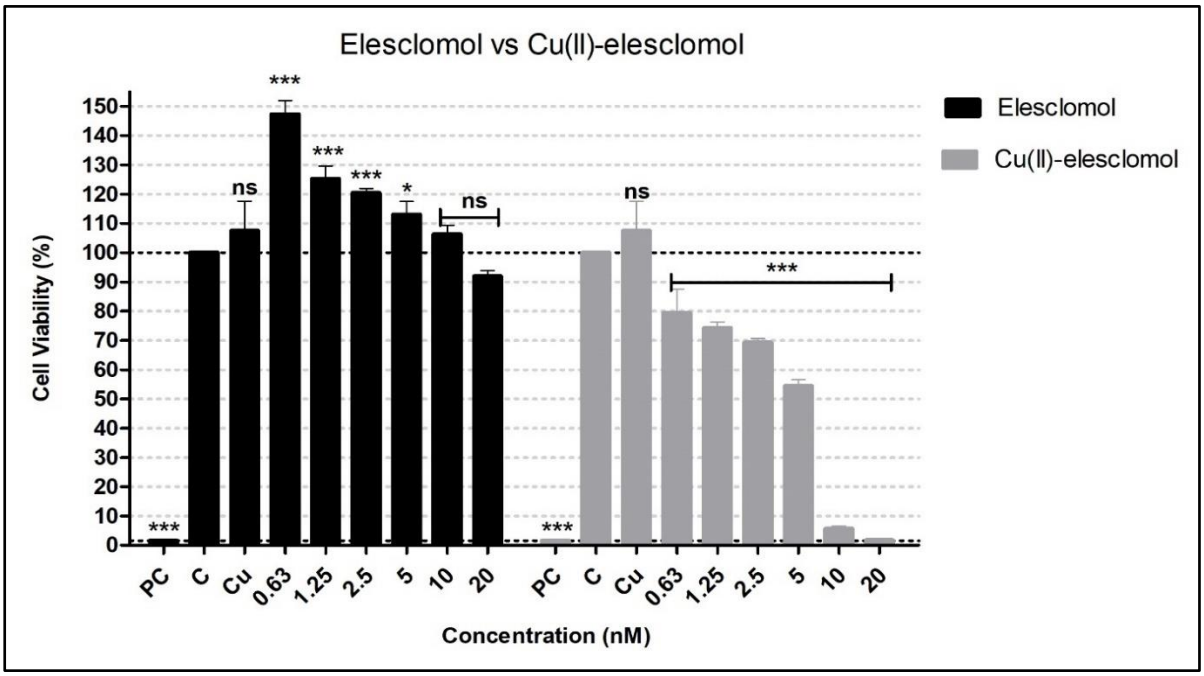

Figure 4.2: Cytotoxic effects against A375 cells following elesclomol and Cu(II)-elesclomol exposure (0.63–20 nM). The percentage cell viability determined by the MTT assay over a period of 24 h, expressed relative to the untreated control (C), which was set at 100% viable. Triton X-100 (0.01%) was used as a positive control (PC). A 10 µM copper control (Cu) was included. Bars signify the mean; and error bars signify the standard deviation (n=3). Asterisks indicate significant statistical differences in cell viability of exposed cells versus control cells (***$P<0.0001$ and *$P<0.05$). Non-significant statistical differences are indicated as ns.

These findings, correspond with results related to existing research with regard to the significance of copper binding to elesclomol and its resulting anticancer activity. Relative to the cell- and positive control, elesclomol displayed no apparent anticancer activity against the A375 melanoma cells. The copper control was included to observe the cytotoxic effects of the copper used. In this study, the copper should be scavenged by the elesclomol to induce oxidative stress while exhibiting no apparent toxicity of its own. Relative to the cell- and positive controls, the copper complied with this requirement, positive control < % cell viability > cell control. These observations are consistent with literature; thus, Cu(ll)-elesclomol was used for further experiments in this study. Results further indicated cytostatic effects at 0.63 nM to 5 nM, and cytotoxic effects at 10 nM and 20 nM.

4.4 *In vitro* efficacy analysis of lipid excipients against A375 cells

Oleic acid, stearic acid and cholesterol were chosen as lipid excipients for this study. The application of lipid-based formulations in cancer therapeutics is an emerging field of research in which lipid-based formulations may improve cancer therapy through enhanced selectivity and reduced toxicity of cancer chemotherapeutic agents. Lipid-based formulations have similarly been shown effective in improving the solubility of hydrophobic agents (Yingchoncharoen *et al*., 2016). The selected lipid excipients chosen in this study, are lipids commonly used in lipid-based formulations (Dwivedi *et al*., 2015; Weber *et al*., 2014).

The cytotoxic effects of the oleic acid, stearic acid and cholesterol were determined against A375 melanoma cells by assessing cell viability (Figure 4.3). The employed MTT assay indicated significant suppression ($P<0.0001$) of melanoma cells in a dose dependant manner for each of the selected lipid excipients ($R^2=0.9955$). Melanoma cells exposed to stearic acid generally display higher sensitivity and significant cytotoxicity, compared to oleic acid and cholesterol.

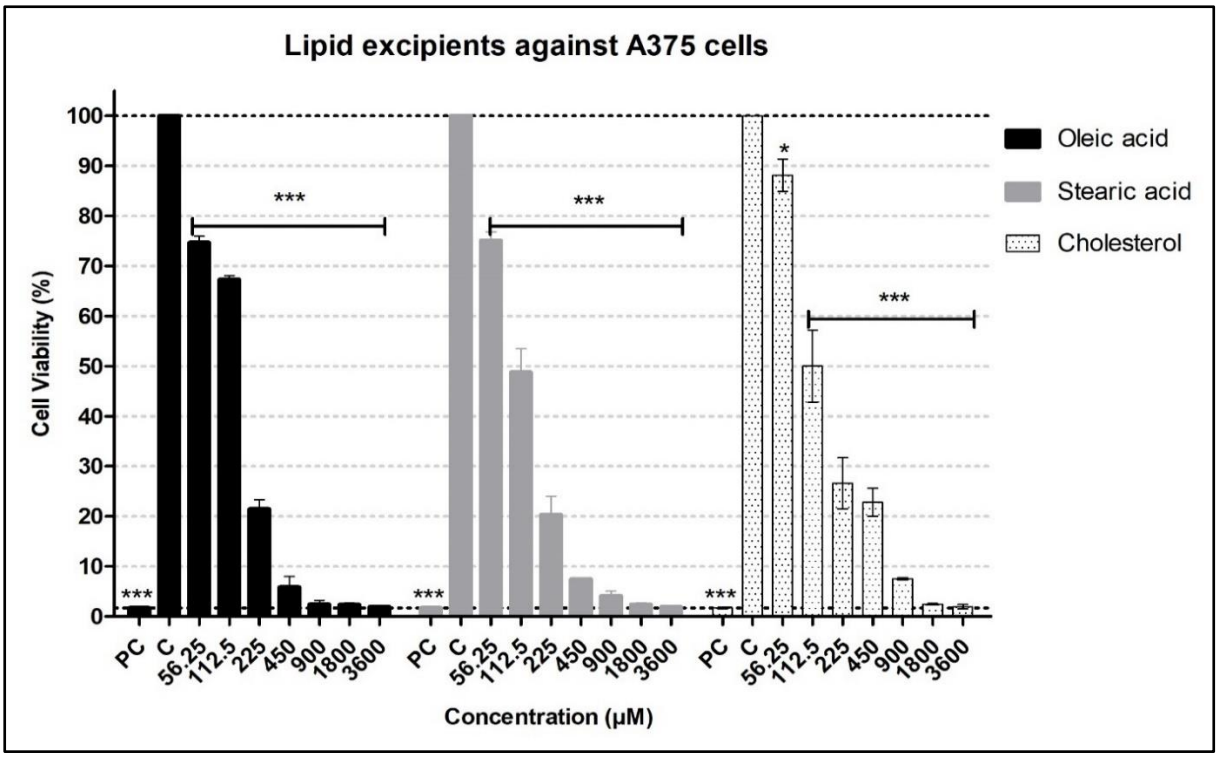

Figure 4.3: Cytotoxic effects against A375 cells following lipid excipient exposure (56.25–3600 µM). The percentage cell viability determined by the MTT assay over a period of 24 h, expressed relative to the untreated control (C), which was set at 100% viable. Triton X-100 (0.01%) was used as a positive control (PC). Bars signify the mean; and error bars denote the standard deviation (n=3). Asterisks indicate significant statistical differences in cell viability of exposed cells versus control cells (***P<0.0001 and *P<0.05).

These results described for the first time the effects of oleic acid, stearic acid and cholesterol on A375 melanoma cells. Based on these observations, it is evident that oleic acid, stearic acid and cholesterol portray significant cytotoxic activity against melanoma cells and may be potentially useful in anticancer therapeutics. Results further indicated cytostatic effects of oleic acid and stearic acid at 56.25 µM and 112.5 µM, and cytotoxic effects at 225 µM to 3600 µM. Cholesterol showed that at 56.25 µM, cells were still viable, at 112.5 µM, cytostatic and at concentrations of 225 µM to 3600 µM, cytotoxic.

4.5 Drug inhibitory concentrations against A375 cells

The half-maximal inhibitory concentration (IC_{50}) is the most widely used measure to determine an agent's efficacy; and it is important for understanding a chemotherapeutic agent's pharmacological and biological characteristics. It indicates the amount of an agent required to inhibit a biological process by half, representing an antagonist drug's potency in pharmacological research. For this reason, the experimental concentrations for combination

treatment were set at IC_{50} values of artemisone and Cu(ll)-elesclomol. Additionally, inhibiting concentrations at 10% and 90% (IC_{10} and IC_{90}) were also investigated. The IC_{10} value is indicative of cell viability at 90%, thus healthy viable cells. At this concentration, the agent induced no cytotoxic effects. The IC_{90} value is suggestive of cell viability at 10%, thus non-viable cells. At this concentration, the agent induced cytotoxic effects. The quantitative colorimetric MTT assay is a common method to determine IC_{50} values of agents based on decreases in intracellular NAD(P)H-dependant oxidoreductase activity. The initial status of living cells is set to a survival rate of 100% of the control wells, whereas a 50% survival concentration is defined as the IC_{50} (Aykul & Martinez-Hackert, 2016; He *et al*., 2016). The MTT assay was employed and IC-values were determined using GraphPad Prism 5 software.

4.5.1 Inhibiting concentrations of artemisone

Using data collected from the MTT assay, the IC_{50} value for artemisone was calculated at 143.5 µM (R^2 = 0.9798) with 95% confidence intervals of 110.8 to 185.8µM. The IC_{10} and IC_{90} values were established as 26.5 µM and 588 µM, respectively. Calculated values correlated well with values obtained from the graph as illustrated in Figure 4.4.

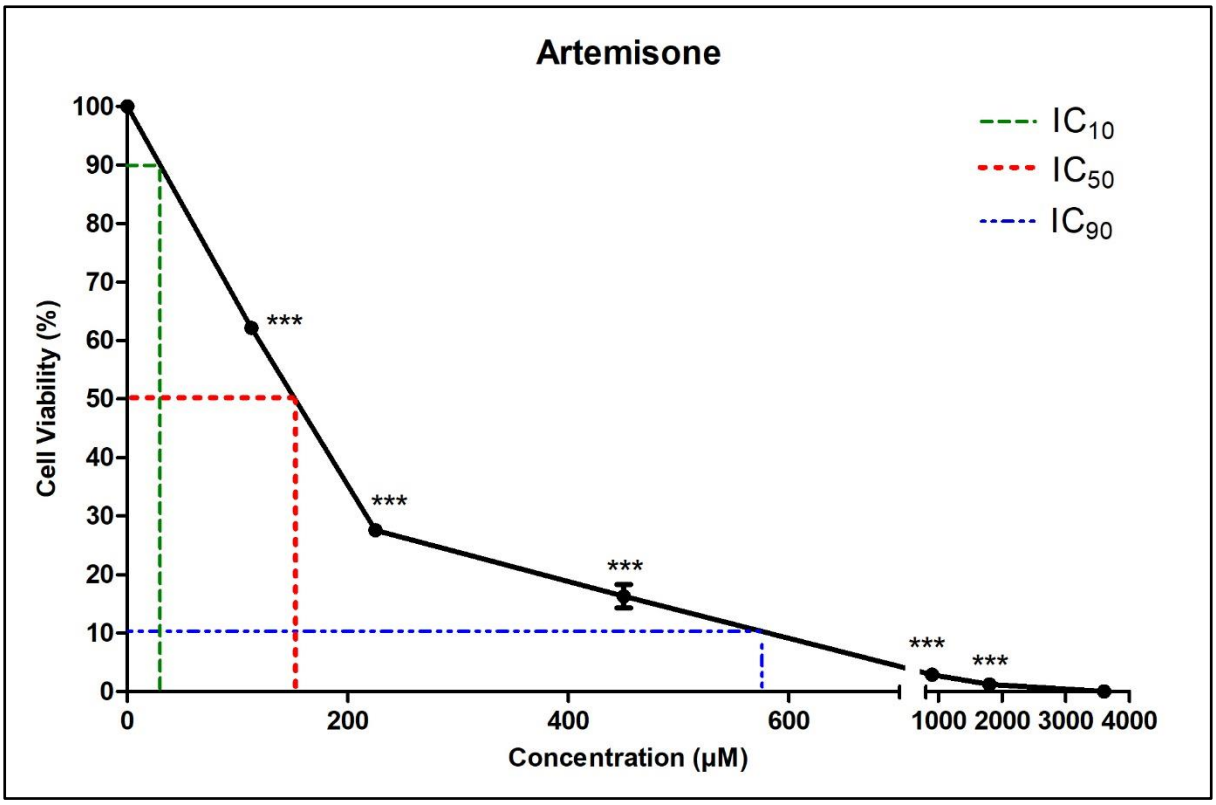

Figure 4.4: Inhibiting concentrations of artemisone at 10%, 50% and 90% against A375. The percentage cell viability determined by the MTT assay over a period of 24 h, expressed relative to the untreated control (C), which was set at 100% viable. Results represented the mean and standard deviation (n=3). Asterisks indicate significant statistical differences in cell viability of exposed cells versus control cells (***P<0.0001).

4.5.2 Inhibiting concentrations of Cu(II)-elesclomol

Using data collected from the MTT assay, the IC_{50} for Cu(II)-elesclomol was calculated at 5.53 nM (R^2 = 0.9561) with 95% confidence intervals of 3.606 to 8.482µM. The IC_{10} and IC_{90} values were obtained at 0.295 µM and 9.69 µM, respectively. Calculated values correlated well with values read from the graph as illustrated in Figure 4.5. These findings describe, for the first time, the IC-values for Cu(II)-elesclomol against A375 melanoma cells.

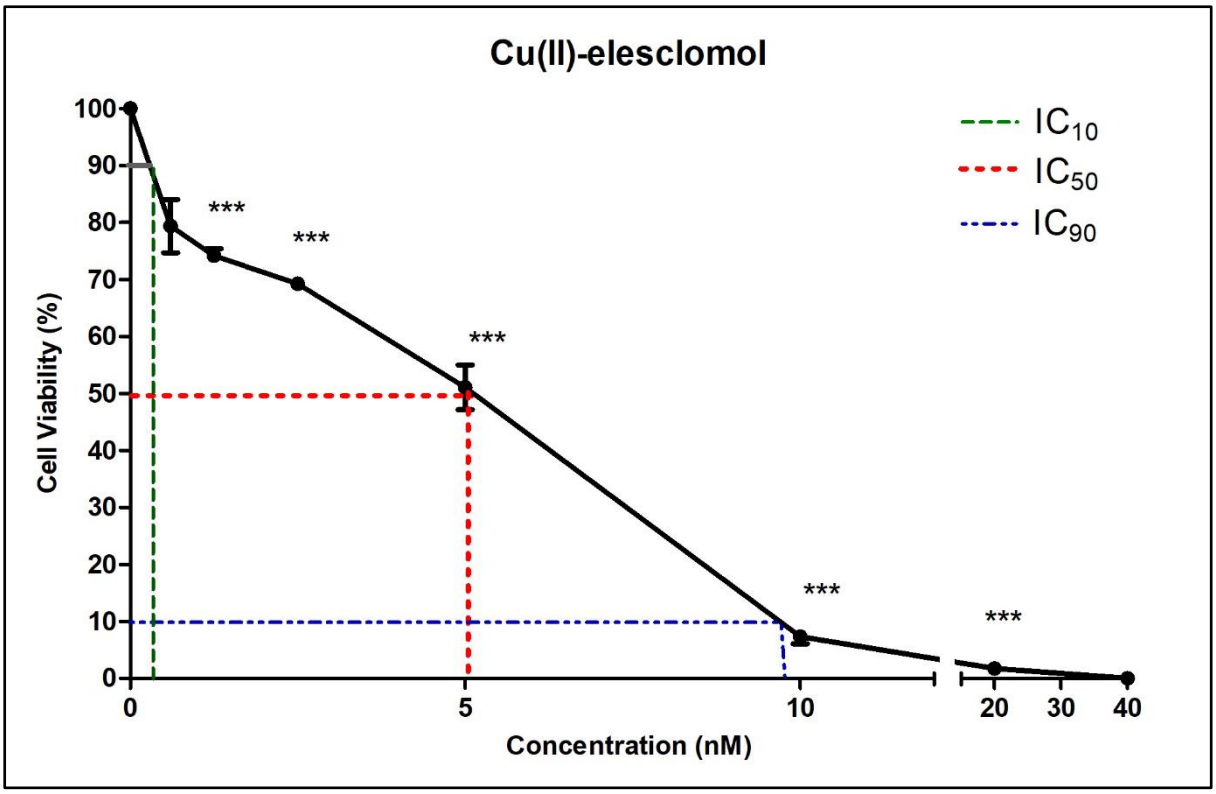

Figure 4.5: Inhibiting concentrations of Cu(II)-elesclomol at 10%, 50% and 90% against A375. The percentage cell viability determined from the MTT assay over a period of 24 h, expressed relative to the untreated control (C), which was set at 100% viable. Results represented the mean and standard deviation (n=3). Asterisks indicate significant statistical differences in cell viability of exposed cells versus control cells (***P<0.0001).

Cu(II)-elesclomol has shown anticancer efficacy against a broad range of cancer cell lines, including melanoma cell cultures (Kirshner *et al*., 2008). However, the effects of Cu(II)-elesclomol against A375 melanoma cells have not been defined previously. A study conducted by Blackman and colleagues (2011) found that Cu(II)-elesclomol on Hs249T melanoma cells exhibited an IC_{50} value of 11 nM, whereas in this study the IC_{50} value of 5.53 nM against A375 melanoma cells was considerably lower.

Based on these observations, the concentration ranges for the remainder of the experiments were set. The concentration range for artemisone treatments at IC_{10}, IC_{50} and IC_{90} was set at 30 µM, 140 µM and 600 µM, respectively (rounded off to the closest 10 or 100). The concentration range for Cu(II)-elesclomol treatments at IC_{10}, IC_{50} and IC_{90} was set at 0.5 nM, 5 nM and 10 nM, correspondingly.

4.6 *In vitro* efficacy analysis of proposed combinations against A375 cells

Several developmental redox chemotherapeutics have displayed potentiating effects on the pharmacodynamic actions of other anticancer agents and radiation, however, when used as single agents offer only modest or no chemotherapeutic benefit. Consequently, many studies investigate the activity of combination redox therapy (Wondrak, 2009).

Herein, the proposed redox agents, artemisone and Cu(II)-elesclomol, were evaluated for their effect on A375 cells as single agents (drug) and as part of combination therapy with lipid excipients; oleic acid, stearic acid and cholesterol (drug-lipid). Additionally, these redox agents were evaluated for their combined effect (drug-drug) and their effect when in combination with the selected lipid excipients (drug-drug-lipid). Cells were exposed to redox agents at their inhibiting concentrations of 10%, 50% and 90% (IC_{10}, IC_{50} and IC_{90}); and combinations with lipid excipients at 45 µM oleic acid, stearic acid and cholesterol. Guidelines for *in vitro* studies, suggest that concentrations that decrease cell viability with more than 30% is an indicator of cytotoxicity, when compared to the untreated control (Tice *et al*., 2000). From the selected lipid excipients, only oleic acid was previously tested against melanoma cells (Section 2.5.4.3) and was thus chosen for optimisation of the lipid concentration. Cell viability of oleic acid was measured in order to assure that the lipid excipient concentration used in this study was non-toxic and that the results represent healthy, but stressed living cells (see Annexure A.1). The anticancer activity of the proposed combinations was analysed with respect to percentage cell viability and intracellular ROS production.

4.6.1 *In vitro* assessment of cell viability

The quantitative colorimetric MTT assay was employed to evaluate the *in vitro* cytotoxicity against A375 melanoma cells relative to the percentage cell viability following 24 h exposure to different combination treatments of artemisone, Cu(II)-elesclomol, oleic acid, stearic acid and cholesterol. As previously mentioned, the MTT assay measures cell viability in terms of the reductive activity of NAD(P)H-dependant cellular oxidoreductase enzymatic conversion of MTT to formazan (Berridge *et al*., 2015). It is a common screening technique used to determine the toxicity of pharmaceuticals and anticancer drugs by estimating the number of viable cells based on metabolic activity (Kupcsik, 2011).

These results indicate a general concentration dependant decline in the percentage cell viability of melanoma cells exposed to treatments (Figures 4.6–4.8). Treatments significantly suppressed melanoma cell growth ($P<0.0001$) relative to the untreated control. Experimental controls (Annexure A.2) show that melanoma cells exposed to lipid excipients at 45 µM resulted in a considerably low viability of the cells ($P<0.0001$). On the other hand, none of the

vehicle controls in this study portrayed a significant impact on cell viability, nor displayed toxicity against A375 melanoma cells.

4.6.1.1 Combination 1: Artemisone with lipid excipients

Results in Figure 4.6 show cells exposed to artemisone and lipid excipient combinations, where artemisone significantly suppressed melanoma cell growth ($P<0.0001$) relative to the untreated cell control ($R^2=0.9965$). Each combination resulted in a concentration dependant decline in the percentage cell viability of melanoma cells, which is an indication of toxicity and anti-cancer activity (Annexure A.3, Table A.2). In contrast, combinations of artemisone with lipid excipients resulted in no significant melanoma cell suppression ($P>0.05$) at IC_{10} and IC_{50} values relative to artemisone mono-treatment. However, lipid excipient combinations at IC_{90} displayed significant differences in melanoma cell suppression ($P<0.0001$) relative to single agent treatment with artemisone. In comparison to the 17.81 ± 3.12% cell viability obtained by artemisone mono-treatment, combinations with lipid excipients reduced cell viability relative to artemisone by 88.66 ± 0.28%, 73.85 ± 0.76% and 82.43 ± 0.30%, individually, for oleic acid, stearic acid and cholesterol (Annexure A.4).

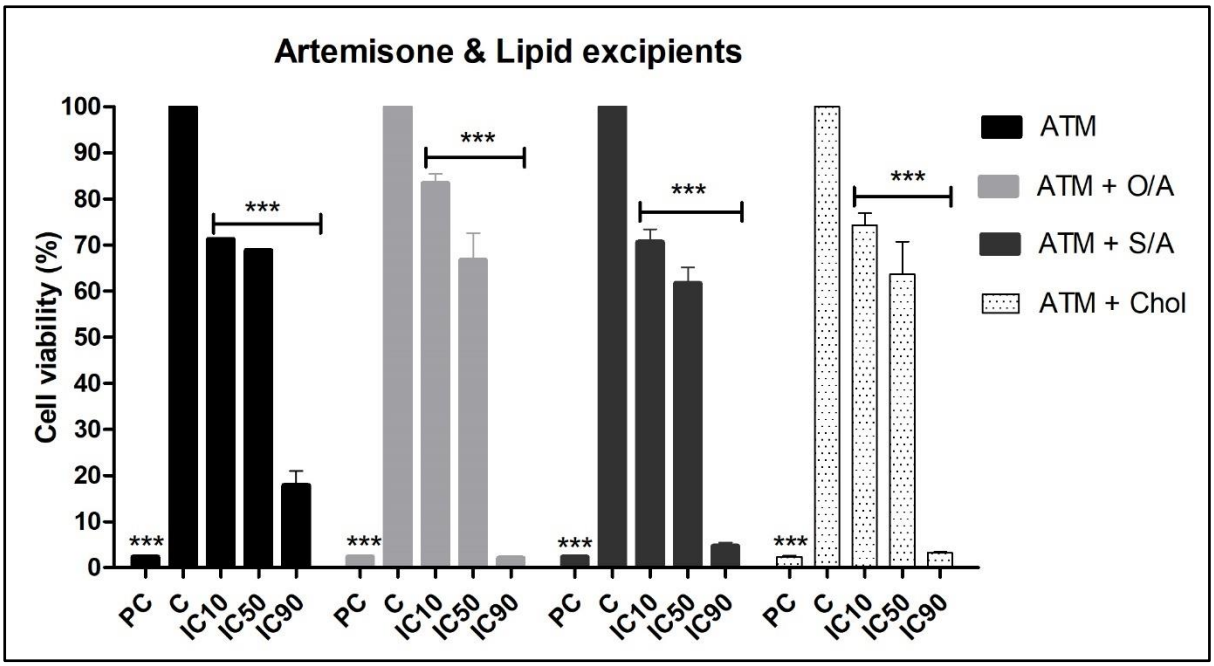

Figure 4.6: Cytotoxic effects against A375 cells following exposure to artemisone and lipid excipient combination treatments. Artemisone (ATM) combinations with lipid excipients, oleic acid (O/A), stearic acid (S/A) and cholesterol (Chol). The percentage cell viability determined by the MTT assay over a period of 24 h, expressed relative to the untreated control (C), which was set at 100% viable. Triton X-100 (0.01%) was used as a positive control (PC). Bars signify the mean and error bars denote the standard deviation (n=3). Asterisks indicate significant statistical differences in cell viability of exposed cells versus control cells (***P<0.0001 and *P<0.05).

These results indicate that combinations of artemisone and selected lipid excipients, oleic acid, stearic acid and cholesterol were able to enhance artemisone's anticancer activity further when combined at higher concentrations.

4.6.1.2 Combination 2: Cu(II)-elesclomol with lipid excipients

Results in Figure 4.7 show cells exposed to Cu(II)-elesclomol and lipid excipient combinations with Cu(II)-elesclomol significantly suppressed melanoma cell growth (P<0.0001) relative to the untreated cell control (R^2=0.9912). Each combination resulted in a concentration dependant decline in the percentage cell viability of melanoma cells, thus indicating toxicity and anticancer activity (Annexure A.3, Table A.3). In contrast, combinations of Cu(II)-elesclomol with lipid excipients caused no significant difference (P>0.05) at IC_{10} values relative to Cu(II)-elesclomol mono-treatment. However, lipid excipient combinations at IC_{50} and IC_{90} displayed significant differences in melanoma cell suppression (P<0.0001) relative to single agent treatment with Cu(II)-elesclomol. Combinations with oleic acid, stearic acid and

cholesterol at IC_{50} values, produced an 85.63%, 47.23% and 54.86%, individual reduction in cell viability relative to the 66.31% cell viability obtained from the single agent Cu(II)-elesclomol treatment. Combinations with oleic acid, stearic acid and cholesterol at IC_{90} values, resulted in a 93.05%, 61.66% and 86.95% respective reduction in cell viability comparative to the 30.80% cell viability obtained by Cu(II)-elesclomol monotreatment (Annexure A.5, Table A.6).

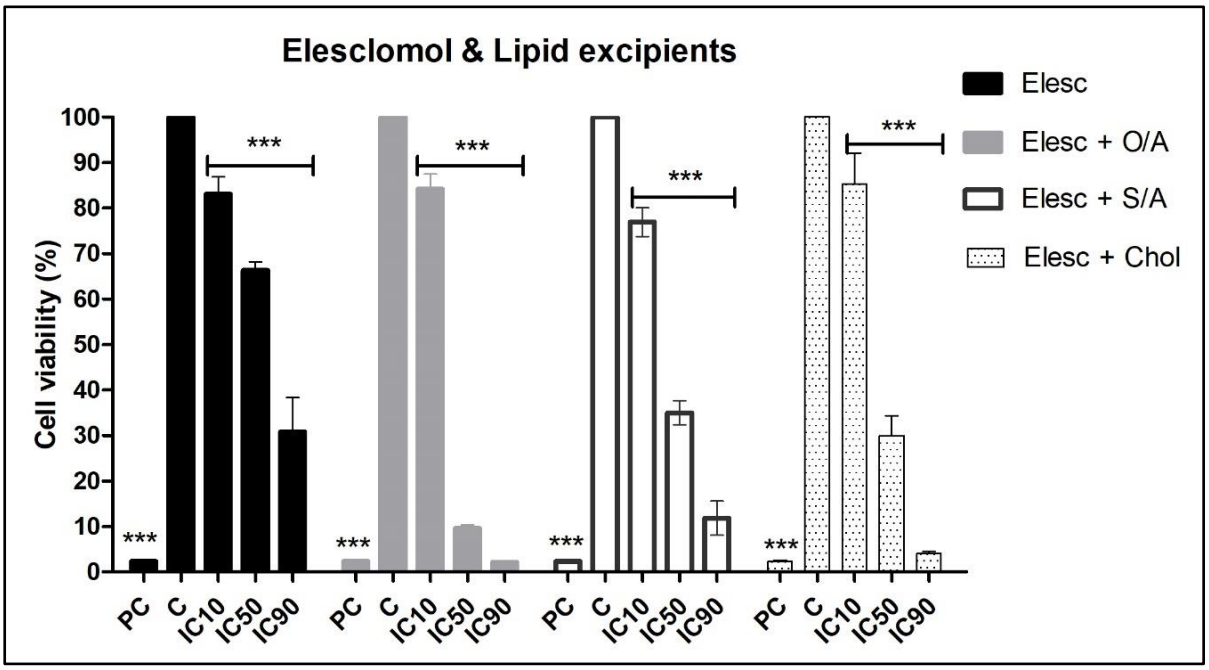

Figure 4.7: Cytotoxic effects against A375 cells following exposure to Cu(II)-elesclomol and lipid excipient combination treatments. Cu(II)-elesclomol (Elesc) combinations with lipid excipients, oleic acid (O/A), stearic acid (S/A) and cholesterol (Chol). The percentage cell viability determined by the MTT assay over a period of 24 h, expressed relative to the untreated control (C), which was set at 100% viable. Triton X-100 (0.01%) was used as a positive control (PC). Bars signify the mean; and error bars denote the standard deviation (n=3). Asterisks indicate significant statistical differences in cell viability of exposed cells versus control cells (***P<0.0001 and *P<0.05).

These results obtained indicate that combinations of Cu(II)-elesclomol and selected lipid excipients (oleic acid, stearic acid and cholesterol) were able to enhance Cu(II)-elesclomol's anticancer activity further when combined at certain concentrations.

4.6.1.3 Combination 3: Artemisone and Cu(II)-elesclomol combination with lipid excipients

Results as shown in Figure 4.8, indicate significant suppression of melanoma cell growth (P<0.0001) relative to the untreated cell control, when exposed to combination treatment of

drug constituents, artemisone and Cu(II)-elesclomol, as well as combinations of drug constituents with lipid excipients (R^2=0.9939). Oleic acid displayed the only exception with the IC_{10} value at a significance of P<0.05. Each of the tested combinations displayed a concentration dependant decline in the percentage cell viability of melanoma cells, thus portraying toxicity and anticancer activity (Annexure A.6).

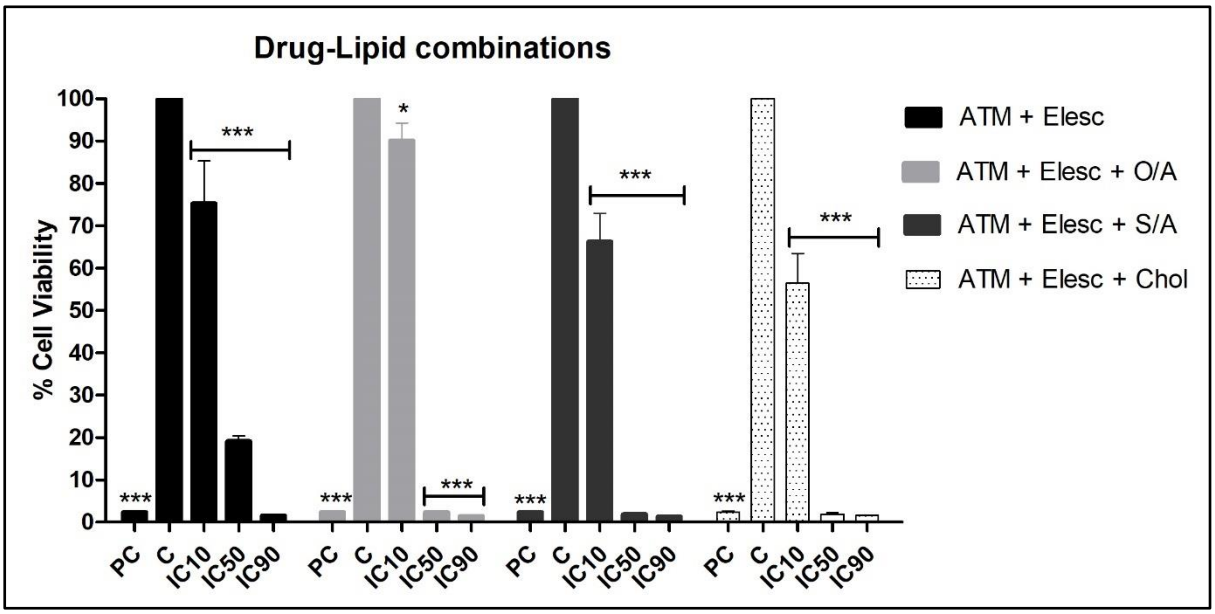

Figure 4.8: Cytotoxic effects against A375 cells following exposure to drug combinations with lipid excipients. Artemisone and Cu(II)-elesclomol combination (ATM + Elesc) with lipid excipients, oleic acid (O/A), stearic acid (S/A) and cholesterol (Chol). The percentage cell viability determined by the MTT assay over a period of 24 h, expressed relative to the untreated control (C), which was set at 100% viable. Triton X-100 (0.01%) was used as a positive control (PC). Bars signify the mean; and error bars denote the standard deviation (n=3). Asterisks indicate significant statistical differences in cell viability of exposed cells versus control cells (***P<0.0001 and *P<0.05).

Significance in melanoma cell suppression relative to drug constituents indicated the following (Annexure A.6):

1. Results relative to artemisone-Cu(II)-elesclomol:
    - IC_{10} – drug combinations with lipid excipients oleic acid and stearic acid displayed no statistical differences (P>0.05). Drug combinations with cholesterol indicated significant suppression in melanoma cell growth (P=0.0035) and resulted in a 24.95% enhanced toxicity relative to the artemisone-Cu(II)-elesclomol treated cells.

- IC_{50} – Combinations with all the lipid excipients showed significant suppression in melanoma cell growth (P<0.0001). Drug combinations with oleic acid, stearic acid and cholesterol, respectively resulted in 88.04%, 90.61% and 90.04% enhanced toxicity relative to the artemisone-Cu(ll)-elesclomol treated cells.
- IC_{90} – combinations with lipid excipients in combination with drug constituents at IC_{90} treatments, displayed no statistical significance (P>0.05).

2. Results relative to artemisone mono-treatment:

- IC_{10} – artemisone-Cu(ll)-elesclomol combinations alone and with lipid excipients stearic acid and cholesterol displayed no statistical significance (P>0.05). Drug combinations with oleic acid, however, depicted a negative impact on melanoma cell growth suppression (P=0.0030) and caused a 20.91% reduced toxicity relative to artemisone treated cells.
- IC_{50} – artemisone-Cu(ll)-elesclomol combinations alone and with lipid excipients indicated significant suppression in melanoma cell growth (P<0.0001). Combinations of artemisone-Cu(ll)-elesclomol alone and with oleic acid, stearic acid and cholesterol, individually resulted in 73.30%, 96.67%, 97.40% and 97.24% enhanced toxicity compared to the artemisone treated cells.
- IC_{90} – artemisone-Cu(ll)-elesclomol combinations alone and with lipid excipients showed significant suppression in melanoma cell growth similar to that observed with IC_{50} treatment (P<0.0001). Combinations of artemisone-Cu(ll)-elesclomol alone and with oleic acid, stearic acid and cholesterol, respectively, resulted in 91.47%, 92.25%, 91.97% and 91.18% enhanced toxicity relative to the artemisone treated cells.

3. Results relative to Cu(ll)-elesclomol mono-treatment:

- IC_{10} – artemisone-Cu(ll)-elesclomol combinations alone and with lipid excipients, oleic acid and stearic acid, displayed no statistical significance (P>0.05). Drug combinations with cholesterol, however, depicted significant suppression in melanoma cell growth (P=0.0026) and produced a 32.03% enhanced toxicity relative to Cu(ll)-elesclomol treated cells.
- IC_{50} – artemisone-Cu(ll)-elesclomol combinations alone and with lipid excipients indicated significant suppression in melanoma cell growth (P<0.0001). Combinations of artemisone-Cu(ll)-elesclomol alone and with oleic acid, stearic acid and cholesterol, individually resulted in 71.24%, 96.56%, 97.30% and 97.13% enhanced toxicity relative to the Cu(ll)-elesclomol treated cells.

- IC_{90} – artemisone-Cu(ll)-elesclomol combinations alone and with lipid excipients portrayed significant suppression in melanoma cell growth similar to that observed with IC_{50} treatment ($P<0.0001$). Combinations of artemisone-Cu(ll)-elesclomol alone and with oleic acid, stearic acid and cholesterol caused a 95.07%, 95.52%, 95.36% and 94.90%, respective, enhanced toxicity compared the Cu(ll)-elesclomol treated cells.

In summary: The results provided in this section illustrate the effect of artemisone, Cu(ll)-elesclomol, oleic acid, stearic acid and cholesterol combinations against A375 melanoma cells. Melanoma cells exposed to combinations of artemisone with lipid excipients, as well as combinations of Cu(ll)-elesclomol with lipid excipients, showed more sensitivity towards treatments at IC_{90}. Combination treatments of both artemisone and Cu(ll)-elesclomol with lipid excipients, on the other hand, displayed the highest sensitivity to treatments at IC_{50}, thus, at lower concentrations of each drug constituent.

Lipid excipient combinations with artemisone (drug-lipid) depicted higher cytotoxicity in comparison to Cu(ll)-elesclomol combinations (drug-lipid) against melanoma cells at IC_{10} treatments. In contrast, Cu(ll)-elesclomol combinations with lipid excipients at IC_{50} treatments, displayed higher sensitivity and cytotoxicity compared to combinations of artemisone. Combinations of lipid excipients with artemisone and those with Cu(ll)-elescmol at IC_{90} treatments, both portrayed similar cytotoxicity against melanoma cells. Combinations of artemisone and Cu(ll)-elesclomol with lipid excipients (drug-drug-lipid) indicated general enhanced cytotoxicity at all concentrations, equated to single drug combinations with lipid excipients.

Combinations of stearic acid generally resulted in higher cytotoxic activity, compared to oleic acid and cholesterol. Combinations of cholesterol displayed higher cytotoxicity versus combinations of oleic acid. However, each of the lipid excipients exhibited enhanced anticancer effects of drug constituents at IC_{50} and IC_{90} treatments.

4.6.2 Oxidative stress targeting in skin cancer

Elevated ROS production and an altered redox status due to high metabolic activities of cancer cells have long been observed; and numerous studies propose that this biochemical feature of cancer cells may be modulated for therapeutic benefits. Carcinogenesis and cancer progression is often promoted by increased ROS production and oxidative stress; however, excessive ROS levels can also be toxic to the cells. Thus, further pharmacological ROS insult could have significant therapeutic implications (Trachootham *et al*., 2009).

This study aimed to develop rational combinations of oxidant and redox drugs, artemisone and Cu(II)-elesclomol, that exploit cancer cells' susceptibility to oxidative stress. The intracellular ROS production of combination therapies was measured using the fluorescent DCFH-DA probe, which penetrates cell membranes where cellular esterase cleaves to the non-fluorescent DCFH-DA and is oxidised by intracellular ROS to the highly fluorescent DCF. These results describe, for the first time, the intracellular ROS generation of artemisone and Cu(II)-elesclomol combinations with lipid excipients, oleic acid, stearic acid and cholesterol.

The experimental controls (Annexure A.2) show that melanoma cells exposed to lipid excipients at 45 µM, increased intracellular ROS accumulation significantly ($P<0.0001$). On the other hand, none of the vehicle controls in this study had a significant impact on ROS accumulation against A375 melanoma cells.

4.6.2.1 Combination 1: Artemisone with lipid excipients

Results in Figure 4.9, indicate no significant increase in intracellular ROS accumulation ($P>0.05$) of cells exposed to artemisone combinations with lipid excipients relative to the untreated cell control ($R^2=0.9389$). Each combination, with the exception of oleic acid ($IC_{90} < IC_{50}$), resulted in a dose dependant increase in intracellular ROS accumulation ($IC_{90} > IC_{50} > IC_{10}$). Likewise, the intracellular ROS accumulation of lipid excipient combinations relative to artemisone mono-treatment, revealed no statistical significance (Annexure A.7, Table A.8).

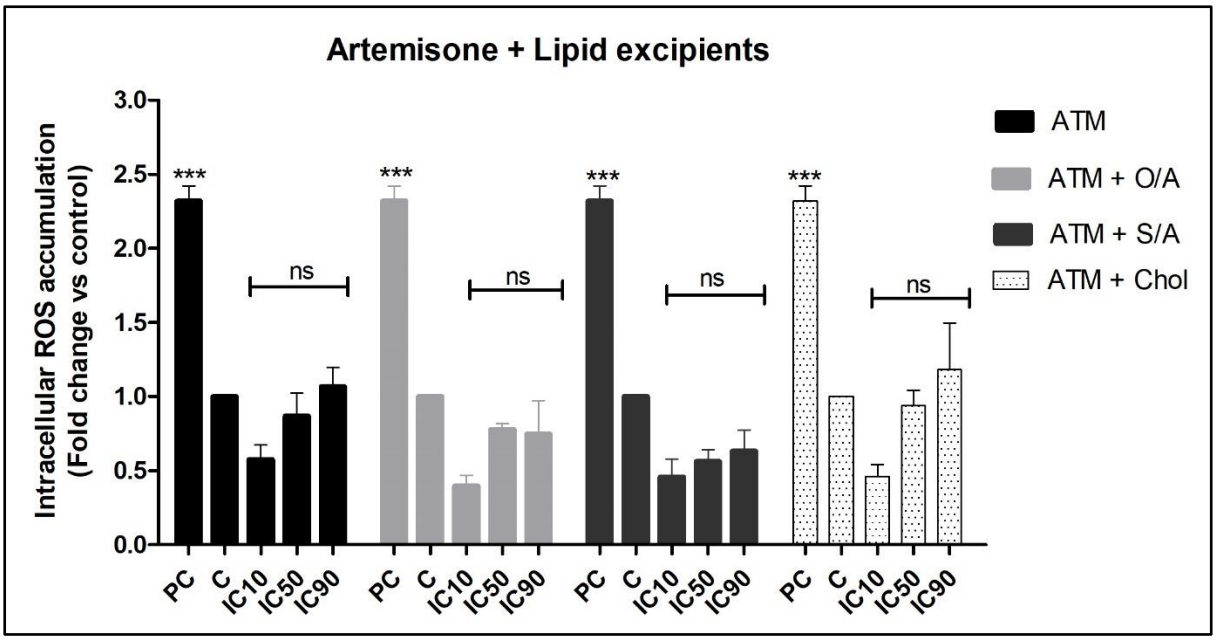

Figure 4.9: Intracellular ROS accumulation in DCFH-DA stained A375 cells after exposure to artemisone and lipid excipient combinations. Artemisone (ATM) combinations with lipid excipients, oleic acid (O/A), stearic acid (S/A) and cholesterol (Chol). Kinetic analysis measurement of fluorescence at excitation 485 nm and emission 535 nm, every 10 min for 1 h. Graphs represented as end point results expressed as a fold change relative to the control (set as 1). Hydrogen peroxide (30%) was used as a positive control (PC). Bars signify the mean and error bars denote the standard deviation (n=3). Asterisks indicate significant statistical differences in cell viability of exposed cells versus control cells (***P<0.0001). Non-significant statistical differences are indicated as ns**.**

The combination of artemisone with cholesterol displayed the most prominent effects, with IC_{50} and IC_{90} treatments resulting in a 0.9 ± 0.11-fold change; and a 1.18 ± 0.32-fold change in intracellular ROS accumulation, respectively. Cells exposure to mono-treatment with artemisone caused similar effects, with IC_{50} and IC_{90} treatments producing a 0.87 ± 0.16-fold change and a 1.07 ± 0.13-fold change in intracellular ROS accumulation, separately. ROS accumulation at IC_{10} treatment values produced no discernible significance. Combinations with both oleic acid and stearic acid, resulted in <0.5-fold changes in intracellular ROS accumulations at all concentrations.

4.6.2.2 Combination 2: Cu(II)-elesclomol with lipid excipients

The findings seen in Figure 4.10 show similar results to that observed in combination 1 (Section 4.6.2.1), indicating no significant increase in intracellular ROS accumulation (P>0.05) of cells exposed to Cu(II)-elesclomol combinations with lipid excipients relative to the untreated cell control (R^2=0.8360). Each combination displayed a dose dependant increase in

intracellular ROS accumulation (IC_{90} > IC_{50} > IC_{10}). Likewise, the intracellular ROS accumulation of lipid excipient combinations compared to Cu(II)-elesclomol mono-treatment, revealed no statistical significance (Annexure A.7, Table A.9).

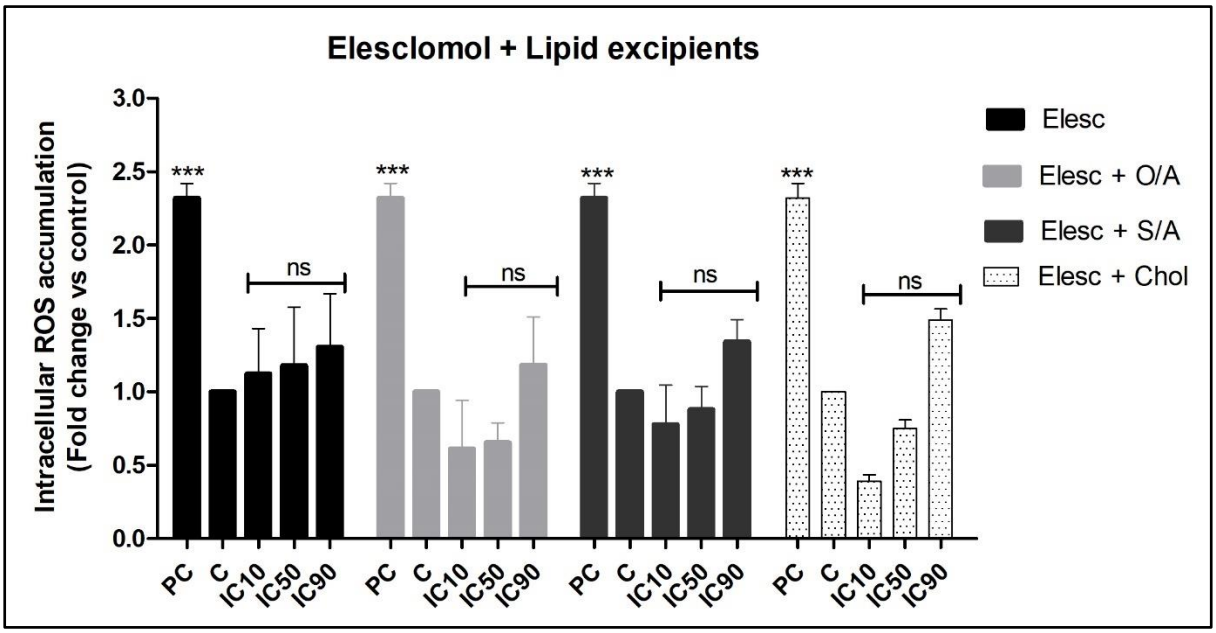

Figure 4.10: Intracellular ROS accumulation in DCFH-DA stained A375 cells after exposure to Cu(II)-elesclomol and lipid excipient combinations. Cu(II)-elesclomol (Elesc) combinations with lipid excipients, oleic acid (O/A), stearic acid (S/A) and cholesterol (Chol). Kinetic analysis measurement of fluorescence at excitation 485 nm and emission 535 nm, every 10 min for 1 h. Graphs represented as end point results expressed as a fold change relative to the control (set as 1). Hydrogen peroxide (30%) as used as a positive control (PC). Bars signify the mean and error bars denote the standard deviation (n=3). Asterisks indicate significant statistical differences in cell viability of exposed cells versus control cells (***P<0.0001). Non-significant statistical differences are indicated as ns**.**

Cell exposure to Cu(II)-elesclomol mono-treatment, generally displayed the most prominent effects causing a 1.12 ± 0.31-fold change, 1.18 ± 0.40-fold change and 1.01 ± 0.36-fold change in intracellular ROS accumulation at IC_{10}, IC_{50} and IC_{90} treatments, respectively. Combinations with oleic acid overall displayed the least prominent effects resulting in a 0.61 ± 0.23-fold change, 0.65 ± 0.40-fold change and 1.18 ± 0.32-fold change in intracellular ROS accumulation at IC_{10}, IC_{50} and IC_{90} treatments, correspondingly. Second to Cu(II)-elesclomol mono-treatment, combinations of stearic acid displayed oxidative effects provoking a 0.61 ± 0.23-fold change, 0.65 ± 0.40-fold change and 1.18 ± 0.32-fold change in intracellular ROS accumulation at IC_{10}, IC_{50} and IC_{90} treatments, individually. Combinations with cholesterol, interestingly, resulted in the lowest fold change at IC_{10} treatment; and the highest fold change at IC_{90} treatment, compared to those observed with the other combinations. At IC_{10},

cholesterol increased the intracellular ROS generation by 0.39 ± 0.03-fold, IC_{50} by 0.75 ± 0.06-fold and IC_{90} by 1.49 ± 0.07-fold.

4.6.2.3 Combination 3: Artemisone and Cu(II)-elesclomol combination with lipid excipients

Data obtained from this experiment revealed varied significance in intracellular ROS accumulation between the different combinations (Figure 4.11). Increased intracellular ROS accumulation, was found to be dose dependant (IC_{90} > IC_{50} > IC_{10}). Cells exposed to the combination treatment of artemisone and Cu(II)-elesclomol, displayed no significant increase in intracellular ROS accumulation (P>0.05), relative to the untreated cell control. Cells exposed to combination treatments of artemisone and Cu(II)-eleclomol with lipid excipients, however, illustrated significantly enhanced intracellular ROS accumulation (P<0.05), relative to the untreated cell control (R^2=0.9154).

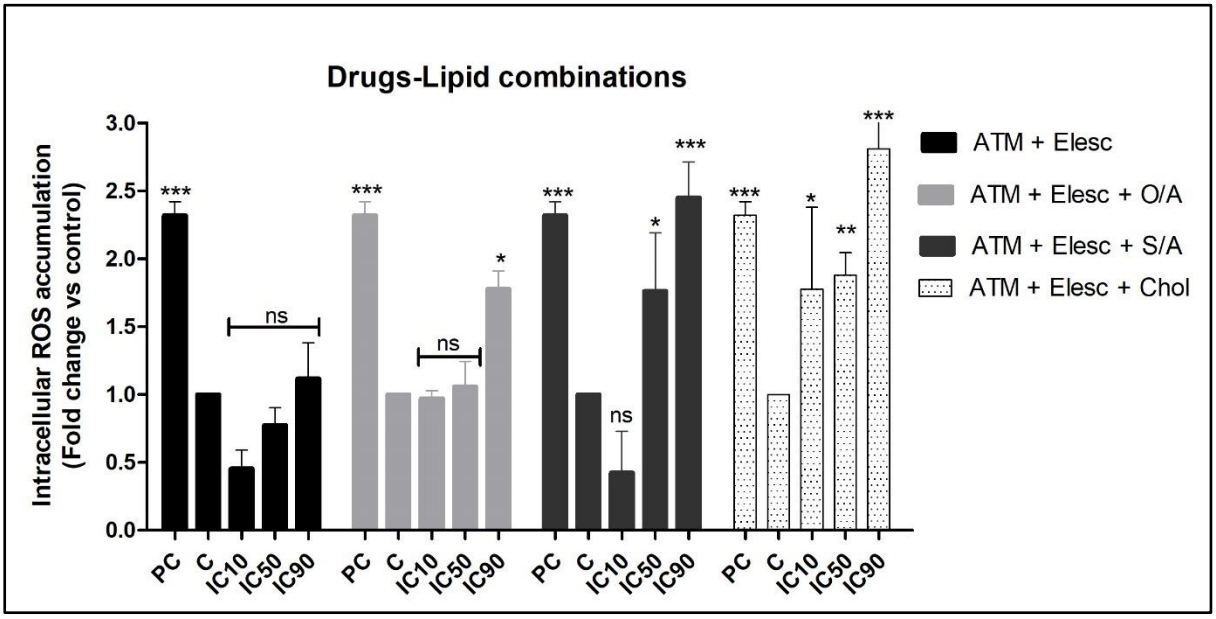

Figure 4.11: Intracellular ROS accumulation in DCFH-DA stained A375 cells after exposure to artemisone and Cu(II)-elesclomol combinations with lipid excipients. Artemisone and elesclomol combination (ATM + Elesc) with lipid excipients, oleic acid (O/A), stearic acid (S/A) and cholesterol (Chol). Kinetic analysis measurement of fluorescence at excitation 485 nm and emission 535 nm, every 10 min for 1 h. Graphs represented as end point results expressed as a fold change relative to the control (set as 1). Hydrogen peroxide (30%) as used as a positive control (PC). Bars signify the mean and error bars denote the standard deviation (n=3). Asterisks indicate significant statistical differences in cell viability of exposed cells versus control cells (***P<0.0001, **P<0.005 and *P>0.05). Non-significant statistical differences are indicated as ns**.**

Combinations with oleic acid, generally displayed the least prominent effects, compared to stearic acid and cholesterol, resulting in a non-significant ($P>0.05$) increase in intracellular ROS accumulation at IC_{10} and IC_{50} treatments, by 0.97 ± 0.06-fold and 1.06 ± 0.19-fold, respectively. On the other hand, treatment at the IC_{90}, caused a significant ($P<0.05$) increase in intracellular ROS accumulation by 1.78 ± 0.13-fold.

Combinations with stearic acid, generally depicted superior effects, compared to oleic acid, that provided a non-significant ($P>0.05$) increase in intracellular ROS accumulation at the IC_{10} treatment (0.42 ± 0.30-fold). However, cells exposed to IC_{50} and IC_{90} treatments, resulted in a significant increase in intracellular ROS accumulation, by 1.76 ± 0.43-fold ($P<0.05$), and 2.45 ± 0.27-fold ($P<0.0001$), correspondingly.

Combinations with cholesterol displayed the most prominent effects of the selected lipid excipients, producing a significant ($P<0.05$) increase in intracellular ROS accumulation at all the treatment concentrations. Results show cell exposure to IC_{10}, IC_{50} and IC_{90} treatments, resulted in increased intracellular ROS accumulation by 1.78 ± 0.60-fold ($P<0.05$), 1.88 ± 0.18-fold ($P<0.005$), and 2.81 ± 0.34-fold ($P<0.0001$), individually.

Significance in intracellular ROS accumulation relative to drug constituents indicated the following (Annexure A.8):

1. Results relative to artemisone-Cu(ll)-elesclomol:
    - IC_{10} – Drug combinations with lipid excipients oleic acid and stearic acid displayed no statistical differences ($P>0.05$). Drug combinations with cholesterol indicated a significant increase in ROS accumulation ($P=0.0044$) and resulted in a $74.72\% \pm 0.6\%$ enhanced ROS accumulation relative to the artemisone-Cu(ll)-elesclomol treated cells.
    - IC_{50} – Combinations with oleic acid prompt no statistical significance ($P>0.05$) relative to the artemisone-Cu(ll)-elesclomol treated cells. Both stearic acid and cholesterol significantly ($P<0.05$) increased ROS accumulation of $55.68\% \pm 0.43\%$, and $58.51 \pm 0.18\%$, respectively, compared to the ROS accumulated after artemisone-Cu(ll)-elesclomol exposure to cells.
    - IC_{90} – All of the combinations with oleic acid, stearic acid and cholesterol displayed a significant increase in ROS accumulation with enhanced ROS levels of $37.08\% \pm 0.13\%$ ($P<0.05$), $54.29\% \pm 0.27\%$ ($P<0.005$), and $60.14\% \pm 0.34\%$ ($P<0.0001$), separately proportionate to the artemisone-Cu(ll)-elesclomol treated cells.
2. Results corresponding to artemisone mono-treatment:

- IC_{10} – The combination of artemisone and Cu(ll)-elesclomol with cholesterol was the only combination to display a significant increase in intracellular ROS accumulation ($P<0.0016$). This combination portrayed a $67.64 \pm 0.6\%$ enhanced ROS accumulation, relative to cells exposed to artemisone mono-treatment.
- IC_{50} – The combination of artemisone and Cu(ll)-elesclomol with stearic acid and those with cholesterol, were the only combinations to depict a significant increase in intracellular ROS accumulation. These combinations caused an enhanced ROS accumulation of $50.68 \pm 0.43\%$, and $53.83 \pm 0.17\%$, respectively for stearic acid and cholesterol, proportionate to cells exposed to artemisone mono-treatment.
- IC_{90} – The combination of artemisone and Cu(ll)-elesclomol was the only treatments that did not result in a significant ($P>0.05$) increase in intracellular ROS accumulation. Combinations with lipid excipients procured an enhanced ROS accumulation of $40 \pm 0.13\%$, $56.41 \pm 0.27\%$, and $61.99 \leq 0.34\%$, individually for oleic acid, stearic acid and cholesterol, corresponding to cells exposed to artemisone mono-treatment.

3. Results proportional to Cu(ll)-elesclomol mono-treatment:
    - IC_{10} – None of the combinations displayed any statistical significance ($P>0.05$), relative to the Cu(ll)-elesclomol treated cells.
    - IC_{50} – The combination of artemisone and Cu(ll)-elesclomol with cholesterol was the only combination to display a significant ($P<0.004$) increase in intracellular ROS accumulation and produced a $37.28 \pm 0.17\%$ enhanced ROS accumulation, comparatively to cells exposed to Cu(ll)-elesclomol.
    - IC_{90} – The combination of artemisone and Cu(ll)-elesclomol with stearic acid and with cholesterol, were the only combinations illustrating a significant increase in intracellular ROS accumulation. These combinations provoked an enhanced ROS accumulation of $46.78 \pm 0.27\%$, and $53.55 \pm 0.34\%$, respectively for stearic acid and cholesterol, proportionate to cells exposed to Cu(ll)-elesclomol mono-treatment.

In summary: The results specified in this section demonstrate the intracellular ROS accumulation of artemisone, Cu(ll)-elesclomol, oleic acid, stearic acid and cholesterol combinations against A375 melanoma cells. The combinations of artemisone and Cu(ll)-elesclomol with lipid excipients (drug-drug-lipid) significantly increased the intracellular ROS accumulation within the melanoma cells compared to the other combinations in this study (drug-lipid and drug-drug). Increased ROS accumulation was found to be dose dependant, with treatments at IC_{90}, displaying the most significant effects.

4.7 References

Aykul, S. & Martinez-Hackert, E. 2016. Determination of half-maximal inhibitory concentration using biosensor-based protein interaction analysis. *Analytical Biochemistry*, 508(2016):97–103.

Bayat, M.R., Homayouni, T.S., Baluch, N., Morgatskaya, E., Kumar, S., Das, B. & Yeger, H. 2017. Combination therapy in combating cancer. *Oncotarget*, 8(23):38022–38043.

Berridge, M.V., Herst, P.M. & Tan, A.S. 2015. Tetrazolium dyes as tools in cell biology: new insights into their cellular reduction. *Biotechnology annual review*, 11(2005):127–152.

Blackman, R.K., Cheung-Ong, K., Gebbia, M., Proia, D.A., He, S., Kepros, J., Jonneaux, A., Marchetti, P., Kluza, J., Rao, P., Wada, Y., Giaever, G. & Nislow, C. 2012. Mitochondrial electron transport is the cellular target of the oncology drug elesclomol. *Plos One*, 7(1):e29798.

Dwivedi, A., Mazumder, A., du Plessis, L.H., du Preez, J.L., Haynes, R.K. & du Plessis, J. 2015. In vitro anti-cancer effects of artemisone nano-vesicular formulations on melanoma cells. Nanomedicine: Nanotechnology, Biology, and Medicine, 11(8):2041–2050.

He, Y., Zhu, Q., Chen, M., Huang, Q., Wang, W., Li, Q., Huang, Y. & Di, W. 2016. The changing 50% inhibitory concentration (IC_{50}) of cisplatin" a pilot study on the artifacts of the MTT assay and the precise measurement of density-dependant chemoresistance in ovarian cancer. *Oncotarget*, 7(43):70803–70821.

Kirshner, J.R., He, S., Balasubramanyam, V., Kepros, J., Yang, C., Zhang, M., Du, D., Barsoum, J. & Bertin, J. 2008. Elesclomol induces cancer cell apoptosis through oxidative stress. *Molecular Cancer Therapeutics*, 7(8):2319–2327.

Kupcsik, L. 2011. Estimation of cell number based on metabolic activity: the MTT reduction assay. (*In* Stoddart, M.J *ed*. Mammalian cell viability. Springer:New York. p.13–19).

Nagai, M., Vo, N.H., Ogawa, L.S., Chimmanamada, D., Inoue, T., Chu, J., Beaudette-Zlatanova, B.C., Lu, R., Blackman, R.K., Barsoum, J., Koya, K. & Wada, Y. 2012. The oncology drug elesclomol selectively transports copper to the mitochondria to induce oxidative stress in cancer cells. *Free Radical Biology and Medicine,* 52(2012):2142–2150.

Simões, M.C.F., Sousa, J.J.S. & Pais, A.A.C.C. 2014. Skin cancer and new treatment perspectives: a review. *Cancer Letters*, 357(2015):8–42.

Tice, R.R., Agurell, E., Anderson, D., Burlinson, B., Hartmann, A., Konayashi, H., Miyamae, Y., Rojas, E., Ruy, J.C. & Sasaki, Y.F. 2000. Single-cells gel/comet assay: guidelines for *in vivo* and *in vitro* toxicology testing. *Environmental and molecular mutagenesis*, 35(3):206–221.

Trachootham, D., Alexandre, J. & Huang, P. 2009. Targeting cancer cells by ROS-mediated mechanisms: a radical therapeutic approach? *Nature reviews: Drug discovery*, 8(7):579–591.

Weber, S., Zimmer, A. & Pardeike, J. 2014. Solid lipid nanoparticles (SLN) and nanostructured lipid carriers (NLP) for pulmonary application: a review of the state of the art. *European Journal of Pharmaceutics and Biopharmaceutics*, 86(1):7–22.

Wondrak, G.T. 2009. Redox-directed cancer therapeutics: molecular mechanisms and opportunities. *Antioxidants & Redox Signalling,* 11(12):3013–3069.

Yingchoncharoen, P., Kalinowski, D.S. & Richardson, D.R. 2016. Lipid-based delivery systems in cancer: what is available and what is yet to come. *Pharmacological Reviews*, 68(3):701–787.

CHAPTER 5

IN VITRO CYTOTOXICITY ANALYSIS AGAINST HUMAN MELANOMA CELLS

CONCLUSION & FUTURE RECOMMENDATIONS

5.1 Concluding discussion

Genetic alterations in the redox status of cancer cells, promote a continuous and elevated production of ROS, associated in the initiation and progression of tumours (Trachootham *et al*., 2009; Wondrak, 2009). The body's potent antioxidant system effectively neutralises ROS produced in normal cells, however, owing to high metabolic rates of cancer cells, ROS is generated at levels beyond the capacity of this antioxidant system. Many cancers are characterised by poor prognosis and high mortality, despite extensive research and substantial efforts for developing targeted cancer chemotherapeutics (Panieri & Santoro, 2016). Skin cancer represents the most frequent occurring cancers and melanoma, the leading cause of skin cancer related deaths (Lewies *et al*., 2017; Simões *et al*., 2015). Breakthroughs in chemotherapeutics have been achieved in certain cancers, though marginal advances have been made in treatments for other malignancies such as metastatic melanomas (Wondrak, 2009). Strategies aimed at altering redox dysregulation in the presence of ROS inducers, present a promising new approach to cancer chemotherapeutics. This can be achieved by elevating oxidative stress beyond the toxicity threshold of cancer cells, sparing normal cells (Panieri & Santoro, 2016).

This study aimed to investigate the *in vitro* cytotoxic activity and intracellular ROS-generation of artemisone and elesclomol in combination with selected lipid excipients, oleic acid, stearic acid and cholesterol. Redox directed combinations were investigated in which artemisone and Cu(ll)-elesclomol were combined, for the first time, to potentially target hypoxic and proliferating cancer cells based on the susceptibility of cancer cells to oxidative stress. Further reduced toxicity and enhanced selectivity of chemotherapeutic agents was investigated by combining lipid excipients, oleic acid, stearic acid and cholesterol with artemisone and Cu(ll)-elesclomol.

The MTT assay was employed to evaluate the metabolic activity of melanoma cells and to draw conclusions on cell proliferation, viability and cytotoxicity (Shoemaker, 2006). The *in vitro* efficacy of each constituent used in this study, was investigated. Artemisone and elesclomol (alone and copper-bound) displayed toxic effects broadly consistent with existing research.

The results obtained with the MTT assay indicates that artemisone suppresses melanoma cell growth in a dose dependant manner, with a IC_{50} value of 143.5 µM. These observations are in line with previous findings of artemisone's toxicity on A375 melanoma cells, wherein Dwivedi and collaborators (2015), showed similar effects of artemisone against A375 cells at a IC_{50} of 149.43 µM. The findings of elesclomol alone and bound to copper, showed coherent to existing literature. The results underlined the significance of copper for elesclomol to be able to exhibit cytotoxic effects. Nagai *et al*. (2012) first found that elesclomol displayed no cytotoxic activity if not bound to copper. Observations in this study showed Cu(ll)-elesclomol to display significant toxicity against A375 melanoma cells, opposed to elesclomol to be non-toxic. The concentration copper used in this study, 10 µM copper sulphate (per 20 nM elesclomol), displayed similar toxicity relative to 10 µM copper chloride, used in other studies of Cu(ll)-elesclomol (Yadav *et al*., 2013). Studies on the efficacy of the selected lipid excipients against A375 melanoma cells, demonstrates cytotoxic effects at 225–3600 µM. Stearic acid generally displayed the most potent cytotoxicity, followed by cholesterol then oleic acid.

One of the objectives was to establish the inhibiting concentrations of artemisone and Cu(ll)-elesclomol at 10%, 50% and 90%. As mentioned earlier, the IC_{50} value of artemisone was found to be broadly consistent with results relating to existing research. The IC_{10}, IC_{50} and IC_{90} values for artemisone was calculated at 26.5 µM, 143.52 µM and 588 µM, respectively. Results describe for the first time the IC_{50} value of Cu(ll)-elesclomol against A375 melanoma cells. The IC_{10}, IC_{50} and IC_{90} values for Cu(ll)-elesclomol was calculated at 0.295 nM, 5.53 nM and 9.69 nM, respectively.

Combination therapy of two or more constituents that yield similar effects, exploits the chances for enhanced efficacy, ameliorated toxicity and decreased occurrence of drug resistance (Foucquier & Guedj, 2015; Tallarida, 2011). This approach has been applied in several developmental chemotherapeutic therapies involving redox combinations, in an attempt to enhance the actions of the anticancer agents (Wondrak, 2009). This study attempted to develop synergistic combinations that targets hypoxic and proliferated cancer cells, relying on cancer cell's susceptibility to oxidative stress. The main objective of this study, was evaluating the efficacy of the combinations relative to the percentage cell viability and intracellular ROS accumulation on A375 melanoma cells.

Combinations of artemisone with lipid excipients resulted in enhanced cytotoxicity relative to the untreated control, however, only at the IC_{90} treatment displayed significance relative to artemisone. The conclusion can be made that combinations of lipid excipients enhances the *in vitro* efficacy of artemisone at high concentrations. No significant increase in the intracellular ROS generation was observed with regard to these combinations. Combinations of Cu(ll)-

elesclomol with lipid excipients resulted in a dose-dependent reduction in cell viability and enhanced cytotoxicity relative to the untreated control, however, only IC_{50} and IC_{90} treatments, displayed significance relative to Cu(II)-elesclomol treated cells. The conclusion can be made that combinations of lipid excipients enhances the *in vitro* efficacy of Cu(II)-elesclomol at moderate to high concentrations. No significant increase in the intracellular ROS generation was observed with regard to these combinations. Combinations with lipid excipients displayed enchantment of drug constituents, artemisone and Cu(II)-elesclomol. Combinations with oleic acid, resulted in the most significant reduction in cell viability of melanoma cells, then combinations with cholesterol. Combinations with stearic acid, displayed the least prominent reduction in cell viability, compared to the other lipids. Low ROS levels may be an indicative of apoptosis, whereas high ROS levels are often associated necrosis or caspase-independent apoptosis pathways (Lewies *et al*., 2017). Therefore, the cytotoxic effects observed in reduced cell viability of melanoma cells, may possibly attributed to apoptosis

Novel combinations of artemisone and Cu(II)-elesclomol with lipid excipients, displayed varied efficacy relative to the untreated cells, artemisone–Cu(II)-elesclomol treated cells, artemisone treated cells and Cu(II)-elesclomol treated cells. Combinations are said to be synergistic when the combined effect is greater than individual potencies of each constituent (Foucquier & Guedj, 2015; Tallarida, 2011). Results gained from the MTT assay, showed synergism of drug constituents and lipid excipients when in combination at specific concentrations. Firstly, cholesterol displayed synergism at IC_{10} and IC_{50} treatments, relative to the artemisone–Cu(II)-elesclomol combination, whereas oleic acid and stearic acid only displayed synergism at the IC_{50} treatment (stearic acid > cholesterol > oleic acid). Synergism, relative to artemisone monotreatment and elesclomol monotreatment, was shown in lipid combinations at IC_{50} and IC_{90} treatments. The DCFH-DA oxidative stress assay, generally showed synergism of combinations at IC_{50} and IC_{90} treatments. Combinations with cholesterol generally showed the most significant increase in intracellular ROS accumulation followed by stearic acid then oleic acid, relative to artemisone–Cu(II)-elesclomol treatments, artemisone monotreatment, as well as Cu(II)-elesclomol monotreatment.

To summarise and conclude, the main findings in this study indicate the neglectable synergism between artemisone and Cu(II)-elesclomol combinations against A375 melanoma cells, however, when combined with lipid excipients, oleic acid, steric acid or cholesterol, significant synergistic effects are induced. It is evident that each of the constituents have potential anticancer activity against A375 melanoma cells, however, the optimum concentrations and combinations are yet to be established. This project provides further new information regarding the effects of artemisone, Cu(II)-elesclomol, oleic acid, stearic acid and cholesterol, specific to

A375 melanoma cells. The study shows the sensitivity of different combinations of drug and lipid excipients against melanoma cells and their effects enhancing toxicity and oxidative stress. The benefits of this study primarily relate novel combinations of artemisone, Cu(II)-elesclomol and lipid excipients for cancer treatment.

5.2 Future recommendations

This study describes the cytotoxicity and ROS generation of drug–lipid combinations, never been considered before, comprising of artemisone, Cu(II)-elesclomol, oleic acid, stearic acid and cholesterol, using the MTT assay and the DCFH-DA assay. The MTT assay is a widely adopted and popular method to estimate the *in* vitro cell viability of cultured cells, however, other cell viability assays offer much greater sensitivity compared to the MTT assay (Berridge *et al*., 2015). Studies have shown liposome delivering drugs (lipid composition) could produce inconsistent values of MTT absorbance. Furthermore, it has been suggested that ROS may affect the MTT assay (Angius & Floris, 2014). Because this study focused on combinations with lipid excipients and cell death resultant from elevated ROS level, it is recommended that an alternative assay to the MTT assay, like the Neutral Red assay, should be employed to investigate cell viability. Gomez Perez and collaborators (2017) showed that copper-bound compounds may interfere with the MTT assay, whereas the Neutral Red assay, appears to display no interference and increased sensitivity for cell viability determination. Cytotoxicity was shown in most of the combinations in this study, however, the exact mode of cells death is yet to be determined. To further validate the observed cytotoxic effects, the Annexin V assay may be employed in future studies to establish whether cell death was a result of apoptosis or necrosis.

This study showed evidence indicating enhanced effect of anticancer agents, artemisone and Cu(II)-elesclomol using combinations of lipid excipients, oleic acid, stearic acid and cholesterol. The concentration of the lipids was fixed at 45 µM for all experiment. It is worth exploring other concentrations in combination with artemisone and Cu(II)-elesclomol. Additionally, lipids from other classes, such as waxes (cetyl palmitate) and triglycerides (tristearin), could also be investigated for their potential in redox combination therapies. Topical and transdermal drug delivery systems have gained much interest in new approaches towards cancer chemotherapy (Haque *et al.*, 2015). Since lipid excipients are popular constituents of topical and transdermal drug delivery systems, exploring the combinations used in this study for their efficacy in topical or transdermal delivery.

Considering the anticancer activity of the combinations used in this study against A375 melanoma cells, it is also recommended that similar studies be performed on other skin cancer lines as well as non-cancerous cell cultures, and *in vivo* melanoma models.

5.3 References

Angius, F. & Floris, A. 2014. Liposomes and MTT cell viability assay: an incompatible affair. *Toxicology in vitro*, 29(2):314–319.

Berridge, M.V., Herst, P.M. & Tan, A.S. 2015. Tetrazolium dyes as tools in cell biology: new insights into their cellular reduction. *Biotechnology annual review*, 11(2005):127–152.

Dwivedi, A., Mazumder, A., du Plessis, L.H., du Preez, J.L., Haynes, R.K. & du Plessis, J. 2015. In vitro anti-cancer effects of artemisone nano-vesicular formulations on melanoma cells. Nanomedicine: Nanotechnology, Biology, and Medicine, 11(8):2041–2050.

Foucquier, J. & Guedj, M. 2015. Analysis of drug combinations: current methodological landscape. *Pharmacy Research & Prespectives*, 3(3):e00149.

Lewies, A., Wentzel, J.F., Van Dyk, H. & Du Plessis, L.H. 2017. The antimicrobial peptide nisin Z induces selective toxicity and apoptotic cell death in cultured melanoma cells. *Biochimie*, 10.1016/j.biochi.2017.10.009 Date of access: 4 Nov. 2017.

Krishner, J.R., He, S., Balasubramanyam, V., Kepros, J., Yang, C., Zhang, M., Du, D., Barsoum, J. & Bertin, J. 2008. Elesclomol induces cancer cell apoptosis through oxidative stress. *Molecular Cancer Therapeutics*, 7(8):2319–2327.

Nagai, M., Vo, N.H., Ogawa, L.S., Chimmanamada, D., Inoue, T., Chu, J., Beaudette-Zlatanova, B.C., Lu, R., Blackman, R.K., Barsoum, J., Koya, K. & Wada, Y. 2012. The oncology drug elesclomol selectively transports copper to the mitochondria to induce oxidative stress in cancer cells. *Free Radical Biology and Medicine,* 52(2012):2142–2150.

Panieri, E. & Santoro, M,M. 2016. ROS homeostasis and metabolism: a dangerous liason in cancer cells. *Cell death & disease*, 7(6):e2253.

Simões, M.C.F., Sousa, J.J.S. & Pais, A.A.C.C. 2014. Skin cancer and new treatment perspectives: a review. *Cancer Letters*, 357(2015):8–42.

Tallarida, R.J. 2011. Quantitative methods for assessing drug synergism. *Genes & Cancer*, 2(11):1003–1008.

Trachootham, D., Alexandre, J. & Huang, P. 2009. Targeting cancer cells by ROS-mediated mechanisms: a radical therapeutic approach? *Nature reviews: Drug discovery*, 8(7):579–591.

Wondrak, G.T. 2009. Redox-directed cancer therapeutics: molecular mechanisms and opportunities. *Antioxidants & Redox Signalling,* 11(12):3013–3069.

Yadav, A.A., Patel, D., Wu, X. & Hasinoff, B.B. 2013. Molecular mechanism of the biological activity of the anticancer drug elesclomol and its complexes with Cu(ll), Ni(ll) and Pt(ll). *Journal of Inorganic Biochemistry,* 126(2013):1–6.

ANNEXURE A: SUPPLEMENTARY RESULTS

A.1 Optimisation of lipid excipient concentration

Table A.1: Cell viability (%) of melanoma cells after exposure to oleic acid.

Concentration (µM)	% Cell viability of A375 melanoma cells				SD	%RSD
	N=1	N=2	N=3	Mean		
720	0.76	0.76	1.27	0.93	0.29	31.66
360	1.77	1.74	2.41	1.97	0.38	19.18
180	2.41	2.41	2.57	2.46	0.09	3.75
90	2.89	2.57	2.88	2.78	0.18	6.54
45	**35.65**	**23.11**	**37.71**	**32.16**	**7.9**	**24.57**
22.5	56.03	56.72	56.92	56.56	0.47	0.83
11.25	57.33	63.67	61.02	60.67	3.18	5.25
5.625	63.67	64.35	70.24	66.09	3.61	5.47
2.8	69.03	65.29	64.35	66.22	2.47	3.74
1.4	73.77	74.06	71.87	73.23	1.19	1.62
0.7	81.50	80.01	76.03	79.18	2.82	3.57

A.2 Experimental controls

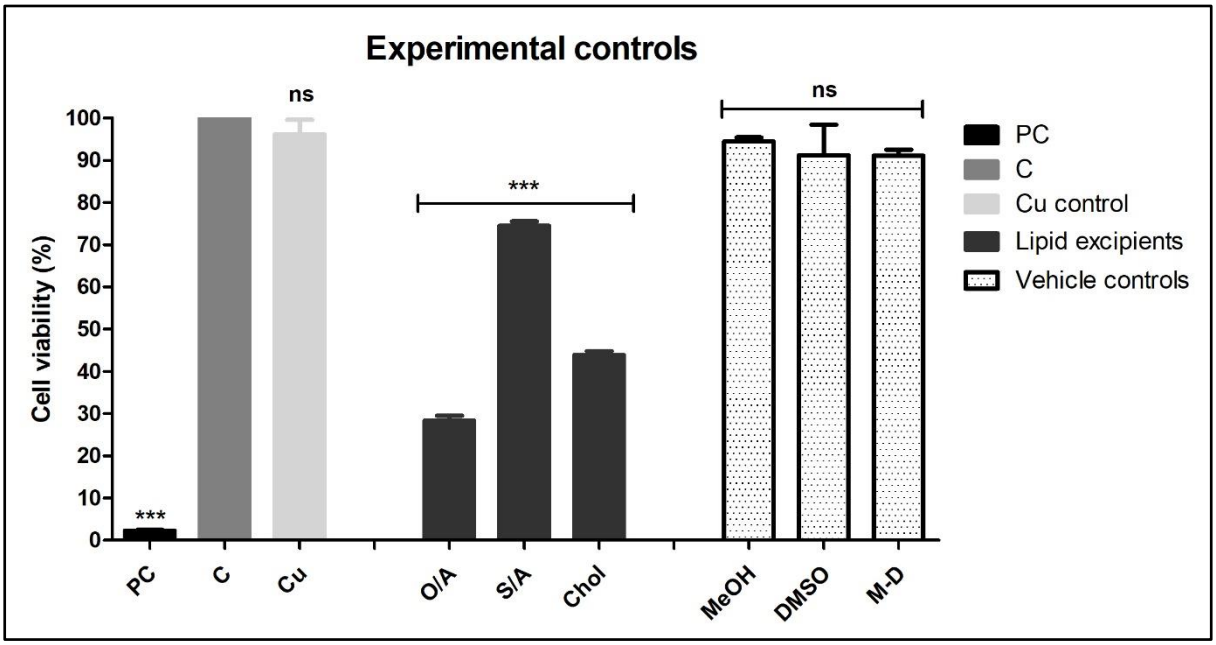

Figure A.1: Cytotoxic effects against A375 cells following exposure to the experimental controls. The percentage cell viability determined by the MTT assay over a period of 24 h, expressed relative to the untreated control (C), which was set at 100% viable. Triton X-100 (0.01%) was used as a positive control (PC). The obtained percentage cell viability given for each experimental control: copper (Cu) at 10 µM, lipid excipients, oleic acid (O/A), stearic acid (S/A) and cholesterol (Chol) at 45 µM and solvents methanol (MeOH), dimethyl sulfoxide (DMSO) and methanol-DMSO combination (M-D). Bars signify the mean and error bars signify the standard deviation (n=3). Asterisks indicate significant statistical differences in cell viability of exposed cells versus control cells (***P<0.0001 and *P<0.05).

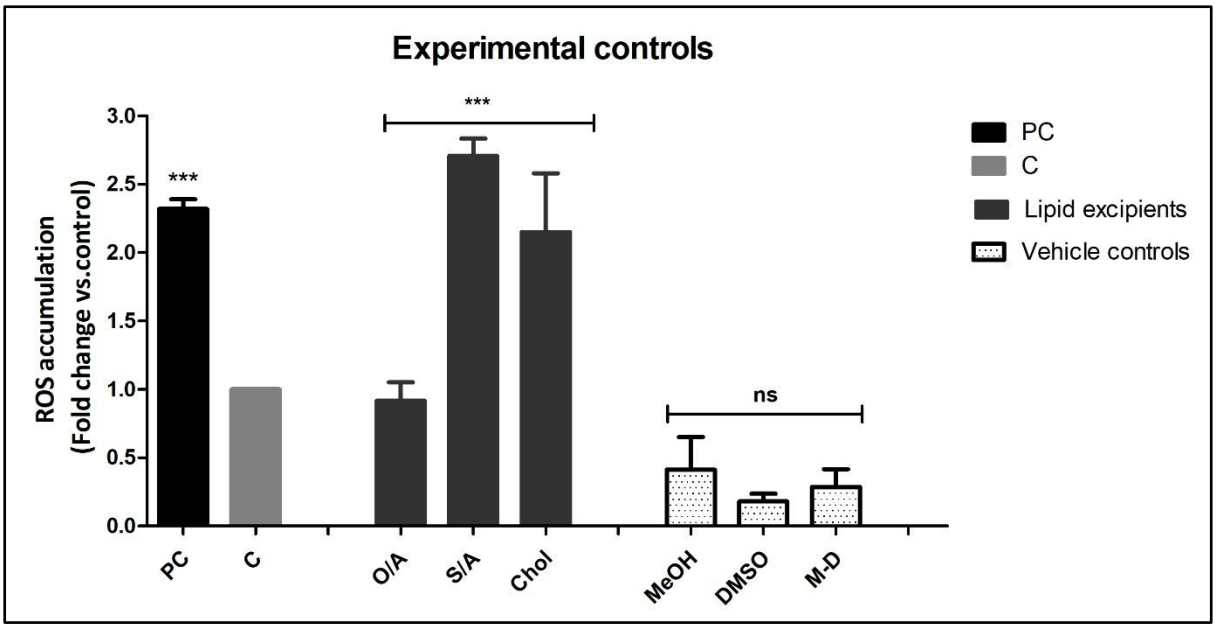

Figure A.2: Intracellular ROS accumulation in DCFH-DA stained A375 cells after exposure to the experimental controls. Kinetic analysis measurement of fluorescence at excitation 485 nm and emission 535 nm, every 10 min for 1 h. Graphs represented as end point results expressed as a fold change relative to the control (set as 1). Hydrogen peroxide (30%) as used as a positive control (PC). The intracellular ROS accumulation given for each experimental control: copper (Cu) at 10 µM, lipid excipients, oleic acid (O/A), stearic acid (S/A) and cholesterol (Chol) at 45 µM and solvents methanol (MeOH), dimethyl sulfoxide (DMSO) and methanol-DMSO combination (M-D). Bars signify the mean and error bars signify the standard deviation (n=3). Asterisks indicate significant statistical differences in cell viability of exposed cells versus control cells (***P<0.0001). Non-significant statistical differences are indicated as ns**.**

A.3 One-way ANOVA analysis of combination treatments relative to untreated control, with Dunnett post-test – *In vitro* assessment of cell viability

Table A.2: One-way ANOVA of melanoma cells exposed to artemisone and lipid excipient combinations after 24 h, relative to untreated cell control.

One-way analysis of variance					
P value	P<0.0001				
P value summary	***				
Are means signif. different? (P < 0.05)	Yes				
Number of groups	14				
F	504,7				
R squared	0,9965				
ANOVA Table	**SS**	**df**	**MS**		
Treatment (between columns)	44590	13	3430		
Residual (within columns)	156,3	23	6,796		
Total	44750	36			
Dunnett's Multiple Comparison Test	**Mean Diff.**	**q**	**Significant? P < 0.05?**	**Summary**	**95% CI of diff**
C vs PC	97,72	45,91	Yes	***	91.27 to 104.2
C vs ATM IC10	28,73	12,07	Yes	***	21.51 to 35.95
C vs ATM IC50	31,15	14,63	Yes	***	24.69 to 37.60
C vs ATM IC90	82,18	38,61	Yes	***	75.73 to 88.64
C vs ATM + O/A IC10	16,62	6,983	Yes	***	9.401 to 23.84
C vs ATM + O/A IC50	33,23	13,96	Yes	***	26.01 to 40.45
C vs ATM + O/A IC90	97,97	46,03	Yes	***	91.52 to 104.4
C vs ATM + S/A IC10	29,38	13,80	Yes	***	22.92 to 35.83
C vs ATM + S/A IC50	38,32	18,00	Yes	***	31.86 to 44.78
C vs ATM + S/A IC90	95,34	44,79	Yes	***	88.88 to 101.8
C vs ATM + Chol IC10	25,68	10,79	Yes	***	18.46 to 32.90
C vs ATM + Chol IC50	36,34	15,27	Yes	***	29.12 to 43.55
C vs ATM + Chol IC90	96,87	45,51	Yes	***	90.41 to 103.3

Table A.3: One-way ANOVA of melanoma cells exposed to Cu(II)-elesclomol and lipid excipient combinations after 24 h, relative to untreated cell control.

One-way analysis of variance					
P value	P<0.0001				
P value summary	***				
Are means signif. different? (P < 0.05)	Yes				
Number of groups	14				
F	242,7				
R squared	0,9912				
ANOVA Table	**SS**	**df**	**MS**		
Treatment (between columns)	47350	13	3642		
Residual (within columns)	420,3	28	15,01		
Total	47770	41			
Dunnett's Multiple Comparison Test	**Mean Diff.**	**q**	**Significant? P < 0.05?**	**Summary**	**95% CI of diff**
C vs PC	97,72	30,89	Yes	***	88.27 to 107.2
C vs Elesc IC10	30,79	9,734	Yes	***	21.34 to 40.24
C vs Elesc IC50	31,15	9,846	Yes	***	21.69 to 40.60
C vs Elesc IC90	82,18	25,98	Yes	***	72.73 to 91.64
C vs Elesc + O/A IC10	19,38	6,125	Yes	***	9.923 to 28.83
C vs Elesc + O/A IC50	29,38	9,289	Yes	***	19.93 to 38.84
C vs Elesc + O/A IC90	97,97	30,97	Yes	***	88.52 to 107.4
C vs Elesc + S/A IC10	29,38	9,287	Yes	***	19.92 to 38.83
C vs Elesc + S/A IC50	38,32	12,11	Yes	***	28.87 to 47.77
C vs Elesc + S/A IC90	95,34	30,14	Yes	***	85.88 to 104.8
C vs Elesc + Chol IC10	28,04	8,864	Yes	***	18.59 to 37.49
C vs Elesc + Chol IC50	32,90	10,40	Yes	***	23.45 to 42.36
C vs Elesc + Chol IC90	96,87	30,62	Yes	***	87.41 to 106.3

Table A.4: One-way ANOVA of melanoma cells exposed to artemisone, Cu(II)-elesclomol and lipid excipient combinations after 24 h, relative to untreated cell control.

One-way analysis of variance					
P value	P<0.0001				
P value summary	***				
Are means signif. different? (P < 0.05)	Yes				
Number of groups	14				
F	325,6				
R squared	0,9939				
ANOVA Table	**SS**	**df**	**MS**		
Treatment (between columns)	55620	13	4279		
Residual (within columns)	341,7	26	13,14		
Total	55960	39			
Dunnett's Multiple Comparison Test	**Mean Diff.**	**q**	**Significant? P < 0.05?**	**Summary**	**95% CI of diff**
C vs PC	97,72	33,02	Yes	***	88.83 to 106.6
C vs A+E IC10	24,77	8,369	Yes	***	15.88 to 33.66
C vs A+E IC50	80,92	27,34	Yes	***	72.03 to 89.81
C vs A+E IC90	98,48	33,27	Yes	***	89.59 to 107.4
C vs A+E + O/A IC10	9,902	3,345	Yes	*	1.009 to 18.79
C vs A+E + O/A IC50	97,72	33,02	Yes	***	88.83 to 106.6
C vs A+E + O/A IC90	98,35	33,23	Yes	***	89.46 to 107.2
C vs A+E + S/A IC10	29,88	9,029	Yes	***	19.94 to 39.82
C vs A+E S/A IC50	98,33	33,22	Yes	***	89.43 to 107.2
C vs E + S/A IC90	98,57	29,79	Yes	***	88.63 to 108.5
C vs A+E + Chol IC10	43,54	14,71	Yes	***	34.64 to 52.43
C vs A+E + Chol IC50	98,10	33,14	Yes	***	89.21 to 107.0
C vs A+E + Chol IC90	98,33	33,22	Yes	***	89.43 to 107.2

A.4 One-way ANOVA analysis of combinations relative to artemisone treated cells, with Dunnett post-test Non-analytical experimental procedures – *In vitro* assessment of cell viability

Table A.5: One-way ANOVA of melanoma cells exposed to artemisone and lipid excipient combinations after 24 h, relative to artemisone.

One-way analysis of variance	IC10	**IC50**	IC90		
P value	P<0.0001	0.0806	P<0.0001		
P value summary	***	ns	***		
Are means signif. different? (P < 0.05)	Yes	No	Yes		
Number of groups	4	4	4		
F	1060	3.710	61.86		
R squared	0,9981	0.6497	0,9587		
Dunnett's Multiple Comparison Test	**Mean Diff.**	**SD**	**Significant ? P < 0.05?**	**Summary**	**95% CI of diff**
ATM IC10 vs ATM + O/A IC10	-12.11	6.53	Yes	**	-17.85 to -6.37
ATM IC10 vs ATM + S/A IC10	0.65	0.38	No	Ns	-4.60 to 5.89
ATM IC10 vs ATM + Chol IC10	68.14	40.30	Yes	***	62.90 to 73.38
ATM IC50 vs ATM + O/A IC50	2.08	0.66	No	Ns	-7.67 to 11.83
ATM IC50 vs ATM + S/A IC50	7.17	2.55	No	Ns	-1.55 to 15.90
ATM IC50 vs ATM + Chol IC50	-2.47	0.79	No	Ns	-12.23 to 7.28
ATM IC90 vs ATM + O/A IC90	15.79	11.95	Yes	***	11.98 to 19.60
ATM IC90 vs ATM + S/A IC90	13.15	9.95	Yes	***	9.35 to 16.96
ATM IC90 vs ATM + Chol IC90	14.68	11.11	Yes	***	10.88 to 18.49

A.5 One-way ANOVA analysis of drug-lipid combinations relative to Cu(II)-elesclomol treated cells, with Dunnett post-test Non-analytical experimental procedures – *In vitro* assessment of cell viability

Table A.6: One-way ANOVA of melanoma cells exposed to Cu(II)-elesclomol and lipid excipient combinations after 24 h, relative to Cu(II)-elesclomol.

One-way analysis of variance	IC10	IC50	IC90		
P value	0.40	P<0.0001	0.0018		
P value summary	ns	***	**		
Are means signif. different? (P < 0.05)	No	Yes	Yes		
Number of groups	4	4	4		
F	1.199	115.8	18.97		
R squared	0,9841	0.9830	0.9046		
Dunnett's Multiple Comparison Test	**Mean Diff.**	**SD**	**Significant? P < 0.05?**	**Summary**	**95% CI of diff**
Elesc IC10 vs Elesc + O/A IC10	-1.12	0.22	No	ns	-17.76 to 15.52
Elesc IC10 vs Elesc + S/A IC10	6.13	1.21	No	ns	-10.51 to 22.78
Elesc IC10 vs Elesc + Chol IC10	-2.26	0.45	No	ns	-17.45 to 12.94
Elesc IC50 vs Elesc + O/A IC50	56,77	18,33	Yes	***	47.17 to 66.37
Elesc IC50 vs Elesc + S/A IC50	31,32	11,08	Yes	***	22.56 to 40.08
Elesc IC50 vs Elesc + Chol IC50	36,36	12,86	Yes	***	27.60 to 45.12
Elesc IC90 vs Elesc + O/A IC90	28,66	6,465	Yes	**	14.92 to 42.40
Elesc IC90 vs Elesc + S/A IC90	18,99	4,791	Yes	**	6.705 to 31.28
Elesc IC90 vs Elesc + Chol IC90	26,78	6,042	Yes	**	13.04 to 40.52

A.6 One-way ANOVA analysis of drug-lipid combinations relative to drug constituents, with Dunnett post-test Non-analytical experimental procedures – *In vitro* assessment of cell viability

Table A.7: One-way ANOVA of melanoma cells exposed to drug-lipid combinations after 24 h, relative to artemisone–Cu(II)-elesclomol.

One-way analysis of variance	**IC10**	**IC50**	**IC90**		
P value	0,0038	P<0.0001	0,1573		
P value summary	**	***	ns		
Are means signif. different? (P < 0.05)	Yes	Yes	No		
Number of groups	4	4	4		
F	11,97	397,6	2,686		
R squared	0,8368	0,9942	0,6171		
Dunnett's Multiple Comparison Test	**Mean Diff.**	**q**	**Significant? P < 0.05?**	**Summary**	**95% CI of diff**
ATM-Elesc IC10 vs Oleic acid	-14,87	2,63	No	ns	-31.70 to 1.96
ATM-Elesc IC10 vs Stearic acid	5,11	0,81	No	ns	-13.71 to 23.93
ATM-Elesc IC10 vs Cholesterol	18,77	3,31	Yes	*	1.93 to 35.60
ATM-Elesc IC50 vs Oleic acid	16,80	28,19	Yes	***	15.03 to 18.57
ATM-Elesc IC50 vs Stearic acid	17,29	25,94	Yes	***	15.31 to 19.27
ATM-Elesc IC50 vs Cholesterol	17,18	28,82	Yes	***	15.41 to 18.95
ATM-Elesc IC90 vs Oleic acid	0,13	1,06	No	ns	-0.27 to 0.53
ATM-Elesc IC90 vs Stearic acid	0,28	2,32	No	ns	-0.12 to 0.69
ATM-Elesc IC90 vs Cholesterol	-0,05	0,46	No	ns	-0.46 to 0.35

A.7 One-way ANOVA analysis of combination treatments relative to untreated control, with Dunnett post-test – Oxidative stress targeting in skin cancer

Table A.8: One-way ANOVA of melanoma cells exposed to artemisone and lipid excipient combinations after 24 h, relative to untreated cell control.

One-way analysis of variance					
P value	P<0.0001				
P value summary	***				
Are means signif. different? (P < 0.05)	Yes				
Number of groups	14				
F	23.63				
R squared	0,9389				
ANOVA Table	**SS**	**df**	**MS**		
Treatment (between columns)	6.523	13	0.5018		
Residual (within columns)	0.4248	20	0.02124		
Total	6.948	3			
Dunnett's Multiple Comparison Test	**Mean Diff.**	**q**	**Significant ? P < 0.05?**	**Summary**	**95% CI of diff**
C vs PC	-1,32	9,92	Yes	***	-1.72 to -0.91
C vs ATM IC10	0,42	3,18	Yes	*	0.01 to 0.83
C vs ATM IC50	0,13	1,11	No	ns	-0.23 to 0.49
C vs ATM IC90	-0,07	0,57	No	ns	-0.43 to 0.29
C vs ATM + O/A IC10	0,60	4,53	Yes	**	0.19 to 1.01
C vs ATM + O/A IC50	0,22	1,67	No	ns	-0.18 to 0.63
C vs ATM + O/A IC90	0,25	1,89	No	ns	-0.15 to 0.65
C vs ATM + S/A IC10	0,54	4,56	Yes	**	0.17 to 0.90
C vs ATM + S/A IC50	0,43	3,67	Yes	*	0.07 to 0.80
C vs ATM + S/A IC90	0,29	2,24	No	ns	-0.11 to 0.70
C vs ATM + Chol IC10	0,53	4,05	Yes	**	0.13 to 0.94
C vs ATM + Chol IC50	0,06	0,46	No	ns	-0.34 to 0.46
C vs ATM + Chol IC90	-0,18	1,52	No	ns	-0.54 to 0.18

Table A.9: One-way ANOVA of melanoma cells exposed to Cu(II)-elesclomol and lipid excipient combinations after 24 h, relative to untreated cell control.

One-way analysis of variance					
P value	P<0.0001				
P value summary	***				
Are means signif. different? (P < 0.05)	Yes				
Number of groups	14				
F	7.842				
R squared	0,8360				
ANOVA Table	**SS**	**df**	**MS**		
Treatment (between columns)	6.395	13	0.4920		
Residual (within columns)	1.255	20	0.06274		
Total	7.650	33			
Dunnett's Multiple Comparison Test	**Mean Diff.**	**q**	**Significant ? P < 0.05?**	**Summary**	**95% CI of diff**
C vs PC	-1,32	5,77	Yes	***	-2.02 to -0.61
C vs Elesc IC10	-0,12	0,60	No	ns	-0.75 to 0.50
C vs Elesc IC50	-0,17	0,87	No	ns	-0.80 to 0.44
C vs Elesc IC90	-0,30	1,49	No	ns	-0.93 to 0.32
C vs Elesc + O/A IC10	0,38	1,89	No	ns	-0.24 to 1.01
C vs Elesc + O/A IC50	0,34	1,51	No	ns	-0.35 to 1.04
C vs Elesc + O/A IC90	-0,18	0,80	No	ns	-0.88 to 0.51
C vs Elesc + S/A IC10	0,22	0,97	No	ns	-0.47 to 0.92
C vs Elesc + S/A IC50	0,12	0,52	No	ns	-0.58 to 0.82
C vs Elesc + S/A IC90	-0,34	1,49	No	ns	-1.04 to 0.36
C vs Elesc + Chol IC10	0,61	2,67	No	ns	-0.09 to 1.31
C vs Elesc + Chol IC50	0,24	1,09	No	ns	-0.45 to 0.95
C vs Elesc + Chol IC90	-0,48	2,39	No	ns	-1.11 to 0.13

Table A.10: One-way ANOVA of melanoma cells exposed to artemisone, Cu(II)-elesclomol and lipid excipient combinations after 24 h, relative to untreated cell control.

One-way analysis of variance					
P value	P<0.0001				
P value summary	***				
Are means signif. different? (P < 0.05)	Yes				
Number of groups	14				
F	19.97				
R squared	0,9154				
ANOVA Table	**SS**	**df**	**MS**		
Treatment (between columns)	18.00	13	1.385		
Residual (within columns)	1.664	24	0.06933		
Total	19.66	37			
Dunnett's Multiple Comparison Test	**Mean Diff.**	**q**	**Significant ? P < 0.05?**	**Summary**	**95% CI of diff**
C vs PC	-1,32	5,49	Yes	***	-2.04 to -0.59
C vs A+E IC10	0,54	2,54	No	ns	-0.10 to 1.19
C vs A+E IC50	0,22	1,04	No	ns	-0.42 to 0.87
C vs A+E IC90	-0,11	0,54	No	ns	-0.76 to 0.53
C vs A+E + O/A IC10	0,02	0,12	No	ns	-0.62 to 0.67
C vs A+E + O/A IC50	-0,05	0,27	No	ns	-0.70 to 0.59
C vs A+E + O/A IC90	-0,77	3,62	Yes	*	-1.42 to -0.12
C vs A+E + S/A IC10	0,57	2,67	No	ns	-0.07 to 1.22
C vs A+E S/A IC50	-0,76	3,17	Yes	*	-1.48 to -0.03
C vs E + S/A IC90	-1,45	6,03	Yes	***	-2.17 to -0.72
C vs A+E + Chol IC10	-0,77	3,60	Yes	*	-1.42 to -0.12
C vs A+E + Chol IC50	-0,87	4,08	Yes	**	-1.52 to -0.22
C vs A+E + Chol IC90	-1,811	7,53	Yes	***	-2.53 to -1.08

A.8 One-way ANOVA analysis of combination treatments relative to artemisone treated cells, with Dunnett post-test – Oxidative stress targeting in skin cancer

Table A.11: One-way ANOVA of melanoma cells exposed to artemisone and lipid excipient combinations after 24 h, relative to artemisone.

One-way analysis of variance					
P value	P<0.0001				
P value summary	***				
Are means signif. different? (P < 0.05)	Yes				
Number of groups	5				
F	139.9				
R squared	0,9894				
Dunnett's Multiple Comparison Test	**Mean Diff.**	**SD**	**Significant ? P < 0.05?**	**Summary**	**95% CI of diff**
ATM IC10 vs PC	-1,74	0.10	Yes	***	-2.07 to -1.416
ATM IC10 vs ATM + O/A IC10	0,17	0.07	No	Ns	-0.148 to 0.50
ATM IC10 vs ATM + S/A IC10	0,11	0.12	No	Ns	-0.17 to 0.41
ATM IC10 vs ATM + Chol IC10	0,11	0.08	No	Ns	-0.21 to 0.44
ATM IC50 vs ATM + O/A IC50	0,08	0.04	No	Ns	-0.22 to 0.40
ATM IC50 vs ATM + S/A IC50	0,30	0.08	Yes	*	0.02 to 0.58
ATM IC50 vs ATM + Chol IC50	-0,07	0.11	No	Ns	-0.38 to 0.24
ATM IC90 vs ATM + O/A IC90	0,31	0.22	No	Ns	-0.27 to 0.91
ATM IC90 vs ATM + S/A IC90	0,36	0.10	No	Ns	-0.22 to 0.95
ATM IC90 vs ATM + Chol IC90	-0,11	0.1	No	Ns	-0.64 to 0.41

A.9 One-way ANOVA analysis of combination treatments relative to Cu(II)-elesclomol treated cells, with Dunnett post-test – Oxidative stress targeting in skin cancer.

Table A.12: One-way ANOVA of melanoma cells exposed to drug-lipid combinations after 24 h, relative to Cu(II)-elesclomol.

One-way analysis of variance					
P value	P<0.0001				
P value summary	***				
Are means signif. different? (P < 0.05)	Yes				
Number of groups	5				
F	139.9				
R squared	0,9894				
Dunnett's Multiple Comparison Test	**Mean Diff.**	**SD**	**Significant? P < 0.05?**	**Summary**	**95% CI of diff**
Elesc IC10 vs PC	-1,74	0.10	Yes	***	-2.07 to -1.416
Elesc IC10 vs Elesc + O/A IC10	0,17	0.33	No	Ns	-0.148 to 0.50
Elesc IC10 vs Elesc + S/A IC10	0,11	0.27	No	Ns	-0.17 to 0.41
Elesc IC10 vs Elesc + Chol IC10	0,11	0.05	No	Ns	-0.21 to 0.44
Elesc IC50 vs Elesc + O/A IC50	0,08	0.14	No	Ns	-0.22 to 0.40
Elesc IC50 vs Elesc + S/A IC50	0,30	0.16	Yes	Ns	-0.44 to 1.04
Elesc IC50 vs Elesc + Chol IC50	-0,07	0.06	No	Ns	-0.38 to 0.24
Elesc IC90 vs Elesc + O/A IC90	0,31	0.33	No	Ns	-0.27 to 0.91
Elesc IC90 vs Elesc + S/A IC90	0,36	0.15	No	Ns	-0.22 to 0.95
Elesc IC90 vs Elesc + Chol IC90	-0,11	0.08	No	Ns	-0.64 to 0.41

A.10 One-way ANOVA analysis of drug-lipid combinations relative to drug constituents, with Dunnett post-test Non-analytical experimental procedures – Oxidative stress targeting in skin cancer

Table A.13: One-way ANOVA of melanoma cells exposed to drug-lipid combinations after 24 h, relative to artemisone–Cu(II)-elesclomol.

One-way analysis of variance	IC10	IC50	IC90		
P value	0,0044	0.0015	0,0010		
P value summary	**	**	**		
Are means signif. different? (P < 0.05)	Yes	Yes	Yes		
Number of groups	4	4	4		
F	10.00	16.58	23.32		
R squared	0,7895	0,8766	0,9210		
Dunnett's Multiple Comparison Test	**Mean Diff.**	**q**	**Significant? P < 0.05?**	**Summary**	**95% CI of diff**
ATM-Elesc IC10 vs Oleic acid	-0,51	1,83	No	Ns	-1.33 to 0.29
ATM-Elesc IC10 vs Stearic acid	0,02	0,10	No	Ns	-0.78 to 0.84
ATM-Elesc IC10 vs Cholesterol	-1,32	4,67	Yes	**	-2.13 to -0.50
ATM-Elesc IC50 vs Oleic acid	-0,28	1,57	No	Ns	-0.81 to 0.25
ATM-Elesc IC50 vs Stearic acid	-0,98	4,90	Yes	**	-1.58 to -0.38
ATM-Elesc IC50 vs Cholesterol	-1,10	6,12	Yes	**	-1.63 to -0.56
ATM-Elesc IC90 vs Oleic acid	-0,66	3,32	Yes	*	-1.27 to -0.04
ATM-Elesc IC90 vs Stearic acid	-1,33	5,99	Yes	**	-2.02 to -0.64
ATM-Elesc IC90 vs Cholesterol	-1,69	7,62	Yes	***	-2.38 to -1.06

Table A.14: One-way ANOVA of melanoma cells exposed to drug-lipid combinations after 24 h, relative to artemisone.

One-way analysis of variance	IC10	IC50	IC90		
P value	0,0016	0.0003	P<0.0001		
P value summary	**	***	***		
Are means signif. different? (P < 0.05)	Yes	Yes	Yes		
Number of groups	5	5	5		
F	9.957	16.93	30.03		
R squared	0,7993	0,8827	0,9376		
Dunnett's Multiple Comparison Test	**Mean Diff.**	**q**	**Significant? P < 0.05?**	**Summary**	**95% CI of diff**
ATM IC10 vs ATM-Elesc IC10	0,12	0,48	No	Ns	-0.61 to 0.85
ATM IC10 vs Oleic acid	-0,39	1,55	No	Ns	-1.12 to 0.33
ATM IC10 vs Stearic acid	0,15	0,60	No	Ns	-0.58 to 0.88
ATM IC10 vs Cholesterol	-1,19	4,71	Yes	**	-1.93 to -0.46
ATM IC50 vs ATM-Elesc IC10	0,09	0,54	No	Ns	-0.40 to 0.59
ATM IC50 vs Oleic acid	-0,19	1,12	No	Ns	-0.69 to 0.31
ATM IC50 vs Stearic acid	-0,89	4,70	Yes	**	-1.45 to -0.33
ATM IC50 vs Cholesterol	-1,01	5,95	Yes	***	-1.51 to -0.51
ATM IC90 vs ATM-Elesc IC10	-0,04	0,27	No	Ns	-0.59 to 0.49
ATM IC90 vs Oleic acid	-0,71	3,95	Yes	*	-1.25 to -0.16
ATM IC90 vs Stearic acid	-1,38	6,87	Yes	***	-1.98 to -0.77
ATM IC90 vs Cholesterol	-1,74	8,67	Yes	***	-2.35 to -1.13

Table A.15: One-way ANOVA of melanoma cells exposed to drug-lipid combinations after 24 h, relative to Cu(II)-elesclomol.

One-way analysis of variance	IC10	IC50	IC90		
P value	0,0035	0.0040	0.0007		
P value summary	**	**	***		
Are means signif. different? (P < 0.05)	Yes	Yes	Yes		
Number of groups	5	5	5		
F	8.083	8.499	16.19		
R squared	0,7638	0,7907	0,8901		
Dunnett's Multiple Comparison Test	**Mean Diff.**	**q**	**Significant? P < 0.05?**	**Summary**	**95% CI of diff**
Elesc IC10 vs ATM-Elesc IC10	0,67	2,42	No	ns	-0.13 to 1.47
Elesc IC10 vs Oleic acid	0,15	0,55	No	ns	-0.64 to 0.95
Elesc IC10 vs Stearic acid	0,70	2,53	No	ns	-0.10 to 1.50
Elesc IC10 vs Cholesterol	-0,65	2,36	No	ns	-1.45 to 0.15
Elesc IC50 vs ATM-Elesc IC10	0.40	1.83	No	ns	-0.25 to 1.05
Elesc IC50 vs Oleic acid	0,12	0,55	No	ns	-0.53 to 0.77
Elesc IC50 vs Stearic acid	-0,58	2,37	No	ns	-1.31 to 0.14
Elesc IC50 vs Cholesterol	-0,70	3,17	Yes	*	-1.35 to -0.05
Elesc IC90 vs ATM-Elesc IC10	0,19	0,83	No	ns	-0.50 to 0.88
Elesc IC90 vs Oleic acid	-0,47	2,08	No	ns	-1.16 to 0.21
Elesc IC90 vs Stearic acid	-1,15	4,50	Yes	**	-1.91 to -0.38
Elesc IC90 vs Cholesterol	-1,51	5,93	Yes	**	-2.27 to -0.74

ANNEXURE B: CERTIFICATE OF EDITING

Gill Smithies

Proofreading & Language Editing Services

59, Lewis Drive, Amanzimtoti, 4126, Kwazulu Natal

Cell: 071 352 5410 E-mail: moramist@vodamail.co.za

Work Certificate

To	Michaela Haigh
Address	Centre of Excellence for Pharmaceutical Studies, Division of Pharmaceutics, Potchefstroom Campus, North West University
Date	7/11/2017
Subject	Chapters 1 and 2: Anti-cancer activities of oxidant-redox drug combinations in lipid excipients
Ref	GS/MH/01

I, Gill Smithies, certify that I have proofed the following,
Chapters 1and 2: Anti-cancer activities of oxidant-redox drug combinations in lipid excipients,
to the standard as required by NWU, Potchefstroom Campus.

Gill Smithies

7/11/2017

ANNEXURE C: ETHICAL TRAINING CERTIFICATE

NORTH-WEST UNIVERSITY
YUNIBESITI YA BOKONE-BOPHIRIMA
NOORDWES-UNIVERSITEIT
POTCHEFSTROOM CAMPUS

Private Bag X6001, Potchefstroom
South Africa 2520

Tel: 018 299-1111/2222
Web: http://www.nwu.ac.za

Health Sciences Ethics Office for Research, Training and Support
Tel: 018-299 2092
Fax:
Email: Minrie.Greeff@nwu.ac.za

6 June 2016

Dear Ms Michaela Christine Haigh

PROOF OF ATTENDANCE

This letter certifies that you have attended the 1-day ethics training, entitled:

The SANS document: As regulation for research with animals

presented by Prof Christiaan B Brink (Chair of AnimCare) on the 20 January 2016.

This proof of attendance, as recognised by AnimCare and the Ethics Office, NWU, is valid for 3 years and expires on the 19th of December 2019.

Yours sincerely

Prof Minrie Greeff
Head of Health Sciences Ethics
Office for Research, Training and Support

Prof Awie Kotzé
Dean of Faculty of Health Sciences